RECLAMATION

Managing Water in the West

Technical Memorandum No. D8330-2005-07

2004 Status Report-Paradox Valley Seismic Network Paradox Valley Project, Southwestern Colorado

U.S. Department of the Interior
Bureau of Reclamation
Technical Service Center
Denver, Colorado

May 2005

U.S. Department of the Interior
Mission Statement

The mission of the Department of the Interior is to protect and provide access to our Nations's natural and cultural heritage and honor our trust responsibilities to Indian tribes and our commitments to island communities.

Bureau of Reclamation
Mission Statement

The mission of the Bureau of Reclamation is to manage, develop, and protect water and related resources in an environmentally and economically sound manner in the interest of the American public.

Technical Memorandum No. D8330-2005-07

2004 Status Report-Paradox Valley Seismic Network Paradox Valley Project, Southwestern Colorado

Prepared by

Kenneth Mahrer
Jon Ake
Daniel O'Connell
Lisa Block

U.S. Department of the Interior
Bureau of Reclamation
Technical Service Center
Denver, Colorado

May 2005

Bureau of Reclamation
Technical Service Center
Seismotectonics and Geophysics Group

Technical Memorandum No. D8330-2005-07

2004 Status Report-Paradox Valley Seismic Network
Paradox Valley Unit
Southwestern Colorado

Prepared By

Kenneth Mahrer
Geophysicist

5/18/05
Date

for Jon Ake
Seismologist

5-18-05
Date

Daniel O'Connell
Seismologist

5/18/05
Date

Lisa Block
Geophysicist

5/18/05
Date

Peer Review

Jerry Wright
Geophysicist

5-18-05
Date

Table of Contents

1.0 EXECUTIVE SUMMARY 3
- **1.1 Background 3**
- **1.2 2004 Activities 5**
  - *1.2.1 November 7th Magnitude M3.9 Event 5*
    - 1.2.1.1 November 7th Magnitude M3.9 Event: Seismograms 5
    - 1.2.1.2 November 7th Magnitude M3.9 Event: Regulations 7
    - 1.2.1.3 November 7th Magnitude M3.9 Event: Foreshocks and Aftershocks ..10
  - *1.2.2 Larger Events at Paradox 11*
  - *1.2.3 McGarr Model: Ratio of Seismic Moment to Injected Volume 13*
  - *1.2.4 Earthtides 15*
- **1.3 Cumulative Findings 17**
- **1.4 Acknowledgements 21**

2.0 LOCAL SETTING 22
- **2.1 PVU Salinity Control Well No. 1 ..... 25**
- **2.2 Wray Mesa Fault and Fracture System 26**

3.0 PARDOX VALLEY SEISMIC NETWORK 28
- **3.1 Paradox Valley Seismic Network 28**
- **3.2 Paradox Data Digitalization and Associated Model 32**
- **3.3 Telemetry, Software, and Strong Motion Instruments 34**
- **3.4 PVSN (Daily-Average) Operational Efficiency 35**

4.0 PVU INJECTION OPERATIONS 37
- **4.1 PVU Operations by Injection Phase 37**
  - *4.1.1 Phase I - (22-May 1996 through 26-July 1999) 37*
  - *4.1.2 Phase II - (27-July 1999 through 22-June 2000) 38*
  - *4.1.3 Phase III - (23-June 2000 through 7-January 2002) 39*
  - *4.1.4 Phase IV - (8-January 2002 through the Present) 39*
- **4.2 PVU Injection History By Year 39**
- **4.3 Injection Adjustments Explanation 40**
  - *4.3.1 Bi-Annual Shutdowns 40*
  - *4.3.2 Reduced Injection Rate 41*
  - *4.3.3 Injectate: 70%:30% PVB:Fresh Versus 100% PVB 42*

5.0 SEISMIC ANALYSIS 43
- **5.1 Typical Seismograms from PVU 43**
- **5.2 Local Seismic Magnitude Scale 44**
- **5.3 Preliminary Event Location Method 44**
- **5.4 Advanced Analysis: Event Re-Location 45**

6.0 OBSERVATIONS 49
- **6.1 Local, Pre-Injection Seismicity 49**
- **6.2 Seismic Events and Well Testing (1991-1995) 49**
- **6.3 Seismic Events and Continuous Injection (1996-Present) 50**
- **6.4 Event Magnitudes 52**
- **6.5 Events by Depth 57**

6.6 Felt Events 57
6.7 2004 Event Locations 58
6.8 1991-2003 Event Locations By Year 63
6.9 Earthquake Recurrence 63
6.10 Focal Mechanisms - Preliminary Analysis 69
6.11 Focal Mechanisms - Advanced 70
6.12 Induced Event Slip Mode 70
6.13 Seismic Magnitude versus Location 71
6.14 Swarm Analysis 71
6.15 Remote (Northern) Seismic Swarms 73
7.0 MODELING 77
7.1 Mohr Circle Analysis 77
7.1.1 General 77
7.1.2 Paradox Injection and Mohr Circle 78
7.2 (Projected) Total Seismic Event Production 80
7.3 A Fractal Model to Accommodate Injectate Volume 81
7.3.1 Background 82
7.3.2 Mathematical Foundation 82
7.3.3 Calculations 84
7.3.4 Fractal Model Implications 86
7.4 Injection Data and Fracture Modeling 87
7.5 Seismicity, Fault Properties, and Injectate Volume 88
7.6 Seismicity and Effective Porosity 89
8.0 CONCLUSIONS 92
8.1 Specific to 2004 92
8.2 Since Inception of Continuous Pumping 92
9.0 MISCELLANEOUS 95
9.1 Supplemental Activities 95
9.2 Accompanying CD File List 95
10.0 REFERENCES 97

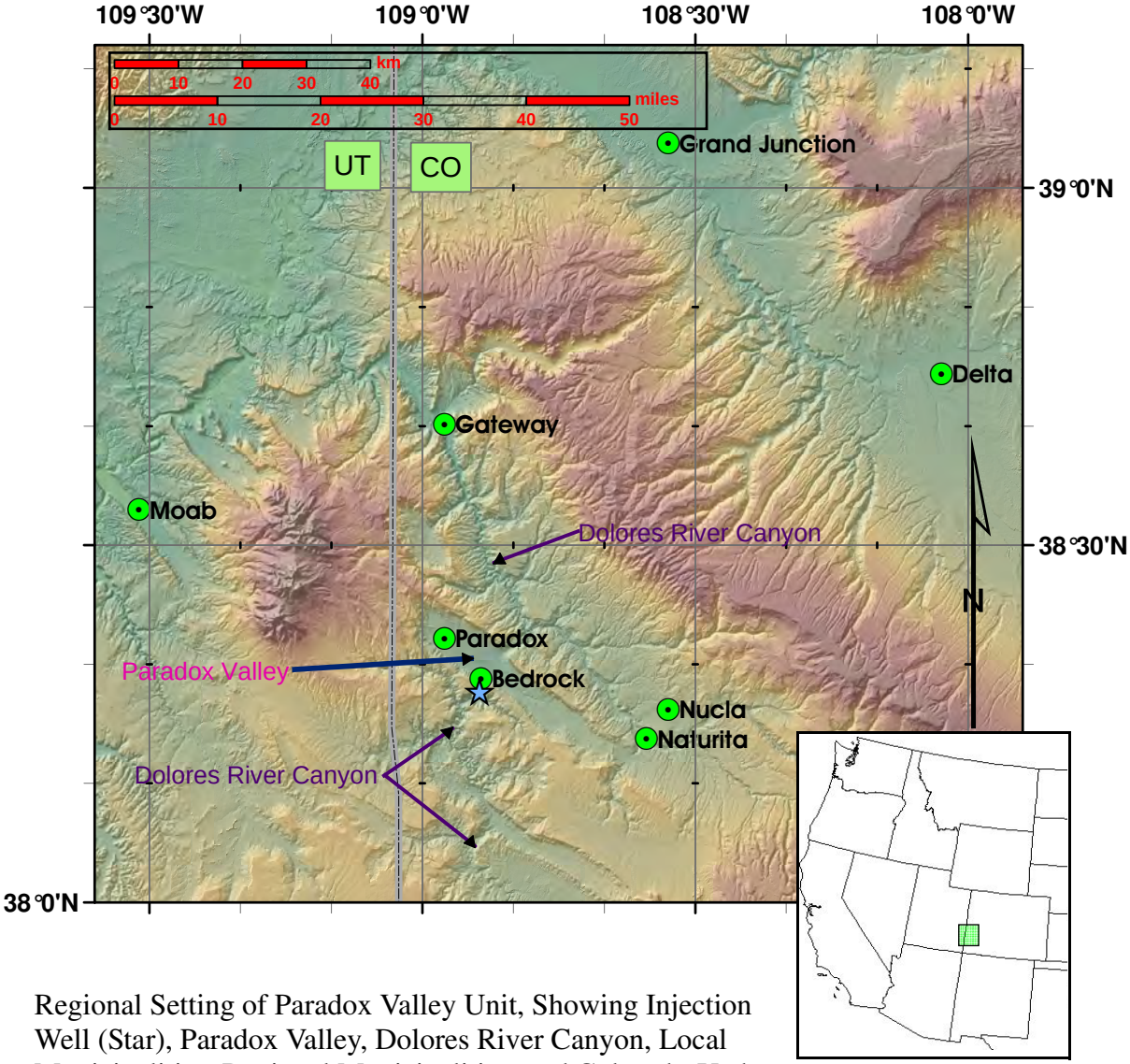

Regional Setting of Paradox Valley Unit, Showing Injection Well (Star), Paradox Valley, Dolores River Canyon, Local Municipalities, Regional Municipalities, and Colorado-Utah Border.

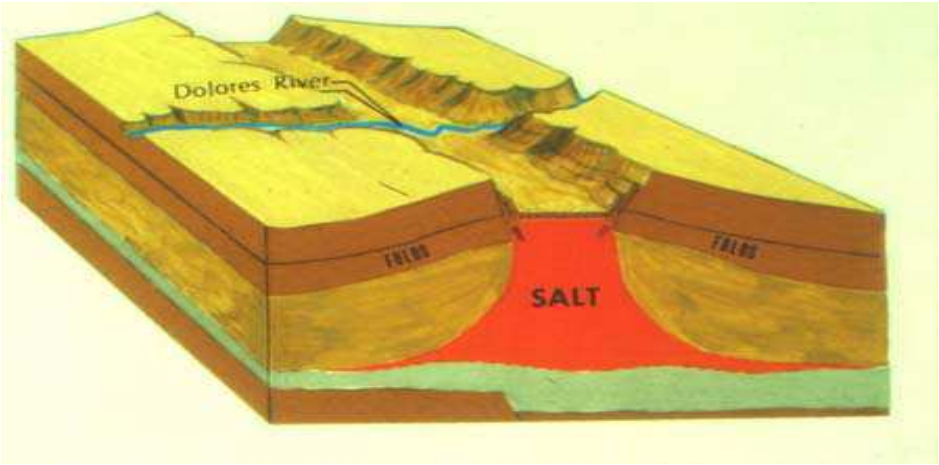

Cartoon of Dolores River across Paradox Valley and Cross Section of Paradox Valley

Dolores River and Paradox Valley
Looking Northeast across the Valley

Paradox Valley Looking
Northwest through the Valley

1.0 EXECUTIVE SUMMARY

Based on other deep-well injection projects, including the Denver Arsenal, CO in the 1960's and Rangley, CO in the later 1960's and early 1970's, the U. S. Bureau of Reclamation (Reclamation) recognized and planned for small earthquakes induced by the Paradox Valley Unit (PVU) injection. In 1985, six years before the onset of injection at PVU, Reclamation began monitoring seismicity in the Paradox Valley region with its surface-based Paradox Valley Seismic Network (PVSN). Recording, analyzing, and interpreting these data were, and still are, the mandate of the PVSN staff. Specifically, PVSN operations (1) gather continuous ground motion data originating in and around Paradox Valley and the surrounding region; (2) electronically collate and telemeter these data to the Denver Federal Center (DFC) in Lakewood, CO; (3) isolate, evaluate, and catalog local, injection-induced seismic events within the data; (4) locate the source (i.e., origin location) of each seismic event; (5) determine cumulative and individual characteristics (e.g., source mechanics or focal mechanisms) of the events, when feasible; (6) identify and evaluate relationships between seismicity, geology, tectonics, subsurface brine and connate water/pressure movements and locations, and injection parameters; (7) maintain a database of both event and injection parameters; (8) and report findings both internally and to the scientific community.

1.1 Background

This report summarizes the calendar year 2004 seismic data, observations, and related work for PVSN and its support staff. Since 1985, Reclamation has operated PVSN, its local, surface-based, 15-station seismometer network, as part of the PVU, a member of the Colorado River Basin Salinity Control family of projects. PVU collects Paradox Valley brine (PVB) prior to it entering the Dolores River, a tributary of the Colorado River. PVU then uses the world's deepest US-EPA Class V disposal well, the PVU Salinity Control Well No. 1, to dispose the brine by injecting it ~4.3 km below the Earth's surface into the Mississippian-aged Leadville Limestone and surrounding formations. Since 1991, the project has disposed more than 4 billion liters of PVB-rich injectate (~600 million+ kg of salts). Between 1991 and 1995 injection was a punctuated sequence of 7 injection tests and an acid stimulation aimed at demonstrating well and reservoir integrity and acquiring a Class V, EPA permit for deep disposal. With the granting of the permit, the injection has been round-the-clock since 1996, with the exception of as-needed maintenance shut downs

and, since 2000, a scheduled, 20-day shut down every 6 months.

Throughout most of the injection well's operating history, the (downhole) injection pressure at PVU has been in the range of 80±2 MPa (~12,000 psi) with surface pressure ranging between 30 and 34 MPa (4,400 and 4,950+ psi), which is about 10 MPA (~1,500 psi) in excess of the formation fracture pressure. The injection has induced an estimated 2+ million microseisms (i.e., seismic events with magnitudes equal to or greater than **M**-3.0 up to the maximum induced event, a magnitude **M**4.3). By the end of December 2004, PVSN has recorded over 4,100 of the largest of these events, specifically those with magnitudes ~**M**0.0 or greater. The recorded data radiate from one of two, disconnected seismic source ("seismogenic") zones: the principal zone, asymmetric, E-W elongated zone that surrounds the injection well and contains more than 90% of the events and the secondary zone, also asymmetric and lying ~8 km northwest of the injection well. From the injection well, the secondary region lies along the local major fault trend of the Leadville Formation and its neighboring formations, the Wray Mesa Fault system.

The PVSN-recorded seismic events are not tensile (i.e., fracture-opening) events created by the injectate or connate fluid wedging open the local rock mass. Although we believe tensile events, which include new fractures and the widening of existing openings, are occurring, these events are physically too small to radiate sufficient energy to be recorded at the surface by any PVSN station; the closest PVSN station is 3 to 4 km from a seismogenic zone. Instead the recorded events are shear slippages or failures along preexisting planes of weakness (e.g., faults, old fractures, etc.). The shear sources are not uniformly or randomly distributed in the seismogenic zones, but define into linear patterns. These well-defined patterns delineate secondary networks of fractures and faults of the Wray Mesa system. The shear planes of slip (i.e., fault-planes of the induced seismicity) align with the linear directions or strikes of these fractures and faults or with their anticipated principal shear stress directions. One very significant finding of the mapped fractures and faults shows that substantial pressure perturbations (either by injectate or connate) have migrated through the Wray Mesa network of faults and fractures at least the 8 km from the injection well to the second seismogenic region.

The estimated maximum volume of the injectate held by the seismically-identified fractures and

faults is nominally only a few percent of the total injectate volume; the remaining injectate has diffused into the local porosity: either into new microfractures created by the injection or the poorly-developed system of pre-existing pores and microfractures. Since the injection pressure exceeds the fracture pressure, the injectate creates new or widens existing pores, fractures, and joints.

Over its history, PVU has instituted strategies to mitigate the risk of inducing larger seismic events while maintaining the economic viability of injection. These strategies have included reducing injection rate and instituting biannual 20-day shut downs. The reduced injection rate allows the injectate more time to diffuse into the reservoir rock matrix. Similarly, the shut downs allow the formation stresses to relax as the injectate leaks off from main fractures into pores and small fractures of the reservoir matrix. Since mid-2002, these changes have substantially reduced seismic event production and seem to have reduced the proclivity to produce larger, felt events.

1.2 2004 Activities

1.2.1 November 7th Magnitude M3.9 Event

On November 7, 2004 at 6:55 AM UTC (Nov. 6, 11:55 PM, local time), PVU witnessed an induced event of magnitude **M**3.9. The event was located 1.57 km south and 0.63 km west of the injection wellhead at a depth of 3.63 km. **Figure 1-1** shows the epicenter of this event (large circle with dot at its center) against a background of epicenters of all PVU-induced events through the end of 2004. The **M**3.9-event is the second largest event induced by the PVU injection; the largest was an **M**4.3 that occurred in May of 2000, more than 4 years earlier. PVU responded very quickly to the November 7th event and ceased injection within approximately 3 minutes of feeling the event. After evaluating the event and its consequences (no reported damage and estimated surface shaking duration of a few seconds), PVU resumed injection at its pre-event rates after 8 days of shutdown.

1.2.1.1 November 7th Magnitude M3.9 Event: Seismograms

Anomalously large events like the **M**3.9 event of November 7th create ground motions that drive

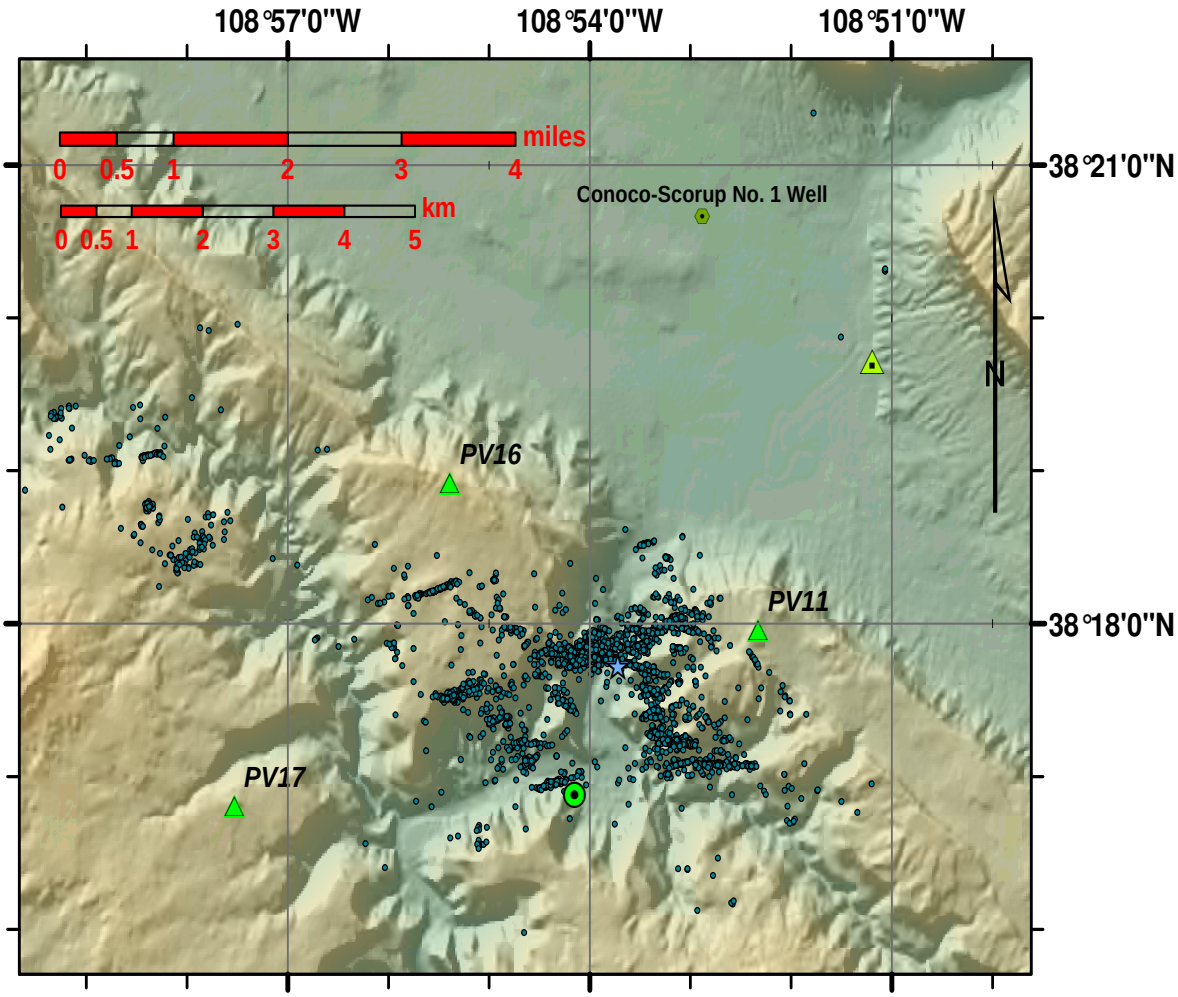

Figure 1-1 Epicenter of November 7, 2004 M3.9 Event. Event is large circle with dot at its center. Also shown are the PVU injection well (star); the epicenters of all the PVU injection-induced events (small circles); and some of the Paradox Valley Seismic Network stations (triangles), including the strong motion instrument near the extraction well field, mid-valley (triangle with dot).

the high-gain instruments of PVSN beyond their operational range. The operational range of the PVSN instruments is limited compared to the range of ground motion data. It must be set to record the most important data. At PVSN we could set this range to record the ground motion (i.e., traces) of anomalously large events, which would preclude recording many of the nominal, more common events, or we could set the range to record the nominal events and preclude recording an acceptable trace for the large events. Because they are much more common and because we can analyze them, we the set range of the instruments to record the ground motion of the nominal-

sized events at PVU (see Chapter **3.0 Paradox VALLEY SEISMIC NETWORK**). Large, very infrequent events, like this **M**3.9 drive the PVSN instruments out of this range. However, the seismograms of large events that are recorded by these instruments can be interpreted to some degree. In addition to the high-gain instruments of PVSN, PVSN also deploys two strong motion instruments, one near the injection wellhead and one in the middle of Paradox Valley, near the PVU extraction well field (dotted triangle in **Figure 1-1**). The strong motion instruments do not record the nominal PVU events, but trigger on and record only larger ground motions. These instruments measure ground accelerations, compared to ground velocities of the nominal PVSN instruments. **Figure 1-2** shows the strong-motion seismograms recorded at the PVU pumping station and **Figure 1-3** shows the seismograms at the injection well. The data in these figures have been numerically integrated to give ground velocities from the recorded accelerations. Note that the peak velocity at the wellhead was approximately 0.5 inches/s, while at the extraction field, approximately 6+ km to the northeast from the wellhead and the epicenter of the **M**3.9 event, the peak velocity was larger, approximately 0.75 inches/s. For comparison, the peak acceleration at the extraction was approximately 0.1 g (1 g = 980 cm/s^2) and at the injection well, it was approximately 0.06 g. At first glance, these data are a bit enigmatic: the site further from the event, the pump station, witnessed 50% or greater ground velocity and acceleration. However, this observation is consistent with linear amplification in softer near-surface materials, as in the soils at the extraction well field site.

1.2.1.2 November 7th Magnitude M3.9 Event: Regulations

The Federal Government has no published regulation regarding acceptable amplitudes of events induced by injection. The same is true for the State of Colorado. However the State of Colorado does have regulations for acceptable ground motion from blasting associated with coal mining (Colorado Division of Mineral and Geology, 1980), specifically the Rules and Regulations of The Colorado Mined Land Reclamation Board Pursuant to the Colorado Surface Coal Mining Reclamation Act, Rule 4: Performance Standard. Under Section 4.08.4(10) states “Except as provided by 4.08.4(10)b, the maximum peak particle velocity in blasting operations shall not exceed the following limits at the locations of any dwelling, public building, school, church, or community or institutional building, outside the permit area:...” At a distance from the blasting site of 5001 or more feet, maximum allowable peak particle velocity (in inches/s) is 0.75. Section 4.08.4(10)b

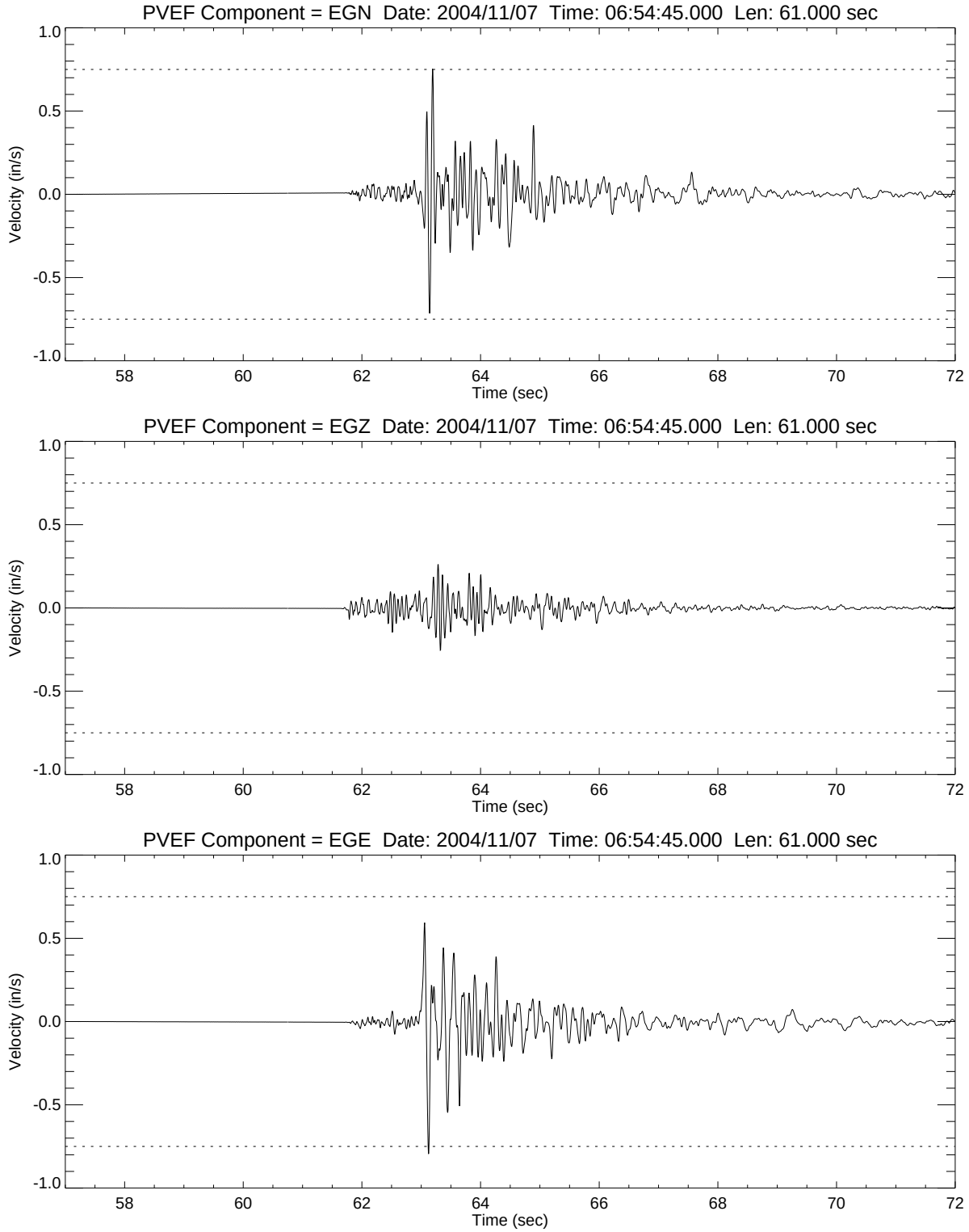

*Figure 1-2 Three-Component Velocity Seismogram of the November 7, 2004, **M**3.9 Event Recorded near Extract Well Field in Paradox Valley (see Figure 1-1). Top panel is north-south motion; middle is up-down; bottom is east-west. Note that vertical scale of each seismogram is the same.*

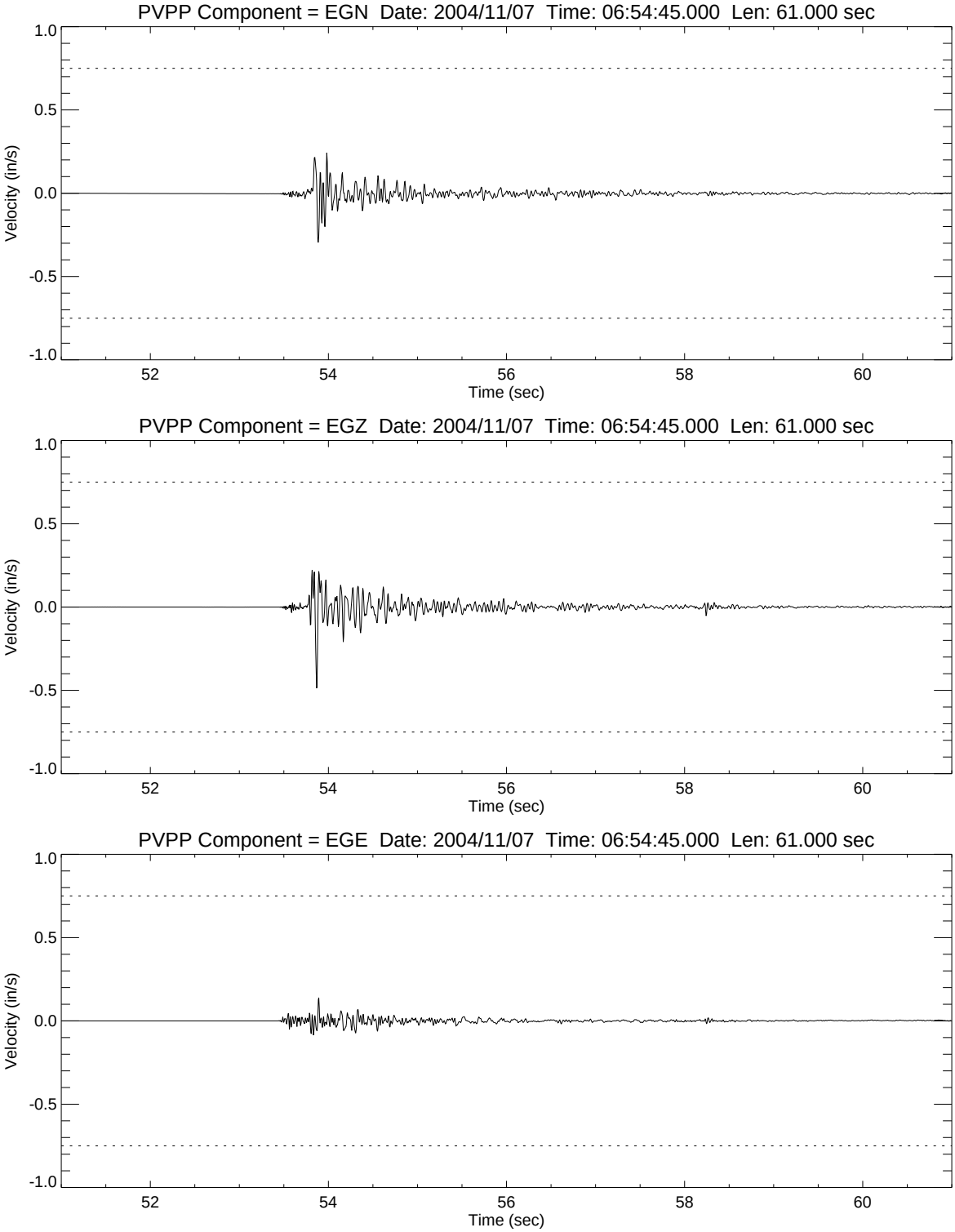

*Figure 1-3 Three-Component Velocity Seismogram of the November 7, 2004, **M**3.9 Event Recorded near Injection Well. Top panel is north-south component; middle is up-down; and bottom is east-west. Note that vertical scale of each seismogram is the same.*

noted in the previous quotation states, "The Division may allow a variance from the maximum peak particle velocity limits if it determines that the structure is owned by the person conducting the surface coal mining operations, and the structure is not leased to another party, or if leased to another party, that a written waiver by the lessee is submitted to the Division prior to blasting."

In accordance with these blasting regulations, the horizontal dashed lines in **Figure 1-2** and **Figure 1-3** are the 0.75 inches/s limits. Note that the **M**3.9 event ground velocity is at the limit at PVU's extraction well field site and below the limit at the injection wellhead.

We offer this section as a reference, since, as noted, we know of no regulations governing acceptable-sized induced seismicity. The applicability of blasting regulations and the noted variance to Paradox injection is not a subject of this report.

1.2.1.3 November 7th Magnitude M3.9 Event: Foreshocks and Aftershocks

In earthquake-proned areas, a major event often "announces its arrival" by a group of foreshocks and its "departure" by a group of aftershocks. To examine whether the November 7th **M**3.9 event generated foreshocks and/or aftershocks, we began by assuming a reasonable distance for the occurrence of foreshocks and aftershocks relative to the location of the **M**3.9 event. We assumed +/- 500 m in both the north-south and east-west directions. This gave a square, 1.0 km on a side and centered on the **M**3.9 event. **Figure 1-4** shows a gridded map of all the event epicenters since 1996 in the southwest quadrant relative to the injection wellhead. [*Note*: There were no events in the region during the '91-'95 injection tests.] Also showed is the 1x1 km dashed square containing the candidate foreshock/aftershock events. **Figure 1-5** shows a close up of the dashed square. In this figure there are 141 events. The occurrence of these 141 events as a function time against a backdrop of the injection (calculated downhole) pressure and the injection phases is shown in **Figure 1-6**. The figure shows that the region was quite active between 1998 and 2000, but with the advent of *Phase III* pumping, the event production rate greatly reduced. From the beginning of *Phase III* to the end of 2004, the region in the dashed square produced 53 events. However, **Figure 1-7** shows a close up of the events in 2004. The figure shows 37 events of which 24 occurred after the **M**3.9 event. Note how few of the events occur prior to the **M**3.9 event. We interpret these results to mean that the **M**3.9 event did not "announce its coming" with identifiable foreshocks,

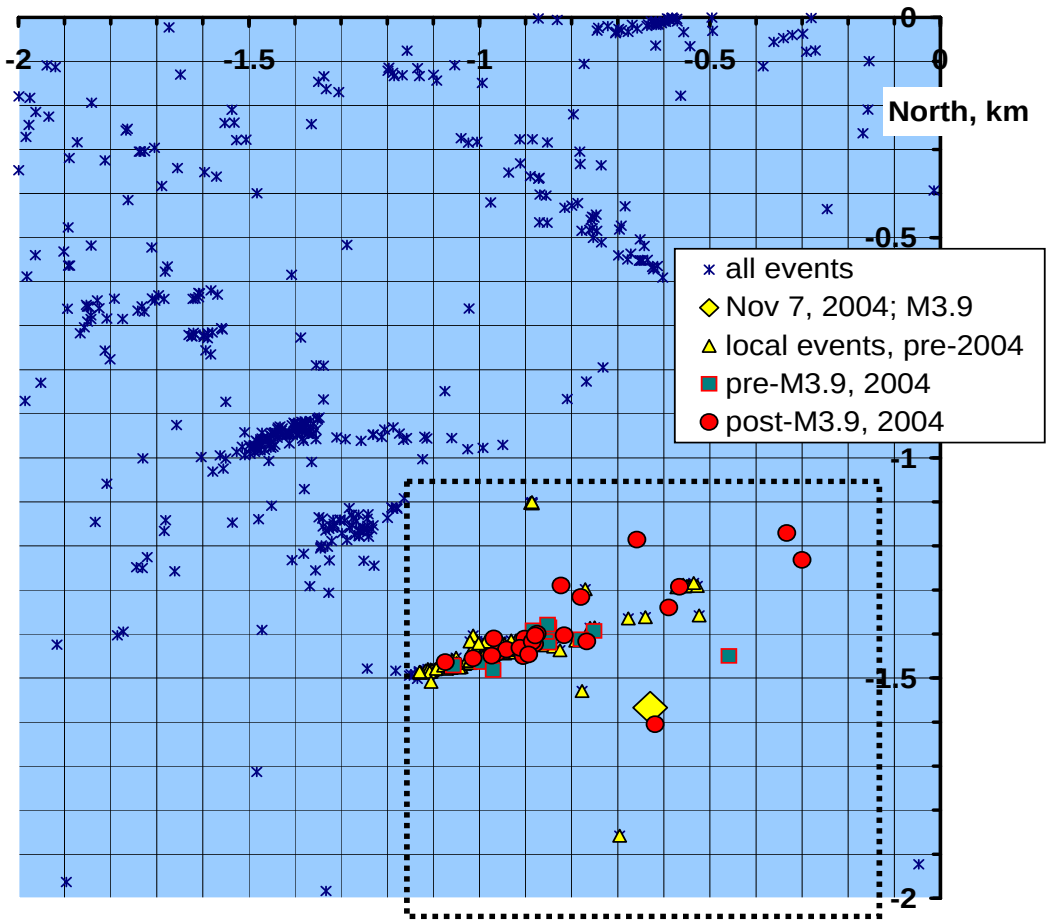

Figure 1-4 Gridded Map of All Event Epicenters Southwest of Injection Well since 1996. Injection well is at northeast corner of map at map coordinates (0,0). Dashed-square is 1x1 km square centered on Nov 7, 2004 ***M****3.9 event. Grid spacing is 0.1 km.*

but left its "mark" with a sequence of approximately 24 aftershocks. In support of this conclusion, we show **Figure 1-8**, a magnitude versus occurrence plot of the events in the aftershock region of the **M**3.9 event. Note that the events generally decrease in size with increasing time, as expected for an aftershock sequence. [At the time of writing this report in the first quarter of 2005, events in the aftershock zone, presumably from the **M**3.9 event, still occur occasionally.]

1.2.2 Larger Events at Paradox

The occurrence of the **M**3.9 in November 2004 motivated us to reexamine the large event occurrence at Paradox. [*Note*: This analysis will continue into 2005.] Injection at Paradox has induced

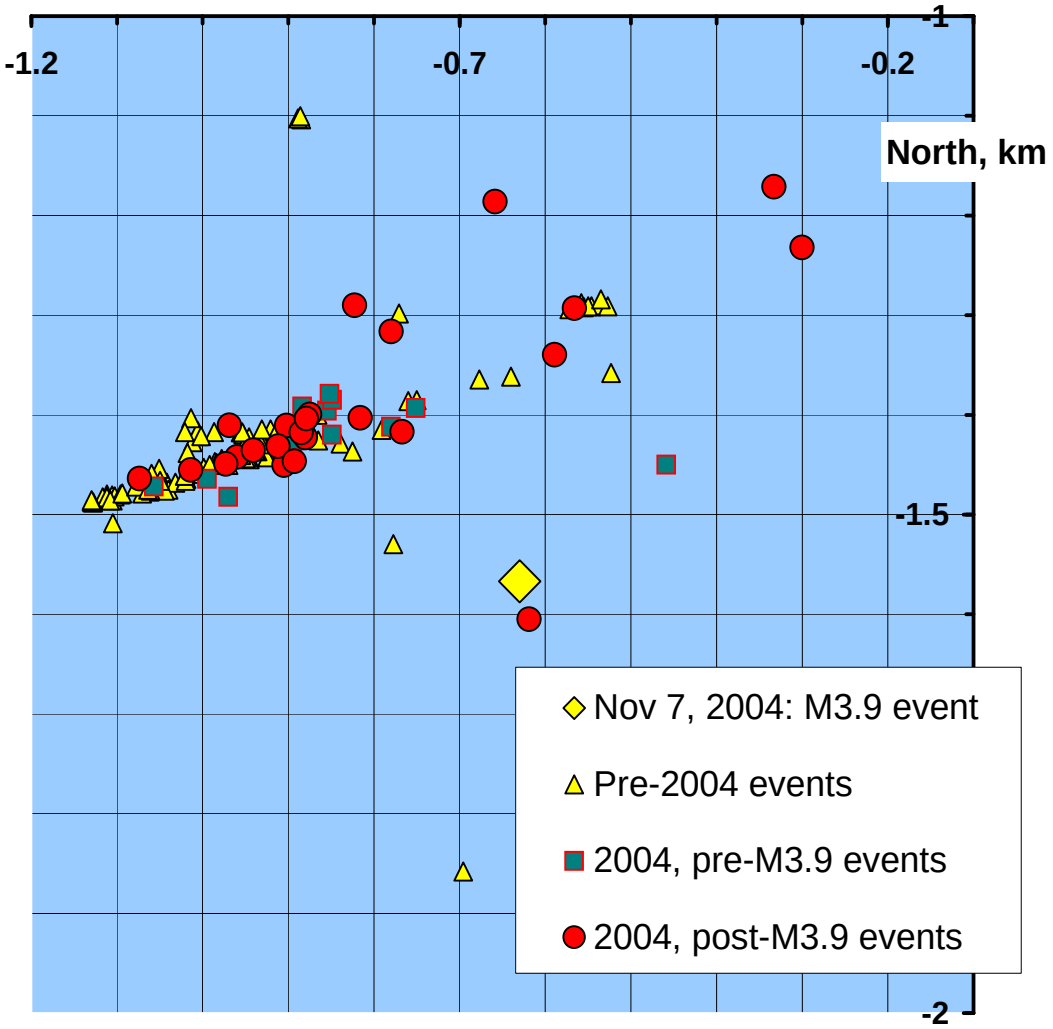

Figure 1-5 Close up of Epicenters in 1x1 km Dashed Square in ***Figure 1-4****. Axis distance designations are in km relative to injection wellhead; grid is 0.1-km spacing*

20 events of magnitude **M**2.5 or greater. All these events occurred since the inception of round-the-clock pumping in 1996. **Figure 1-9** shows a map of these events against a backdrop of all the events at Paradox. Seventeen of these events occurred in the primary seismogenic zone surrounding the injection well and three occurred in the secondary zone to the northwest of the injection well. The figure shows that most of the large events occur in the neighborhood of other large events and that most of the events occur on or near the local edge of the seismogenic zone. Both of these findings require further analysis. Note, also that the June and July 1999 events that initiated PVU's first major injection adjustment (i.e., the inclusion of bi-annual, 20-day shut downs, the changing from *Phase I* to *Phase II* pumping.) were not particularly close to each other, mean-

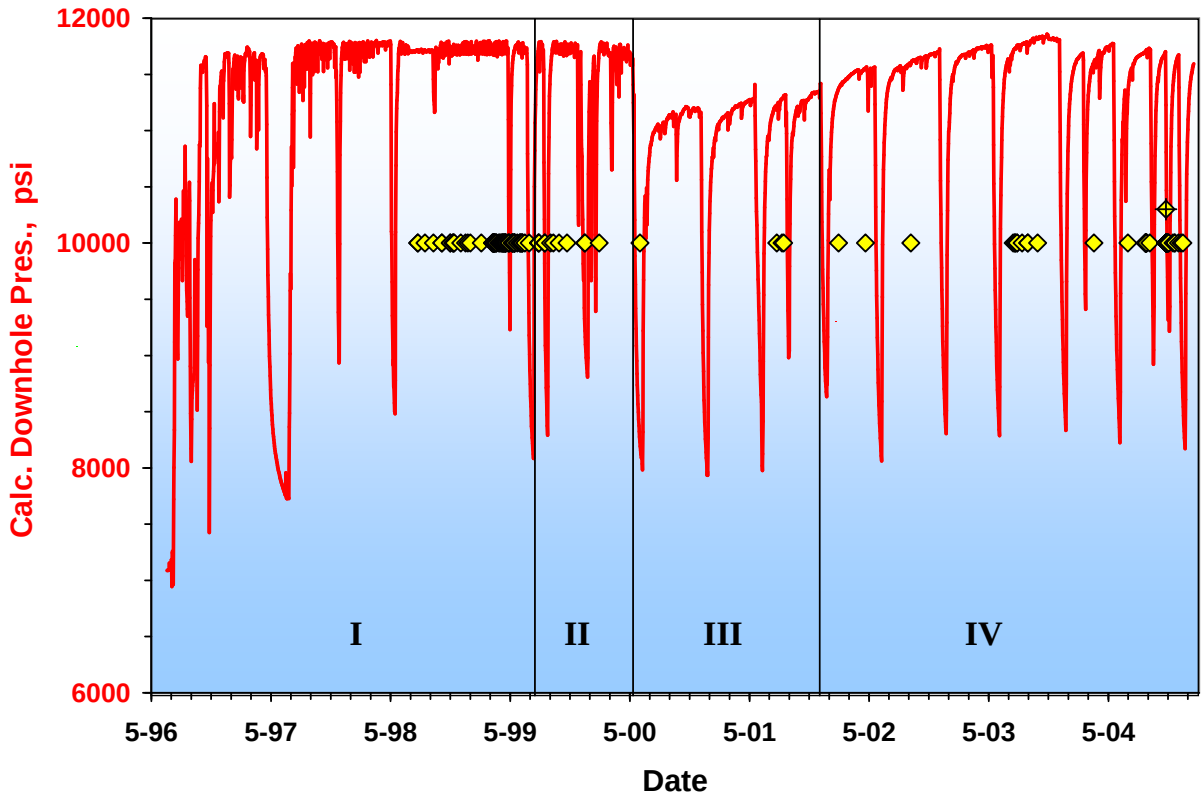

*Figure 1-6 Occurrence (diamonds) of Seismic Events Within Designated Square Region in **Figure 1-4** and in **Figure 1-5**. Also shown are Roman numeraled injection phases and the calculated downhole injection pressure. The **M**3.9 event is shown as a diamond with a plus sign at the far right of and above the line of diamonds.*

ing the second of these was probably not affected by the first. In conjunction with **Figure 1-9** we present **Figure 1-10**,. a plot of depth versus time and downhole injection pressure versus time for the magnitude **M**2.5 and greater events, against a backdrop of the depths of all events at Paradox. One characteristic of this plot is quite obvious; the change in injection schedules associated with *Phase III* and *IV* have certainly reduced the proclivity to create larger events. In addition this figure shows that larger events seem to have shallowed with the onset of the reduced injection rate (i.e., *Phase III*).

1.2.3 McGarr Model: Ratio of Seismic Moment to Injected Volume

McGarr (1976) suggested that, for induced-seismicity, as witnessed at Paradox, the ratio of the sum of the cumulative seismic moment to the cumulative (injected) volume is a constant equal to

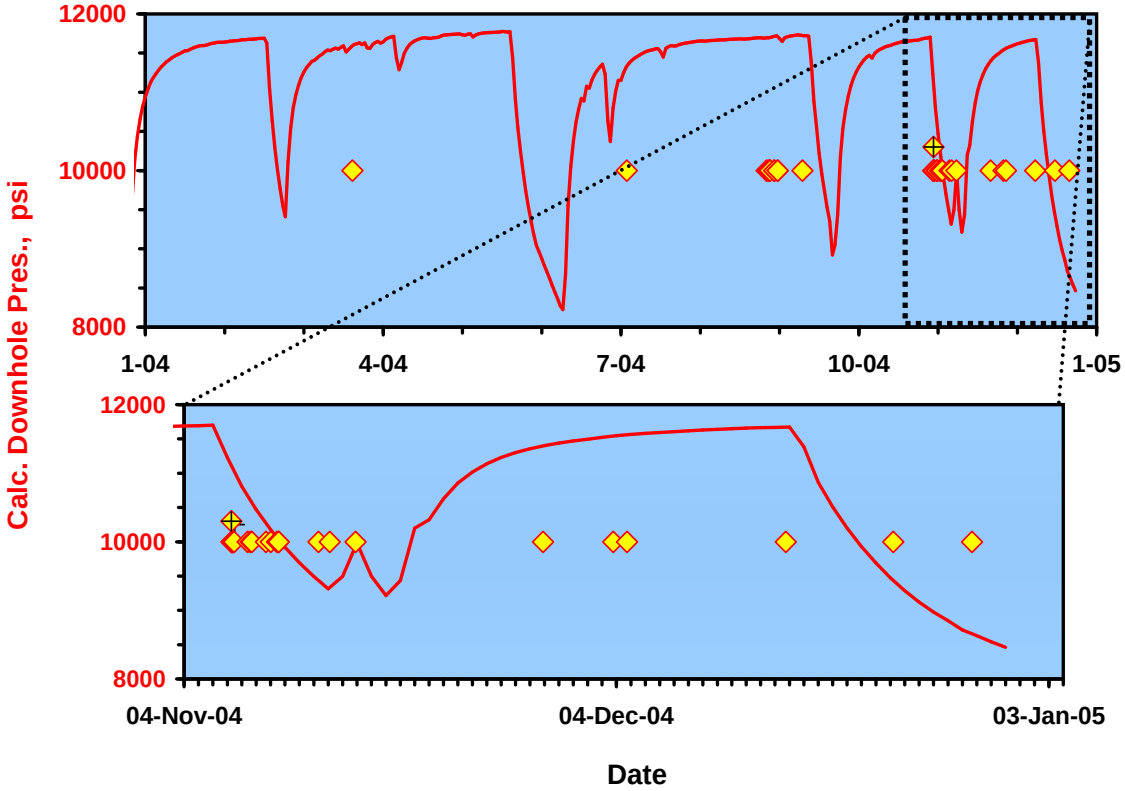

*Figure 1-7 Occurrence (diamonds) of Seismic Events for 2004 Within Designated Square Region in **Figure 1-4** and in **Figure 1-5**. Solid line is calculated downhole (injection) pressure. Insert is close up of two months following the **M**3.9 event. The **M**3.9 event is the diamond with a plus sign.*

a factor, ***K***, close to unity, times the formation shear modulus. McGarr assumes unity for ***K*** and, for limestone, an average value for the shear modulus is ~$2x10^{10}$ N/m^2 (Clark, 1966). **Figure 1-11** shows the cumulative moment-volume ratio for Paradox as a function of time. Also shown are the (calculated) downhole pressure (pressure at ~4.3 km depth, assuming no wellbore friction) and the four pumping phases since 1996. The moment-volume ratio in **Figure 1-11** includes the pump test data which is the vertical offset from the origin.

In **Figure 1-11**, the obvious, large vertical increase in the moment-volume ratio in mid-2000 corresponds to Paradox's largest (i.e., **M** 4.3) induced-event and the three small, but still noteworthy upward "steps" in the ratio, two in mid-1999 and one at the end of 2004, correspond to Paradox's next three largest (i.e., **M** 3.6, **M** 3.5, and the **M** 3.9) induced-events (discussed elsewhere). **Figure 1-11** shows that the moment-volume ratio has not been constant or monotonic but has increased and decreased between ~10^8 and a maximum of ~$1.6x10^9$, immediately following the

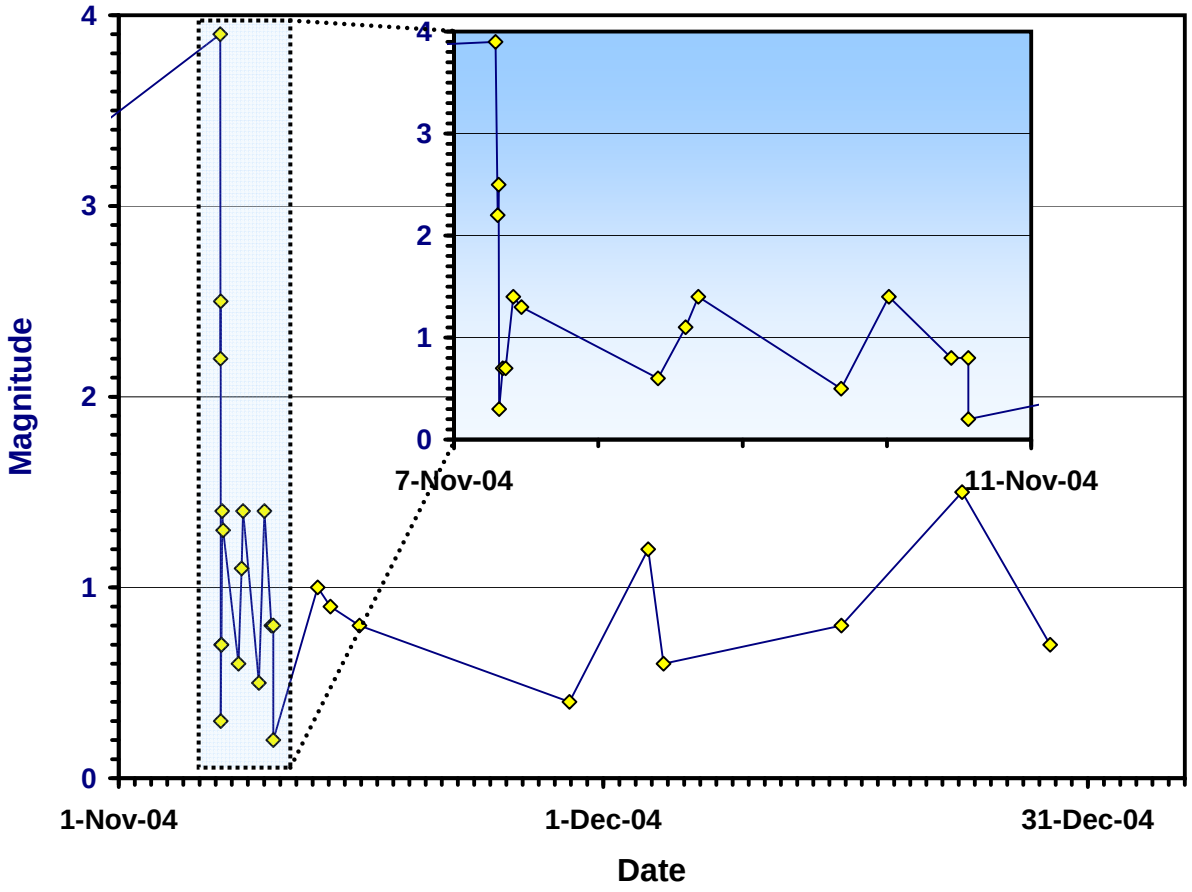

*Figure 1-8 Magnitude versus Occurrence Time of Events Following November 7, 2004 **M**3.9 Event.*

M 4.3 event. Note that with the reduction in injection rate at the inception of *Phase III*, the ratio has been decreasing. In his Discussion section McGarr (1976) does state, "It is worth emphasizing that for situations involving fluid injection or withdrawal, [*the ratio*] is not applicable unless the permeability of the rock is sufficiently low that there is no appreciable fluid flow without fracture." The injection zone at Paradox is highly fractured. We interpret the disparity in the moment-volume ratio as an indication of "appreciable fluid flow without fracturing."

1.2.4 Earthtides

Earthtides are cyclic deformations the Earth witnesses because of the effects of gravity from the Sun and the Moon. These are not to be mistaken with ocean tides, although they are related. The Earth-Sun-Moon gravitational system produces displacements of the solid earth up to about 10 cm from gravitational accelerations (i.e., gravitation forces) that can be as large as 200 to 300

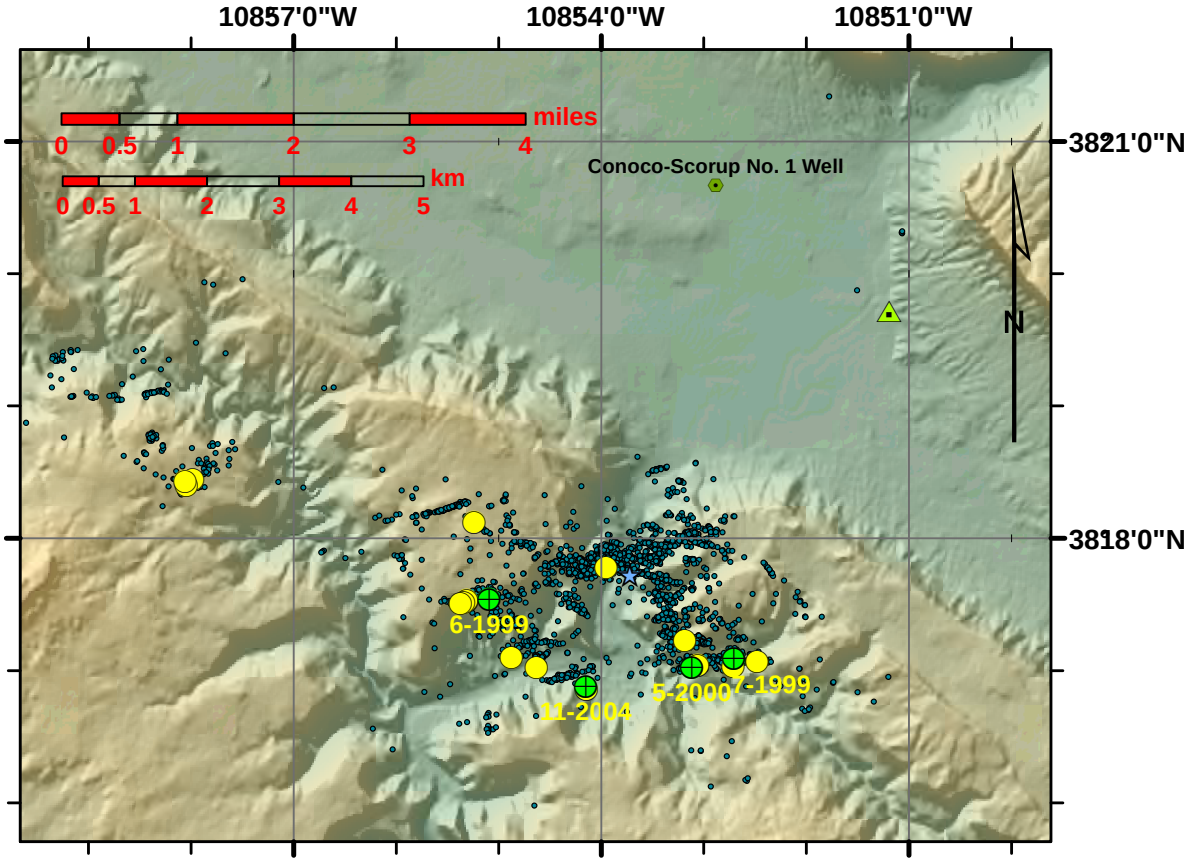

*Figure 1-9 Epicentral Locations of Magnitude **M**2.5 or Greater Events at Paradox. Circles with plus signs are the four largest events, the events with magnitude **M**3.5 or greater, and are annotated by the date of their occurrence. Dotted triangle in middle of Paradox Valley is strong motion instrument at PVU's extraction well field.*

microgal (1 microgal = 10^{-6} gal and 1 gal = 1 cm/s^2; the Earth's gravitation acceleration is 980 gal). With this external force acting on the Earth, one question that arises in seismology is whether or not earthtides affect stress across faults and can trigger earthquakes. Seismologist now know that earthtides do not normally trigger earthquakes. However, the unusual (e.g., fluid-induced) characteristics of earthquakes at Paradox compared to traditional earthquakes and the existence of a large reservoir of injectate caused us to reexamine the question of whether earthtides could be triggering any of the Paradox events. To answer this question we show **Figure 1-12**, a plot of the Sun-Moon earthtides (solid) on which is superimposed occurrences of induced earthquakes (diamonds) for August 2003. The data in **Figure 1-12** are typical of all earthtides-Paradox-event-occurrence data which show that the events at Paradox do not correlate with any phase or phases within the earthtide cycles. If the event-earthtides data did correlate then the occurrence data

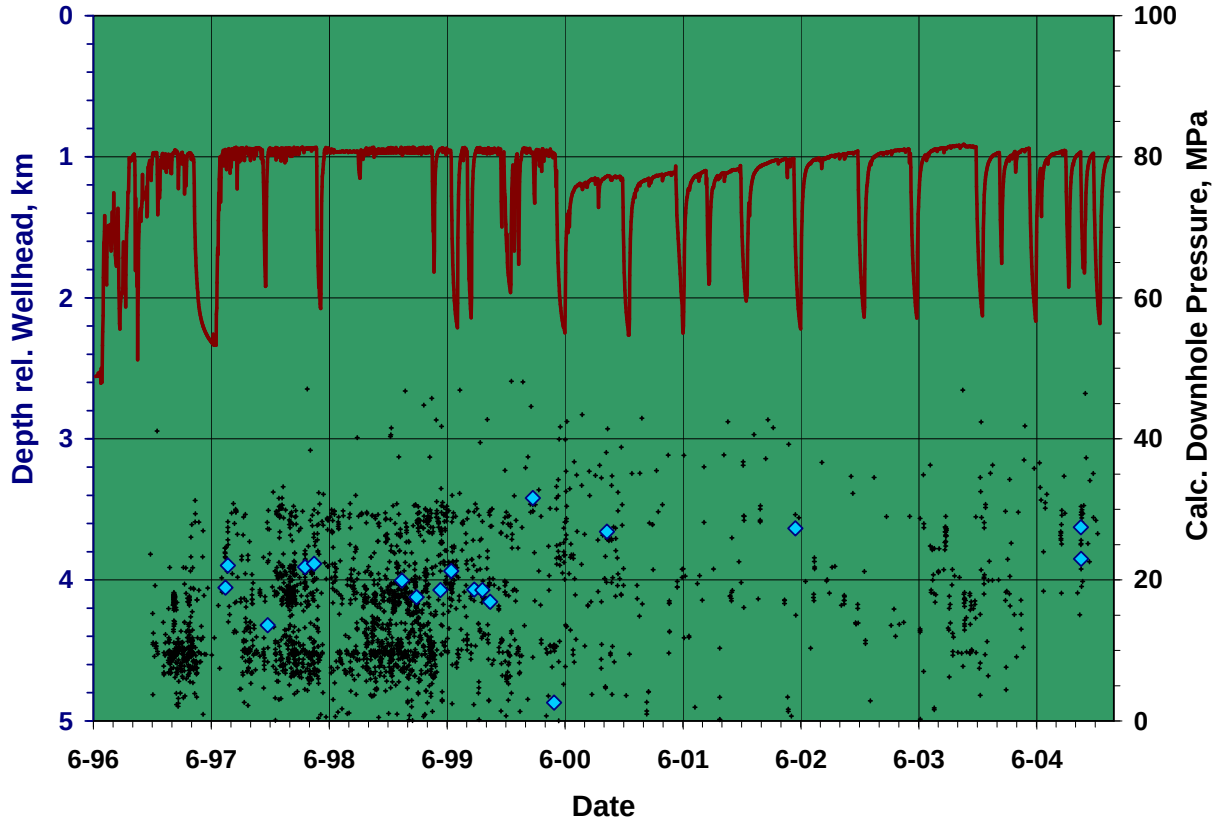

Figure 1-10 Depth of Magnitude M2.5 or Greater Events (blue diamonds) Relative to Injection Wellhead, Calculated Downhole Pressure, and Depths of All Events (black +'s) versus Time.

would not be randomly occurring within the various phases of the earthtides.

1.3 Cumulative Findings

Throughout the continuous pumping, beginning in 1996, the nominal injection pressure at PVU exceeds fracture pressure of the injection reservoir.

The initial induced seismicity was probably due to injectate or connate fluids reducing the friction across faults, liberating pre-existing, *in situ* tectonic stress across the faults. However, some fraction of the later seismicity may also result from inflation by the injectate and the displaced connate fluids changing the *in situ* stresses.

The induced seismicity at Paradox illuminates an extensive, non-symmetric, connected network of fractures, faults, joints, etc. and does not demonstrate the traditional hydraulic fracture picture of two, vertical, symmetric fractures emanating from opposite sides of the

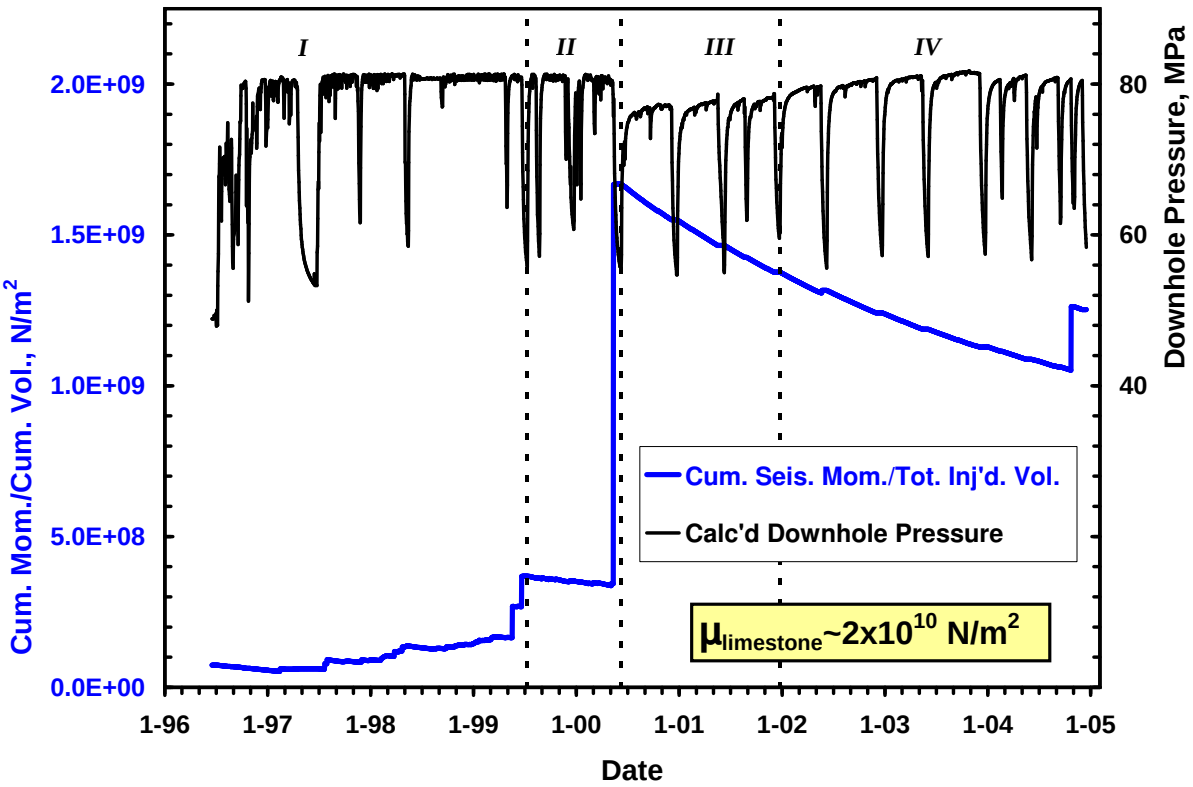

Figure 1-11 Ratio of Cumulative Seismic Moment to Cumulative Injected Volume (blue) and Calculated Downhole Pressure versus Time and versus Injection Phase (Roman numerals). McGarr (1976) posits that the moment to volume ratio in some instances will approximate the rock shear modulus (Greek letter mu with "limestone" subscript).

injection well.

Surface-recorded seismic events are radiated from shear slip on pre-existing faults, joints, or other planes of weakness, not tensile or "new-fracture" openings.

Injection has induced two distinct seismic event zones: a primary zone, asymmetrically surrounding the well to a maximum radial distance of ~3+ km and a secondary zone, centered~8 km to the northwest of the injection well. The second zone lies along the trend of the local fault system, the Wray Mesa system, from the injection well. The primary zone covers a reservoir of between 20 and 30 cubic kilometers

Based on extrapolation of the PVSN data and comparison with data from injection sites that were monitored with *in situ* instruments, our best estimate indicates PVU has induced ~2 million events with magnitudes **M**-3.0 or greater. The smallest events probably include

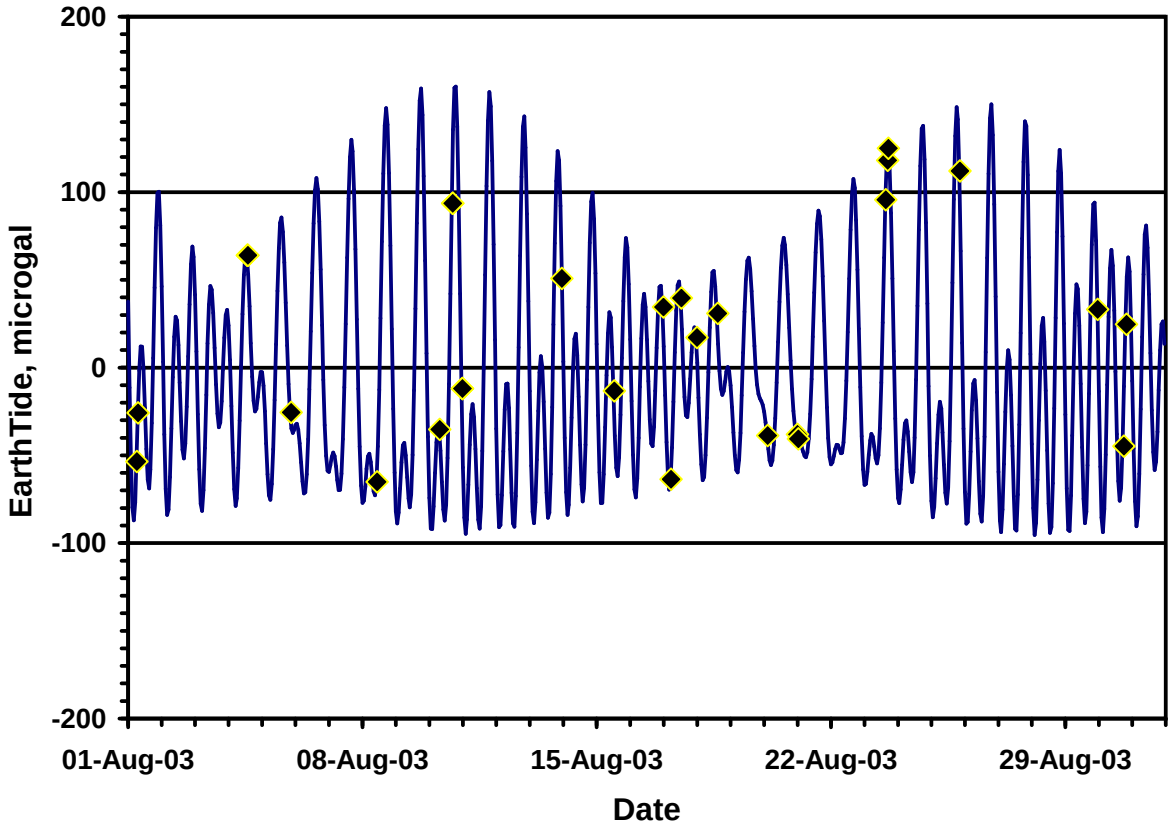

Figure 1-12 Earthtides (i.e., Gravitation Acceleration Potential) due to Sun-Moon System (solid) and Occurrence of Earthquakes (diamonds) at Paradox During August 2003 Superimposed on Earthtide Curves.

both shear and tensile (i.e., crack-opening) events. Being a surface array with its closest instrument ~4 km from the downhole injection interval, PVSN's sensitivity limit is approximately **M**0.0. Thus, PVSN probably only records ~0.1% of the events PVU induces.

More than 99.9% of the over 4,100 surface-recorded events induced at the Paradox Valley injection since 1991 have magnitudes less than **M**2.0. (Human detection threshold ~ **M**2.6.); ~15 events have been felt.

The largest seismic event, an **M**4.3 in May 2000, occurred after ~4 years of continuous injecting.

The first seismic event induced by continuous pumping occurred 111 days after continuous pumping began in late July 1996. During the 7 inject test (1991-95), seismic activity began the same day or within a few days of the onset of injection.

The rate of seismicity is not uniform; there are single, multi-day, and multi-week quiet periods and multi-hour to multi-week active periods.

Spatially, the seismicity occurs as isolated events and occasional swarms; swarms can occur over hours to days in a single location.

The subclass of seismic swarms at Paradox associated with one, large event sometimes show some smaller foreshocks and a few smaller aftershocks or one large event followed by aftershocks.

One seismic zone/swarm region has shown a weak correlation with large-scale pressure changes and is possibly triggered only after pressure exceeds a threshold.

The seismicity occurs within the interior and on the border of the existing seismogenic zones; since about mid-1999, the expansion of the seismogenic zones seems negligible.

By the end of 2004, PVU has injected ~0.004 cubic kilometers of injectate. Since the injectate invasion, increases the connate fluid pressure, the volumetric extent of the injectate is probably less than the volumetric extent defined by the seismicity.

Seismic event are vertically contained between ~2.5 km and ~6 km below the wellhead.

The epicenters group into lineaments that illustrate the secondary fracture and fault network of the Wray Mesa. The alignment of the epicenter lineaments imply the locations of the major, through-going faults of the Wray Mesa system.

The major faults of the Wray Mesa fault system align with the principal stress direction, showing only minor, if any, surface-recordable seismicity. However, these faults align with the predicted hydraulic gradient of the region and, most likely, act as fluid conduits. The location and activation of the secondary seismic zone confirms the fluid-conduit model of these faults.

The fault-planes defined by focal mechanism solutions (i.e., moment tensors) align with the predicted (principle) shear planes and with the secondary faults and fractures of the Wray Mesa.

The 20-day shut down periods relax the *in situ* stress state, resulting in a reduced proclivity for large events.

Since 2002, the increased percentage of Paradox Valley Brine in the injectate has not directly affected seismicity. It has increased the bottom-hole pressure, slightly, due to increased specific gravity of the injectate.

The storage of injectate must be facilitated by existing pore space and by the injection pressure creating new (pore or fracture) volume, since injection can hydraulically fracture the rock matrix; the identified primary and secondary faults and fractures of the Wray Mesa system can only accommodate a few percent of the injectate volume.

The *b*-value, a parameter relating the number of seismic events and the size of events has been altered by the changes in injection phases.

1.4 Acknowledgements

This study and the continuous operation of the Paradox Valley Seismic Network are made possible through the continued and generous support of Andy Nicholas, Project Manager at the Paradox Valley Unit, Colorado. We are greatly appreciative. In addition, Dee Overturf and Tom Bice (US Geological Survey, Denver) provided outstanding field support throughout the history of this project. Rick Martin, US Bureau of Reclamation, Denver (Reclamation), developed and installed PVSN and recognized many of the potential issues during early stages of the project. Chris Wood (Reclamation) developed software. Ute Vetter (formerly with Reclamation) provided technical support. Over the history of this project, we have benefitted from stimulating discussions with Roger Denlinger, Evelyn Roeloffs, Steve Hickman, Art McGarr (all at the US Geological Survey), Jim Bundy (Subsurface Technology, Inc.) and Ivan Wong (URS Corporation).

2.0 LOCAL SETTING

The Paradox Valley Unit is located in western Montrose County approximately 90 km southwest of Grand Junction, CO and 16 km east of the Colorado-Utah border. Paradox Valley is about 40 km long on a N55^{o}W axis and from 5 to 10 km wide (**Figure 2-1**, **Figure 2-2** & **Figure 2-3**). The most prominent local feature is the LaSal Mountains in the Manti-LaSal National Forest, which rise to an elevation of about 3.7 km above msl and border Paradox Valley on the northwest. Paradox Valley has a relatively flat floor enclosed by steep walls of sandstone. Elevations vary from about 1.5 km above mean sea level (msl) in the valley to slightly more than 2.0 km above msl along the valley rim.

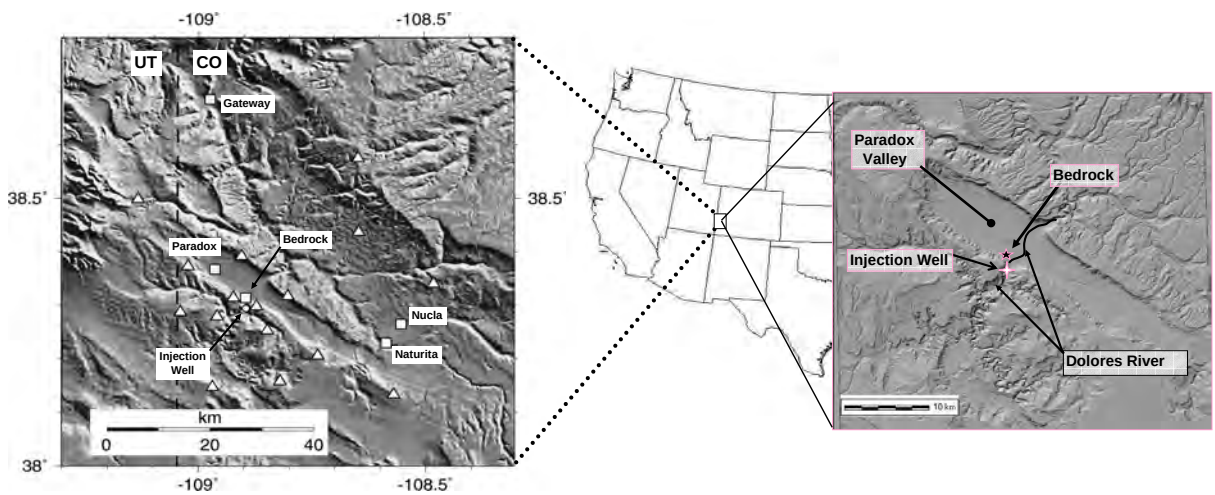

Figure 2-1 Location Map of Paradox Valley Unit, Dolores River, and Local Topography. See Figure 2-2 for expanded version of map.

Paradox Valley is one of five northwest-striking, collapsed diapiric salt anticlines in southwestern Colorado and southeastern Utah. The formation of these anticlines began about 250 mya when the emergence of mountainous uplifts placed intensive lateral stresses on the intervening sedimentary formations, causing faulting and fracturing along weak axial zones. Subsequently the stresses relaxed and combined with the weight of overlaying strata forced a deeply buried, salt-rich layer to flow upward into the faulted area creating the anticline. As pressures eased, the crest of the anticline gradually dropped downward into fault blocks. That and subsequent erosion created Par-

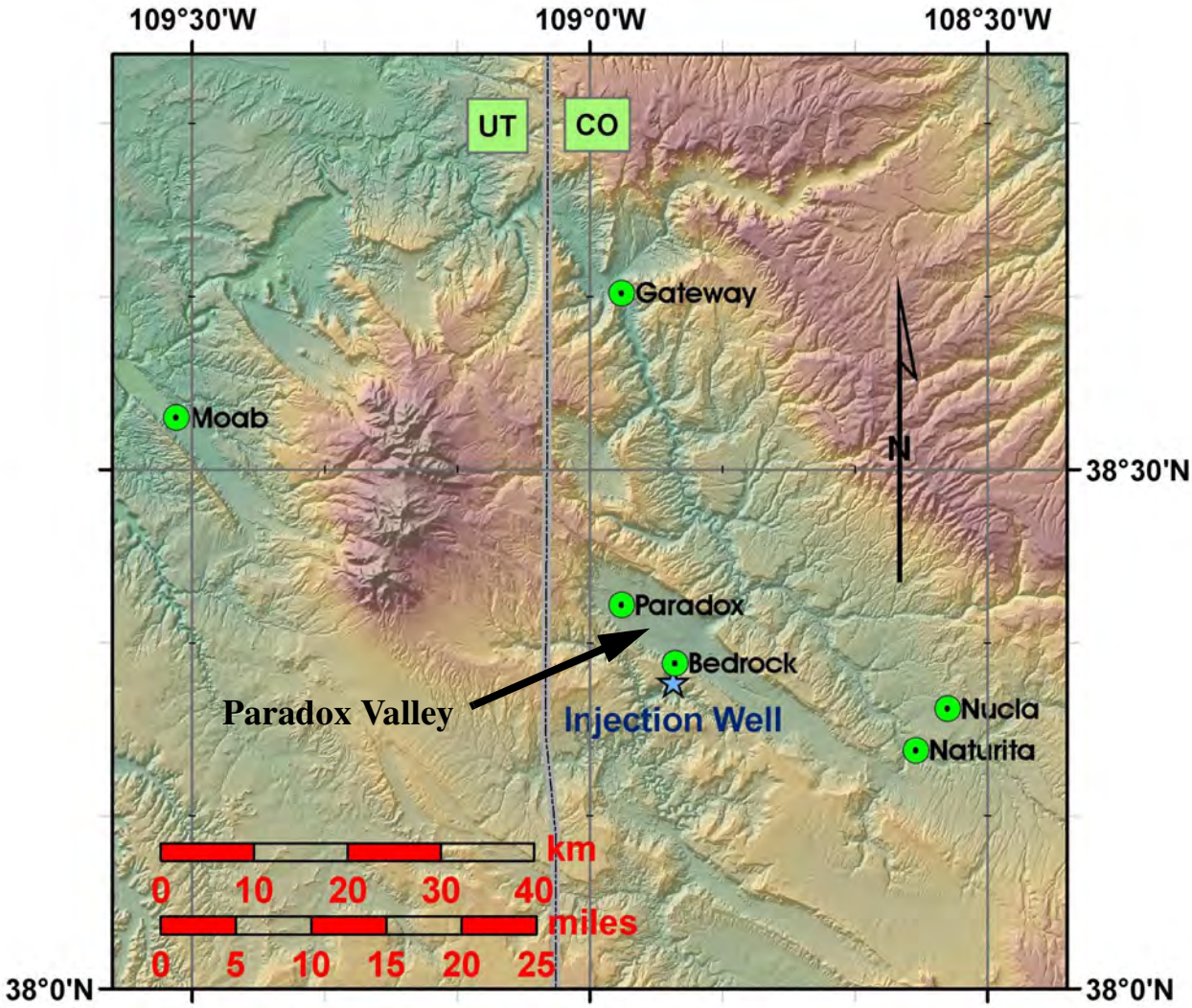

Figure 2-2 Local Topographic Setting of PVU Injection Well, Paradox Valley, Local and Regional Municipalities.

adox Valley. Currently, the Dolores River flows across the strike (i.e., axis) of the valley near Bedrock, CO (**Figure 2-2** and **Figure 2-3**).

The Dolores River originates in the San Juan Mountains southwest of Paradox Valley in southwest Colorado and flows generally north, northwest for about 300 km to Paradox Valley and another 110 km north, northwest to its confluence with the Colorado River northeast of Moab, Utah. Small tributaries in the unit area include La Sal Creek, which enters from the northwest about 8 km upstream from Paradox Valley, and West and East Paradox Creeks, which enter from the northwest and southeast within the valley. East Paradox Creek is intermittent, however, and

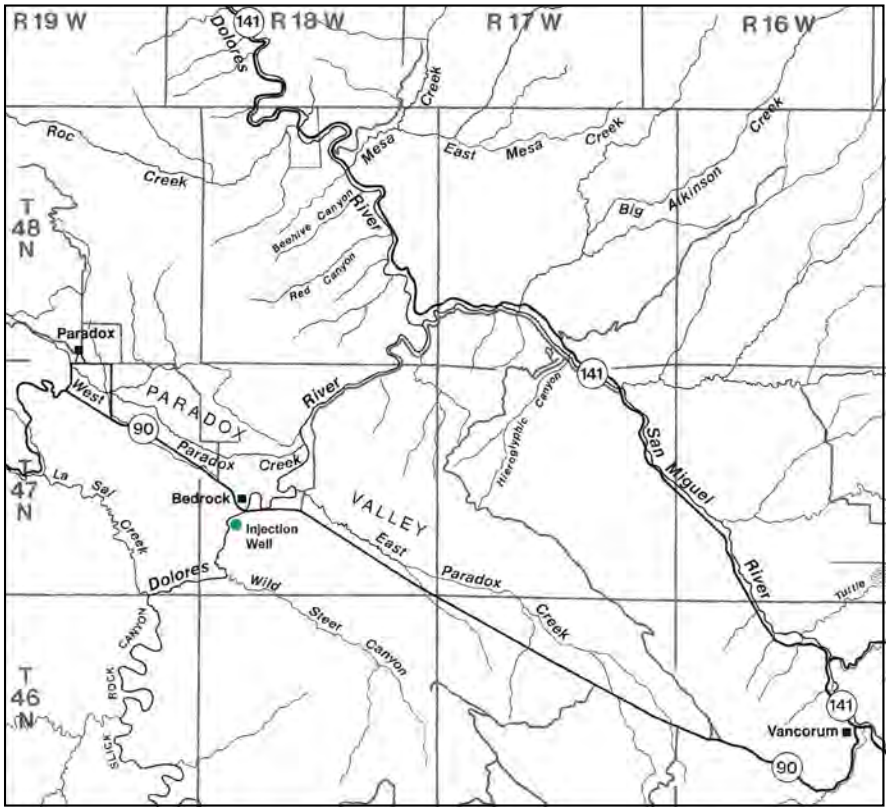

Figure 2-3 Paradox Valley Unit Injection Well and Local Geography. Figure is adapted from Parker (1992). Each square is approximately 10 km by 10 km

has essentially no effect on the river flow. Over its path through Paradox Valley, the Dolores can pick up more than 180,000 metric tonnes (200,000 standard tons) of salts annually, primarily from brine-saturated groundwater, (called Paradox Valley Brine or PVB), percolating through seeps and springs in the salt body and into the Dolores. There are two general types of seeps and springs: brackish water with total dissolved solids (tds) varying from about 1,500 milligrams per liter (mg/l) to 4,000 mg/l and the Paradox Valley Brine with ~260,000 mg/l. (For reference, the EPA defines fresh water as tds less than between 400 mg/l and 500 mg/l.) Water pumped from the 9 extraction wells near the river has a salinity of ~260,000 mg/l (260,000 mg/l or ppm is saturation, the maximum salt carrying capacity of fresh water). This brine, which is nearly eight times the salinity of ocean water, consists mostly of sodium and chloride, with much smaller amounts of sulfate, potassium, magnesium, calcium, and bicarbonate. Heavy metals, particularly iron and

lead, and non-radioactive strontium are also present in small amounts. Noticeable amounts of hydrogen sulfide gas are released as the brine surfaces, creating a noxious odor.

2.1 PVU Salinity Control Well No. 1

The PVU Salinity Control Well No. 1 (**Figure 2-4**) was completed in 1987 at a total depth (t.d.) of

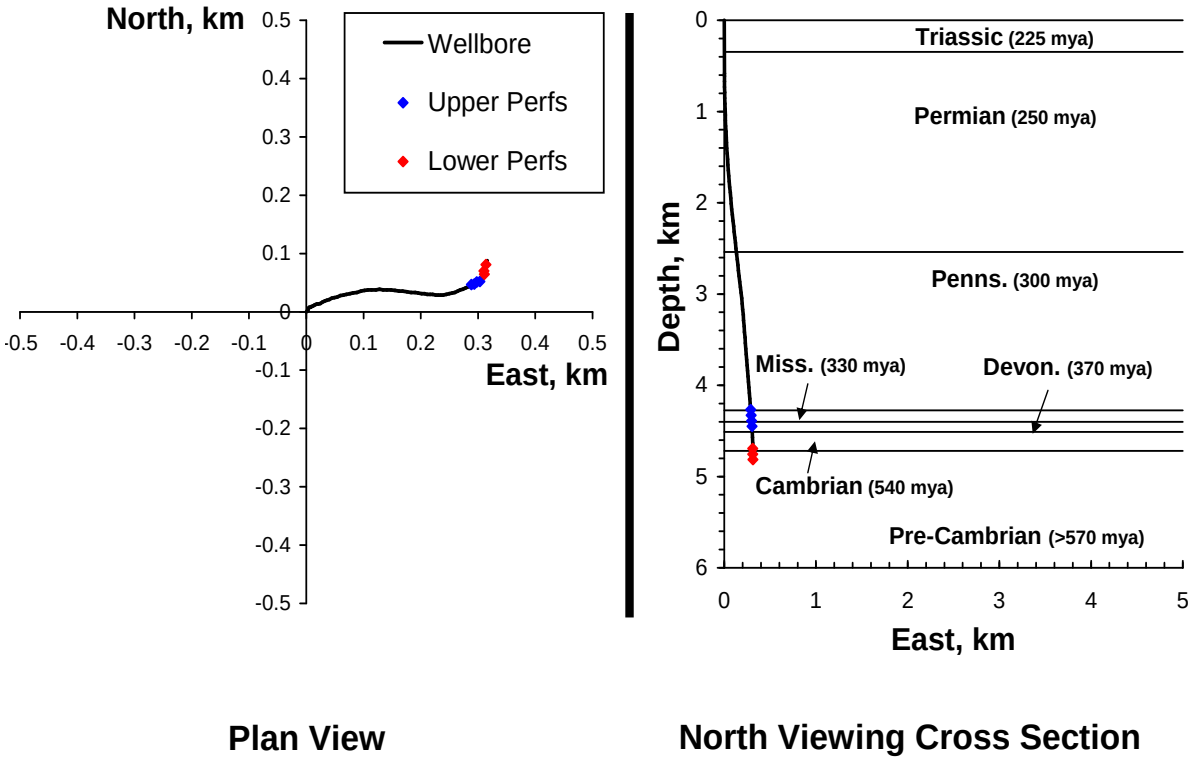

Figure 2-4 Plan View and North-Viewing Cross Section of PVU Injection Well: Salinity Control Well No. 1. Figures include the near-wellbore stratigraphic column, based on well logging of Salinity Control Well No. 1, and locations of casing perforations.

4.88 km (16,000 ft). The well was built to EPA Underground Injection Code (UIC) Class I standards ("Isolate hazardous, industrial and municipal wastes through deep injection"), but was permitted in 1995 by EPA as a Class V disposal well ("Manage the shallow injection of non-hazardous fluids"). The well is located in SW SE section 30, township 47N, range 18 W Paradox Valley, Montrose County, CO. Its latitude and longitude are 38° 17' 43. 62" N and 108° 53' 43.32" W, respectively. The wellhead elevation (i.e., ground surface) is 1.523 km (4,996 ft) above

mean sea level. The Kelly bushing of the well, a marker frequently used by drillers and well loggers, is listed at 9.8 m (32 ft) above ground surface.

The well penetrates Triassic rock at the surface through Precambrian rock at t.d. and has a minor drift to the east and slightly to the north. Log-based, near-wellbore stratigraphy, the perforation intervals, and a plan view of the well are shown in **Figure 2-4**. Based on interpretation of regional core and log data, the Mississippian Leadville carbonate was selected as the prime injection zone with the upper Precambrian as a secondary zone (Bremkamp and Harr, 1988). The well casing of PVU No. 1, Inconel (C-276, a nickel-molybdenum-chromium alloy), was perforated at ~20 perforations/m in two major intervals between 4.3 km and 4.8 km.

2.2 Wray Mesa Fault and Fracture System

The Wray Mesa fault system has been active creating an extensive fracture network. PVU Salinity Control Well No. 1 was sited so that injectate would intersect the generally NW-SE trending faults of the Wray Mesa and its fracture system. The main trend of the Wray Mesa fault system (N55^{o}W) parallels the general trend of Paradox Valley (**Figure 2-2**). In their 1988 report, Bremkamp and Harr predicted that the PVU injectate would move in the direction of least reservoir resistance and lowest hydrostatic pressure. This direction is to the northwest and up dip along the fracture permeability of the Wray Mesa system. Our findings, as discussed below and based on injection-induced, seismic source locations, support their prediction. **Figure 2-5** shows Bremkamp and Harr's (1988) original northeast-southwest cross section of Paradox Valley and bordering region. Note the Wray Mesa Fault system. The Bremkamp and Harr's (1988) cross section runs through the injection well and shows their original interpretation of the Wray Mesa faults. [A note of caution: the surface topography in **Figure 2-5** west of the salt anticline (i.e., Paradox Valley) appears to be at the same level as the valley. However, the actual surface west of the valley shows a sharp elevation increase to plateaus (**Figure 2-1** and **Figure 2-2**). This discrepancy occurs because the survey used by Bremkamp and Harr did not follow the plateau topography, but instead followed the incised canyon of the Dolores River before using the primary surface topography of the plateaus bordering Paradox Valley.]

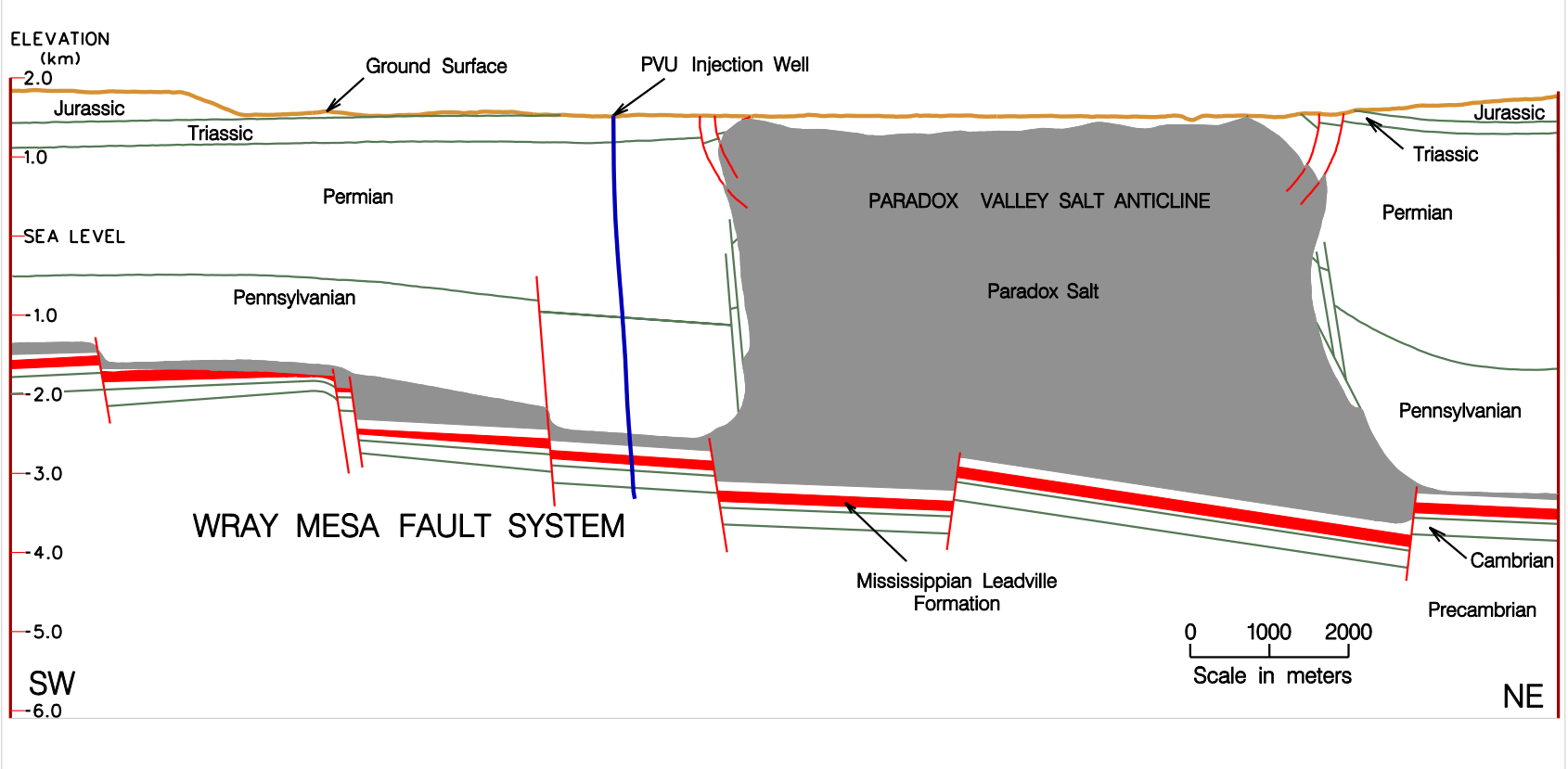

Figure 2-5 Bremkamp and Harr's (1988) Northeast-Southwest Cross Section Through Paradox Valley and its Bordering Region. Cross Section runs through the injection well and surface topography reflects surveyors path up the canyon of the Dolores River and not the local mesa topography.

3.0 PARADOX VALLEY SEISMIC NETWORK

3.1 Paradox Valley Seismic Network

Paradox Valley Seismic Network (PVSN) is operated by the Bureau of Reclamation, Seismotectonics Group out of the Denver Federal Center and provides seismograph coverage for roughly 5500 km^2 of the Colorado Plateau centered on the intersection of the Dolores River and the west side of Paradox Valley (**Figure 3-1**). PVSN was installed in late 1983 and has operated continu-

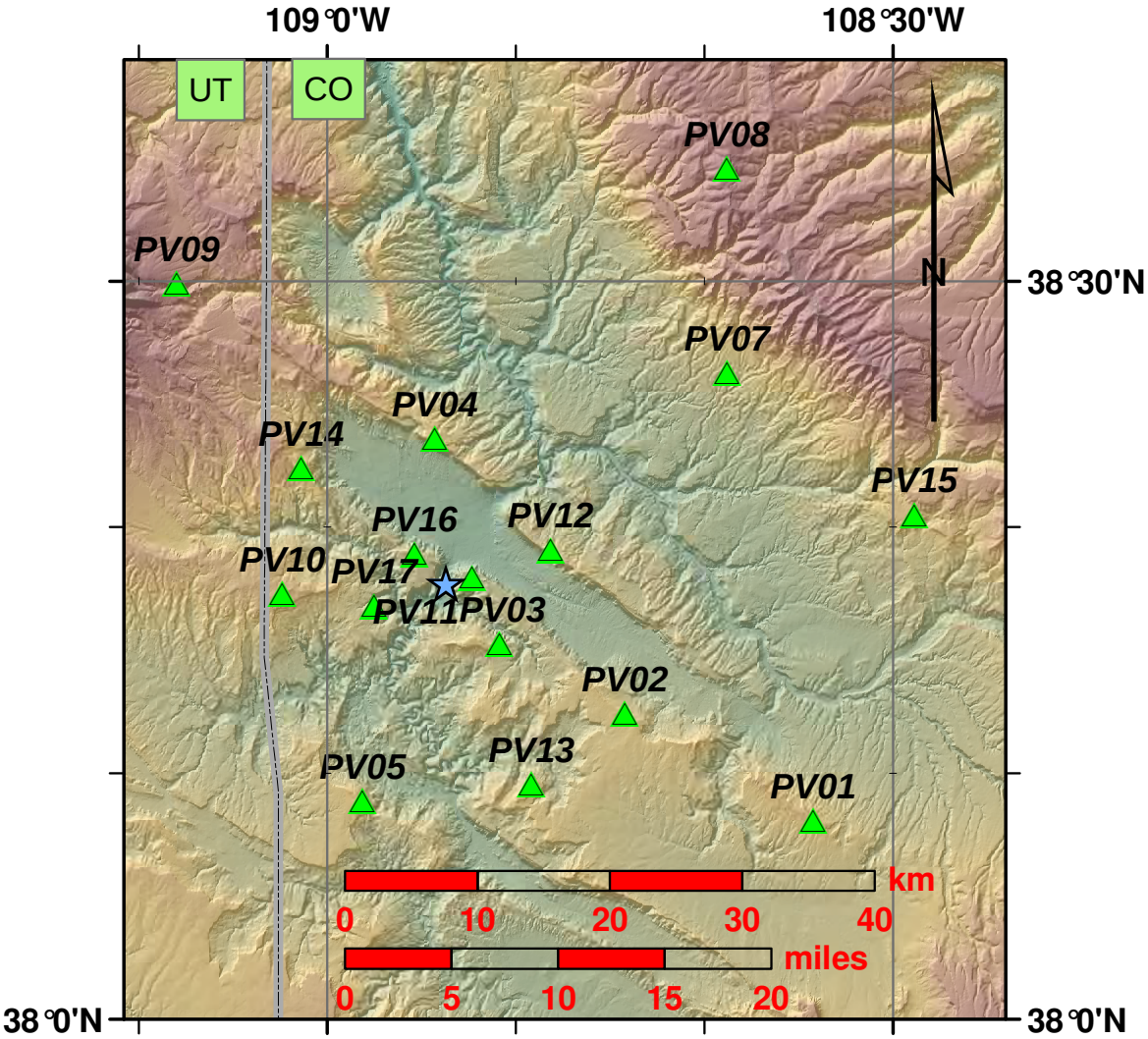

Figure 3-1 Regional Topography, Locations, and Designations of Paradox Valley Seismic Network Stations (triangles) and Injection Well (star).

ously since that time. For each station shown in **Figure 3-1**, **Table 3-1** gives station name, latitude, longitude, elevation, and operational parameters ; **Table 3-2** gives the legal description of

Table 3-1 PVSN Station Locations and Characteristics

Station Designation	Station Name	Latitude deg., N	Longitude deg., W	Elevation m, msl	Date Installed	Gain, dB/ Filters, Hz
PV01	The Burn	38.13	108.57	2190	5/83	78 / 0.2-25
PV02	Monogram Mesa	38.21	108.74	2158	5/83	78 / 0.2-25
PV03	Wild Steer	38.25	108.85	1975	5/83	78 / 0.2-25
PV04	Carpenter Flats	38.39	108.91	2152	5/83	78 / 0.2-25
PV05	E. Island Mesa	38.15	108.97	2150	5/83	78 / 0.2-25
PV07	Long Mesa	38.44	108.65	2001	6/83	78 / 0.2-25
PV08	Uncompahgre Butte	38.58	108.65	2941	6/83	78 / 0.2-25
PV09	North LaSalle	38.50	109.13	2640	6/83	78 / 0.2-25
PV10	Wray Mesa	38.29	109.04	2300	6/83	78 / 0.2-25
PV11Z	Davis Mesa	38.30	108.87	1881	12/89	78 / 0.2-25
PV11N	Davis Mesa	38.30	108.87	1881	12/89	60 / 0.2-25
PV11E	Davis Mesa	38.30	108.87	1881	12/89	60 / 0.2-25
PV12	Saucer Basin	38.32	108.80	2091	12/89	78 / 0.2-25
PV13	Radium Mtn	38.16	108.82	2158	12/89	78 / 0.2-25
PV14	Lion Creek	38.37	109.02	2240	12/89	78 / 0.2-25
PV15	Pinto Mesa	38.34	108.48	2280	6/95	78 / 0.2-25
PV16Z	Nyswonger Mesa	38.32	108.92	2045	7/99	78 / 0.2-25
PV16N	Nyswonger Mesa	38.32	108.92	2045	7/99	60 / 0.2-25
PV16E	Nyswonger Mesa	38.32	108.92	2045	7/99	60 / 0.2-25
PV17	Wray Mesa East	38.28	108.96	1985	tbd	--

Notes: Elevations are relative to mean sea level (msl), the surface elevation of the injection well is 1540 m above msl. Stations designated with a,"Z", "N", or "E" suffix stand for instruments that sense motion in the vertical, north-south, or east-west directions, respectively. Stations without a suffix have vertical-only motion sensors.

the station locations. Within the limits of terrain accessibility and radio telemetry linkage, the net-

Table 3-2 PVSN Sites - Legal Description

Station Desig.	Geographic Name	Legal Description
PV01	The Burn	T45N R15W S19 C,NM
PV02	Monogram Mesa	T46N R17W S27 C,NM
PV03	Wild Steer	T46N R18W S10 C,NM
PV04	Carpenter Flats	T48N R18W S30 C,NM
PV05	E. Island Mesa	T45N R19W S16 C,NM
PV07	Long Mesa	T48N R16W S9 C,NM
PV08	Uncompahgre Butte	T50N R16W S22 C,NM
PV09	North LaSalle	T26S R25E S35 U,SLC
PV10	Wray Mesa	T47N R20W S35 C,NM
PV11	Davis Mesa	T47N R18W S29 C,NM
PV12	Saucer Basin	T47N R18W S24 C,NM
PV13	Radium Mtn	T45N R18W S14 C,NM
PV14	Lion Creek	T48N R20W S36 C,NM
PV15	Pinto Mesa	T47N R15W S12 C,NM
PV16	Nyswonger Mesa	T47N R19W S24 C,NM
PV17	Wray Mesa East	T47N R19W S34 C,NM

work is loosely arranged in two concentric rings centered on the brine injection well. The outer ring diameter is approximately 80 km.

Each PVSN station consists of a ground motion sensor or sensors (i.e., seismometer), amplifier, voltage control oscillator (VCO), low power telemetry radio, solar panel, and broadcast tower with antenna. All systems are powered by solar-recharged batteries. Most of the stations operate single, vertical-motion-only seismometers. The Davis Mesa and Nyswonger Mesa stations (PV11 and PV16, respectively), operate three-component seismometers, recording vertical, east-west, and north-south motion. When completed, PV17 will also be a three-component site.

The seismometers at all existing sites are Teledyne Geotech Model S-13's, a high-quality, reliable, ground velocity measuring instrument with flat response between 1 and 20 Hz. At all sites, the amplifiers and VCO's are also Teledyne Geotech (model 4250). The pass band (i.e. filters) of each field amplifier is set to minimize long-period noise (**Table 3-1**). **Figure 3-2** shows the typical

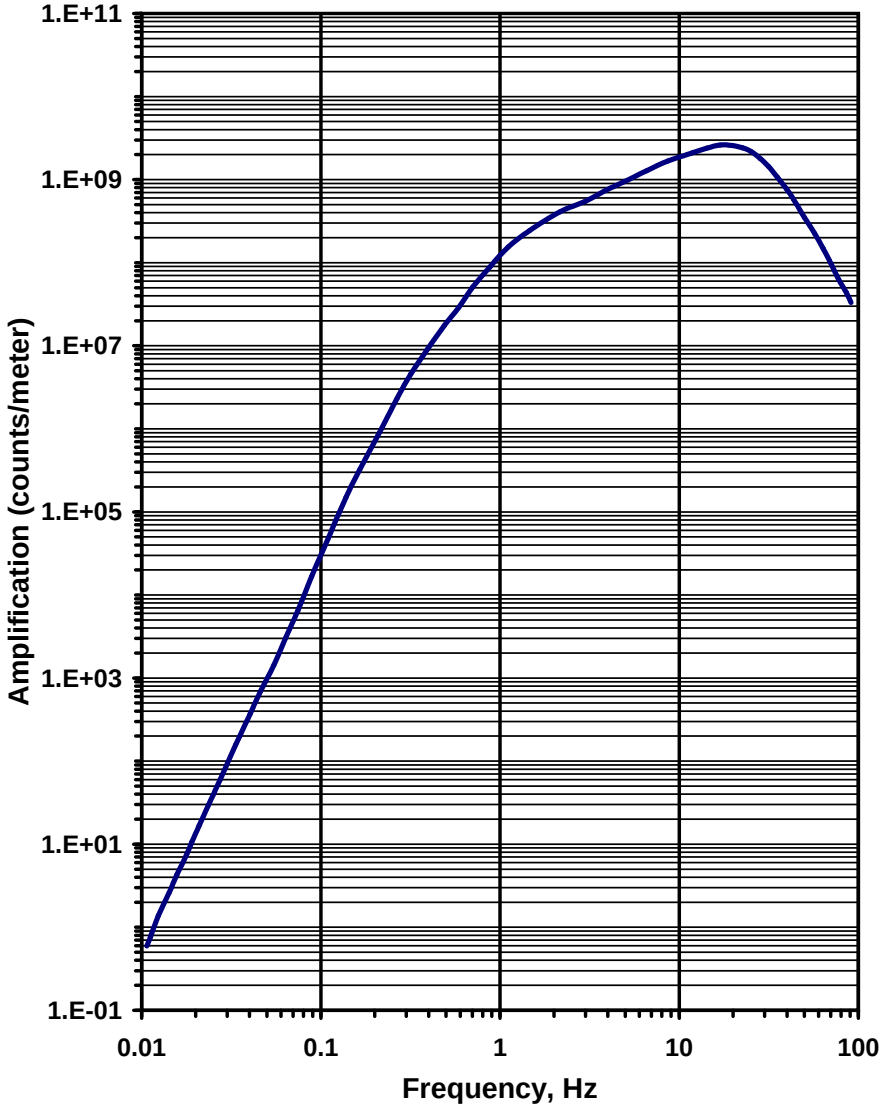

Figure 3-2 Typical response (i.e., amplification) of a vertical-component Teledyne Geotech S13 seismometer and electronics at each PVSN site.

frequency response/amplification curve of the full electronics and seismometer system at each PVSN site. Nominal gain is 48 dB for the curve shown, Teledyne Geotech model 42.5 amplifier/ voltage control oscillator (VCO) and model 4612 discriminator. Damping is 71% critical damping.

3.2 Paradox Data Digitalization and Associated Model

PVSN data telemetry begins with continuous analog signals broadcast from each seismometer site to a receiver in Nucla, CO. At Nucla, these signals are each digitized at a frequency of 100 samples per second (Hz) and then are transmitted as digital data to the Denver Federal Center for analysis. All signals received by PVSN are comprised of a band of frequency components. Based on the Nyquist Theorem, any component of a digitized signal with frequencies higher than half the sampling frequency will be lost by the digitizing process. All components below half the sampling frequency are captured. The question arises as to whether 100 Hz is a high enough sampling frequency to capture the information within the signal or could vital information be lost by the digitalization of the data at Paradox. To show that information is not being lost, we constructed a mathematical model of the expected frequency components of a typical signal. To create this model, we used standard, accepted conventions from earthquake seismology. The mathematics of this model is beyond the scope of this report. However, we heuristically explain below how we created the model, its assumptions and results, and demonstrate that 100-Hz sampling does not compromise (i.e., lose) the signal information from the Paradox data.

Figure 3-3 shows a model that progressively includes phenomenon that affect the data from events generated by Paradox injection. The figure shows the amplitude of the frequency components of a typical signal at various stages of its evolution from creation, propagation through the earth and then recording by a typical PVSN instrument. Each stage selectively affects the amplitude (i.e., the energy content) of the signal coming into and leaving that stage. The output of a stage is the input of the next stage. **Figure 3-3(a)** shows a typical source spectrum (i.e., the frequency components) from 3 different magnitude earthquakes (i.e., **M**0, **M**2, **M**4) using the single-corner ω^2 Brune model (Brune, 1970, 1971). Note that each spectrum runs from 0.1 Hz to 500 Hz and shows significant seismic energy across this passband. This signal contains all the source information that can be gleaned from seismic analysis. **Figure 3-3(b)** shows the spectrum after the seismic energy has propagated through a generalized Earth model (modeled propagation distance = 8 km). Propagating through the earth causes some loss of energy (i.e., called “path attenuation” with assumed quality factor, Q = 300; Lee and Wallace, 1995), as shown by the reduced amplitudes of these spectrum. **Figure 3-3(c)** shows the next stage of the model, energy loss by

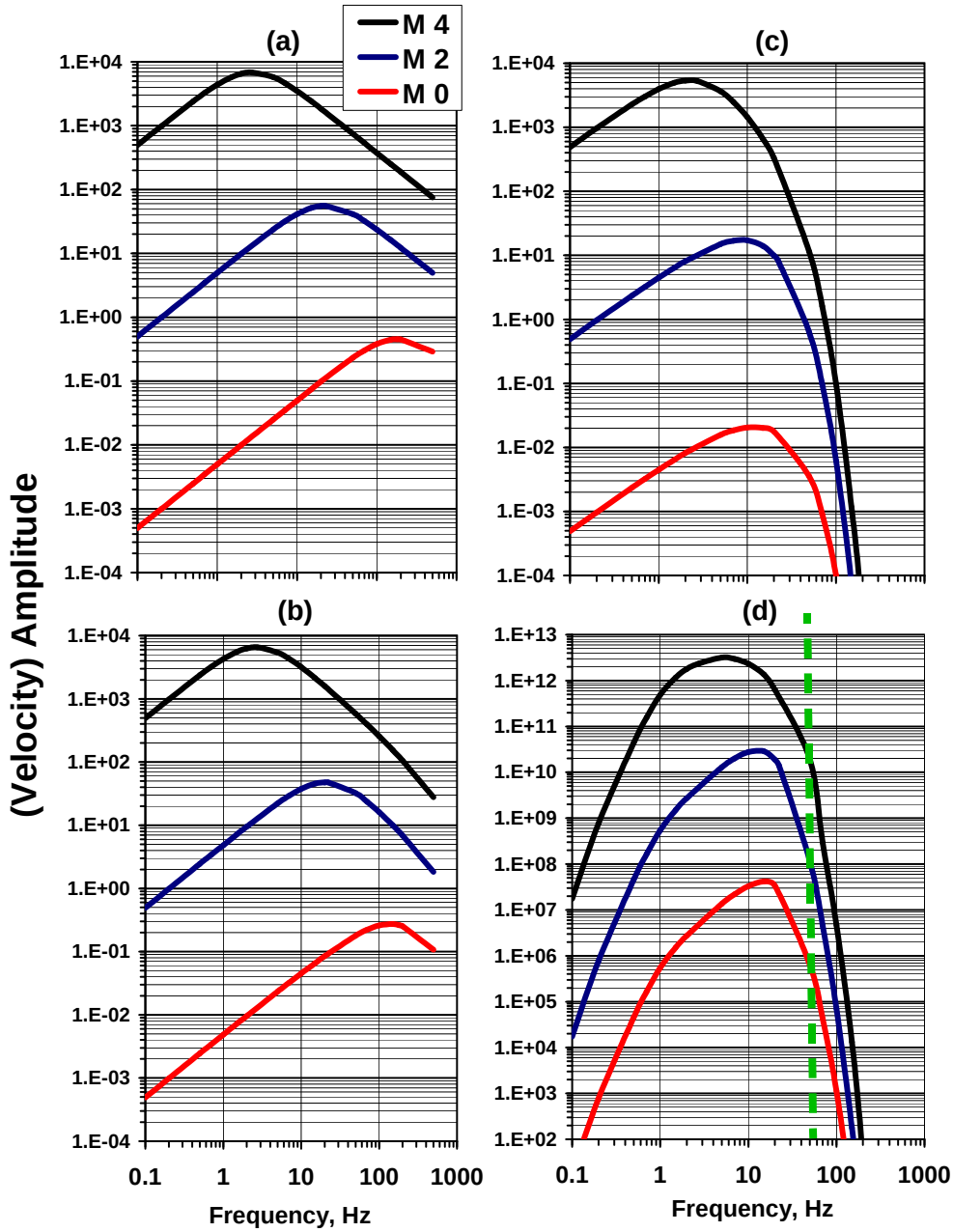

*Figure 3-3 Signal Spectrum for Magnitude **M** 0, 2, and 4 Events. Panel (a) shows source spectrum based on an ω^2 Brune Model; (b) shows the Brune Model combined with path attenuation; (c) shows the Brune Model and path attenuation combined with near-surface attenuation; and (d) shows the Brune Model, path attenuation and near-surface attenuation combined with the PVSN system response (Figure 3-2). Dashed (green) line in (d) is 50 Hz, half the 100-Hz digitizing frequency of the Paradox data.*

"near-surface attenuation" (i.e., called "kappa" with assumed kappa = 0.025 s; Anderson and Hough, 1984) caused as the signal reaches the Earth's surface, the location of the PVSN seismom-

etry. Near-surface attenuation is a significant and unavoidable factor, as long as the seismometers are at the surface. Finally **Figure 3-3(d)** shows the effect of the PVSN system response (**Figure 3-2**) to the signal incoming (i.e., source, path-attenuated, plus near-surface attenuated) to the PVSN site seismometer and electronics. **Figure 3-3(d)** models the modeled spectrum or frequency content of the signal that a typical PVSN station would output (i.e., transmit) to Nucla for digitizing at 100-Hz sampling. Note that the portion of the signal in **Figure 3-3(d)** above 50 Hz (i.e. right of the dashed green line) is insignificant compared to the signal below 50 Hz. This model shows, as stated earlier, that 100-Hz digital sampling captures nearly all of the energy (i.e., information) of signals generated at PVSN.

3.3 Telemetry, Software, and Strong Motion Instruments

In October of 2000, Reclamation upgraded the data telemetry system and the detection, location and archiving software (Mahrer et al., 2001). Upgrading the software included adapting, refining, and implementing Earthworm, software developed by the US Geological Survey and used in its seismic arrays.

As noted above, at Nucla, the radio signals from each PVSN site are digitized and transmitted via a digital telephone link to the Bureau of Reclamation processing center at the Denver Federal Center (DFC) in Lakewood, Colorado. At the DFC, Earthworm detects events in the data stream, then classifies, locates, and archives the detected events. Subsequently, each event is re-evaluated by a Bureau of Reclamation seismologist.

In addition to the high-gain PVSN instruments/array noted in **Table 3-1** and **Table 3-2**, PVSN includes two strong-motion, digital-recording instruments (Springnether Force Balance Accelerometers, FBA-23's recorded by Kinemetrics K2 digital data recorders). One is sited near the injection wellhead; the other is at PVU's pumping station (38.33^{o}N 108.85^{o}W). Both instruments are triggered instruments (i.e., they only record ground motion greater than a fixed amplitude) and both have telephone links to the DFC. The data from these instruments are not part of our normal analysis stream, but, if either or both instruments are triggered, their data can be and have been integrated into the analysis. In the May 2000, M4.3 event, the data from these instru-

ments was used for analysis, since the induced ground motion had overdriven the other high-gain PVSN instruments.

3.4 PVSN (Daily-Average) Operational Efficiency

[*Operational Efficiency (OE) is the percentage of data channels online and working, based on 100% being all channels working, everyday for the whole year. The daily-averaged OE is calculated by summing the number of online, working PVSN data channels for each day of the year and dividing that total by 6935 (i.e., 19 channels x 365 days or 366 for leap year), the maximum number of possible data channel days for a year. If DFC witnesses a power failure resulting in the loss of data recording, this is included in the calculation as if all PVSN stations were down for the duration of the power failure. Note also that a data channel may be entered as operating for a fractional part of a day. This can occur because the power at each site is a combination of solar cells (daytime) and batteries (night) and the batteries age and won't accept a full recharge from the solar cells. Thus a site will only be operational during daylight and none or limited hours at night.*]

During 2004, the seismic network and telemetry system operated at 80% efficiency. Previous years averaged about 90% efficiency. **Figure 3-4** shows individual data channel online percentages and the operational efficiency of the whole network ("cumulative") for 2004. In the figure, the suffixes on PV11 and PV16, "V", "N", and "E", correspond to the vertical, north-south, and east-west instruments at these three-component sites, respectively. **Figure 3-5** shows the total number of seismic data channels in operation at any time during 2004. Note that the data drop outs in the figure were caused by short-term power failures and power (maintenance) shut downs at the DFC. Note also that throughout 2004, PV08 and PV14 were offline.

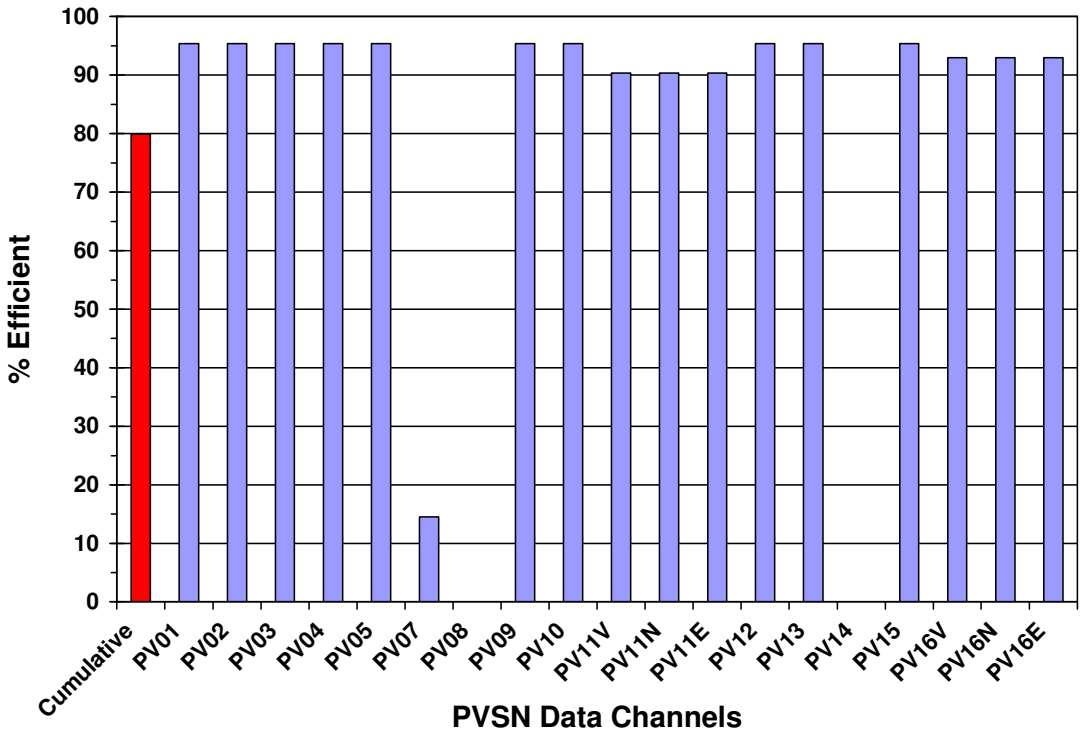

Figure 3-4 PVSN Operational Efficiency: Cumulative (red) and By Individual Data Channel (blue).

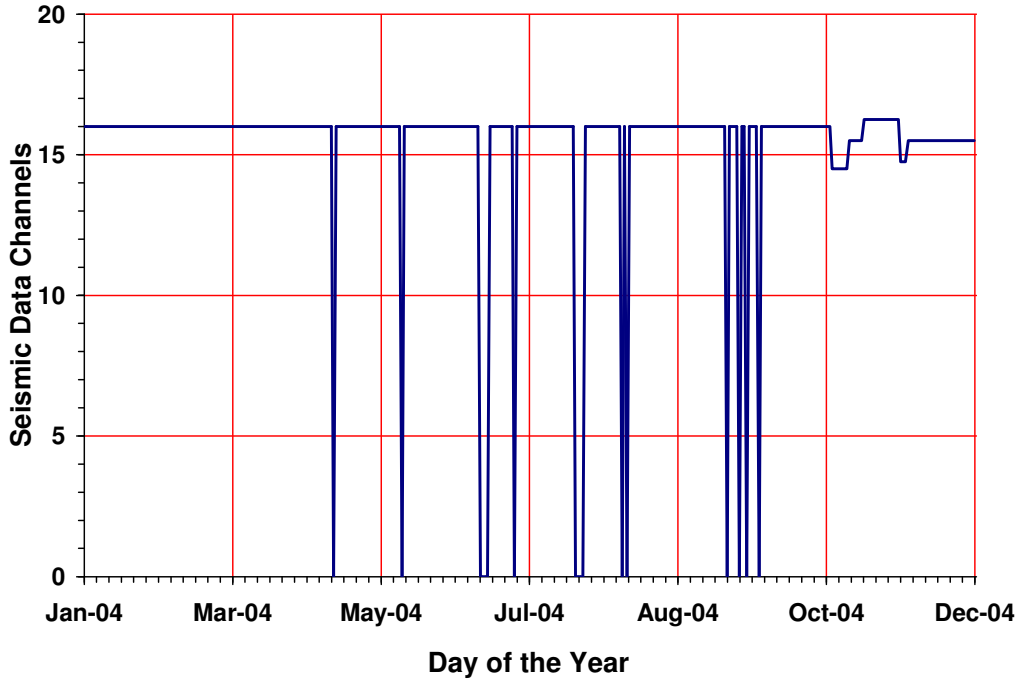

Figure 3-5 PVSN Cumulative Operations, Number of Seismic Data Channels Online in Operation versus Day of the Year.

4.0 PVU INJECTION OPERATIONS

PVU operates the Salinity Control Well No. 1 which is located at 38.2995^{o} N and 108.8953^{o} W along the western boundary of Paradox Valley, approximately 1.5 km up the canyon formed by the Dolores River (**Figure 2-1**, **Figure 2-2** & **Figure 2-3**). As shown in **Figure 2-4**, the well is essentially vertical, deviating only ~0.3 km to the east and slightly to the north over its 4.8+ km depth. **Figure 2-4** also shows the two major perforation intervals of the wellbore casing. The upper perforation interval is within the primary injection target, the Mississippian-aged Leadville Limestone formation.

4.1 PVU Operations by Injection Phase

As noted throughout this report, from 1991 through 1995 PVU pumped a series of 7 injection tests. These tests were conducted to acquire an EPA permit for continuous brine disposal. Following these tests, the EPA granted the permit, and, in May 1996, PVU began continuous injection. Since continuous injection began, PVU has instituted and maintained three major injection changes. Each change was invoked to mitigate the potential for unacceptable seismicity or improve injection economics. Each change was maintained for a sufficient period to be considered a sustained and evaluatable injection period. We chose the nomenclature "*Phase*" for each sustained injection period. We created this distinction to differentiate and evaluate operational parameters and resulting reservoir response(s), including induced seismicity, during the separate phases. Described below are the four injection phases. **Table 4-1** summarizes the injection phases. In the table the averaging of values includes both active pumping and shutdown days.

4.1.1 Phase I - (22-May 1996 through 26-July 1999)

The initial phase, *Phase I*, followed inception and a few months of building up injection pressure; during this phase PVU injected at maximum: ~1290 l/min (~345 gpm) at ~33 MPa (~4,900+ psi) surface pressure which corresponded to ~80 MPa (~11,600 psi) downhole pressure at 4.3 km (14,080 ft) depth. The injectate during *Phase I* was 70% Paradox Valley Brine (PVB), 30% fresh water. Throughout *Phase I*, injection was continuous with the exceptions of unscheduled mainte-

Table 4-1 Phases of Continuous Pumping, Associated Time-Averaged Injection Parameters, and Injection Characteristics

Phases	Approx. Duration	Avg. Wellhead Pressure	Avg. Pressure @ 4,300 m* depth	Avg. Inj. Rate	Injectate: %PVB:% H_2O	Biannual 20-day Shutdown	Approx. No. Recorded Seismic Events***
	days	(MPa)	(MPa)	(l/min)		y/n	
I	1100	29.6	76.7	1029.6	70:30	No	2500
II	332	29.3	76.3	934.6	70:30	Yes	446
III	566	27.5	74.6	732	70:30	Yes	219
IV	1090+**	28.2	77.4	734	100:0	Yes	301

*Depth = Top of the casing perforation interval, i.e., the top of the injection target horizon, the Leadville Limestone, which well testing indicates has the greatest injectivity
**Number includes days through 12/31/04
***Includes all recorded events not only magnitude M>=0, as used in later analysis.
MPa = megapascals, 1.0 MPa = 145 psi, l/min = liter/minute, 1.0 l/min = 0.26 gal/minute

nance and pressure diffusion shut downs. [*Note*: A pressure diffusion shut down is a stoppage of injection because the wellhead pressure is approaching the wellhead safety limit. By shutting down injection and waiting, the pressure reduces to an acceptable margin from the safety limit; the pressure reduction is due to fluid diffusion into the reservoir rock matrix (i.e., diffusing from the pressured fractures and faults into the small fractures and pores of the rock matrix).] During *Phase I*, shut downs ran for minutes, hours, a few days or a few weeks up to a maximum of 71 days in mid 1997; this shut down was needed to replace the injection pumps.

4.1.2 Phase II - (27-July 1999 through 22-June 2000)

Following a magnitude **M**3.5-event in June 1999 and a magnitude **M**3.6 event a month later, in July 1999, PVU augmented injection to include a 20-day shutdown (i.e., “shut-in”) every six months (one in December-January and one in May), but, during injection continued at the same pressure and rate as *Phase I*.

4.1.3 Phase III - (23-June 2000 through 7-January 2002)

Following a magnitude **M**4.3 earthquake in May 2000, the largest to date induced by injection at Paradox, PVU reduced the injection rate ~33% to ~870 l/min (~230 gpm) while maintaining the 70:30 ratio of brine to fresh water and the bi-annual, 20 day shutdowns. The lower injection rate reduced surface pressure about 10%. This change constitutes *Phase III* injection.

4.1.4 Phase IV - (8-January 2002 through the Present)

In January 2002, PVU began *Phase IV*, injecting 100% brine (i.e., PVB) using the *Phase III* injection schedule: ~870 l/min (~230 gpm) and a 20-day shutdown every six months. Since the specific gravity of PVB is ~5% greater than the 70:30 mixture, surface pressures initially decreased while maintaining the same downhole pressure. [Note: At the beginning of *Phase IV*, the surface pressure was ~30 MPa (~4,400 psi), and downhole pressure was ~79 MPa (~11,500 psi). Figures giving injection pressure and injection rates along with induced seismicity per day can be found in chapter **6.0 OBSERVATIONS**.

4.2 PVU Injection History By Year

Table 4-2 summarizes PVU Well No. 1's annual injection history. For expected reader convenience, the values in **Table 4-2** are in standard units, millions of gallons (Mgal) and thousands of tons (ktons).

Table 4-2 Annualized Summary of PVU Injection

Year	Phase	Injectate (approx.)	Paradox Valley Brine (approx.)	Salt Disposed (approx.)
		Mgal	Mgal	ktons
1991	Tests	11.7	3.9	4.3
1992	Tests	9.8	7.8	8.4
1993	Tests	26.2	10.0	10.8

Table 4-2 Annualized Summary of PVU Injection

Year	Phase	Injectate (approx.)	Paradox Valley Brine (approx.)	Salt Disposed (approx.)
		Mgal	**Mgal**	**ktons**
1994	Tests	81.7	58.7	63.7
1995	Tests	34.4	24.1	26.2
1996	*Phase I*	44.6	31.1	33.7
1997	*Phase I*	127.8	89.4	97.0
1998	*Phase I*	166.2	116.1	126.0
1999	*Phases I & II*	150.4	104.5	113.3
2000	*Phases II & III*	112.4	85.4	92.7
2001	*Phase III*	99.6	69.7	75.6
2002	*Phase IV*	103.0	103.0	111.8
2003	*Phase IV*	104.2	104.2	113.0
2004	*Phase IV*	94.8	94.8	102.8
TOTAL		**1,167**	**902.7**	**978.5**

4.3 Injection Adjustments Explanation

As noted above, PVU has instituted 3 major injection changes, resulting in 4 injection phases. Each of these changes invoked a strategy either to help reduce unacceptable seismicity or to optimize brine emplacement. The motivations behind these strategies are discussed in the following sections.

4.3.1 Bi-Annual Shutdowns

The scheduled shut downs were included so that the injectate from the pressurized fractures and faults could diffuse into the formation rock matrix (i.e., *in situ* stress relaxation). Scheduled shutdowns were implemented to mitigate seismicity following the **M** 3.5 event and a month later the **M** 3.6 event in mid 1999. Prior to these events, we had noted that the rate of seismicity in the

near-wellbore region (i.e., within about a 2-km radius from the wellbore) reduced during and following unscheduled, maintenance shutdowns and during the shutdowns following the injection tests of 1991 through 1995. Based on these observations and following the two mid-1999 (large) events, PVU began a program of two scheduled, 20-day shutdowns each year, one in December-January and one in May-June. As detailed below (e.g., **Figure 6-4**), the shut downs reduced the seismicity, but did not sufficiently reduce the proclivity to produce large seismic events.

During 2004, PVU witnessed all or parts of three, scheduled shutdowns: 12/20/03 to 1/7/04, 6/2/04 to 6/20/04, and 12/18/04 to 1/06/05.

4.3.2 Reduced Injection Rate

Prior to May 27, 2000, PVU pumped injectate at a maximum rate of ~ 1,100 lpm (1,100 liter/min =345 gal/min). To maintain this rate, 3 constant-rate pumps were used with each operating at ~115 gpm. This rate resulted in an average wellhead pressure of ~4,800+ psi.

During 3-pump operations, the surface pressure on occasion approached the wellhead pressure safety limit of 5,000 psi; at these times PVU would shut down one injection pump and sometime two pumps, reducing injection rate, and letting pressure drop a few hundred psi before returning to 3-pump operations; this resulted in an overall average injection rate of ~300 gpm. These shutdowns normally lasted hours.

Immediately following the May 27, 2000 **M** 4.3 event, PVU shutdown for 28 days. During this shutdown period, PVU evaluated the existing injection strategy and its effect on seismicity and decided to institute a new strategy to reduce the seismic threat. The new strategy changed operations from 3 injection pumps to 2 pumps. On June 23, 2000 PVU resumed pumping using 2 pumps, resulting in an injection rate of ~230 gpm. At this reduced rate, surface pressure normalized between ~4,400 and 4,500 psi. When first initiated, it was believed that reducing the injection rate combined with previously-instituted, bi-annual 20-day shutdowns would reduce the potential for large events. Together, the bi-annual, 20-day shutdowns and lower injection rate reduced earthquake production. From 1998 through the **M** 4.3 event, PVSN recorded an average

~81 earthquakes/month; following the reduced injection in late June 2000 through the end of 2001, that average dropped to ~13 earthquakes/month.

As demonstrated by the May 27th 2000 event, 20-day shutdowns alone were not sufficient for stemming large event production. The combination of shutdowns and reduced injection rate is not a perfect solution; however, these are the only means to date that we have found to mitigate unacceptable seismicity. No matter what method of event control or mitigation is invoked, mitigation is not equivalent to elimination. As we understand seismic source generation, larger (i.e., **M** 3 or greater) events are still probable, as demonstrated by the November 7, 2004 **M** 3.9 event. However, we believe that careful monitoring and the methods discussed above will continue to minimize the rate of event production.

4.3.3 Injectate: 70%:30% PVB:Fresh Versus 100% PVB

Beginning with continuous operations in 1996, PVU diluted the injectate to 70% PVB and 30% Dolores River fresh water. A geochemical study had predicted when 100% PVB interacted with connate fluids and the dolomitized Leadville Limestone at downhole (initial) temperatures and pressures, PVB would precipitate calcium sulfate that would restrict permeability (Kharaka, 1997). During October 2001, with the decreased injection volume discussed above, the injectate concentration question was reconsidered. Temperature logging in the injection interval recorded substantial near-wellbore cooling, indicating that if precipitation occurred, it would not be near, and possibly clog, the wellbore perforations. Further discussions indicated that, if precipitation occurs, its maximum expected rate is ~8 tons of calcium sulfate per day. To put this amount into perspective, injection at ~230 gpm, assuming a density of 8.33 lbs/gal, gives a daily injection tonnage of ~1380 tons/day. The maximum expected precipitate is ~0.6% of the daily injection mass. Injecting 100% PVB began on January 8, 2001, after the December-January-2001 20-day shutdown and has been maintained through the end of 2004. To date, the only affect has been increasing bottom hole pressure because of the increased density of 100% PVB over the 70%:30% mix. No discernible affect on the induced seismicity has been seen.

5.0 SEISMIC ANALYSIS

5.1 Typical Seismograms from PVU

The following figure, **Figure 5-1**, shows typical seismic signals (i.e., seismograms) recorded by

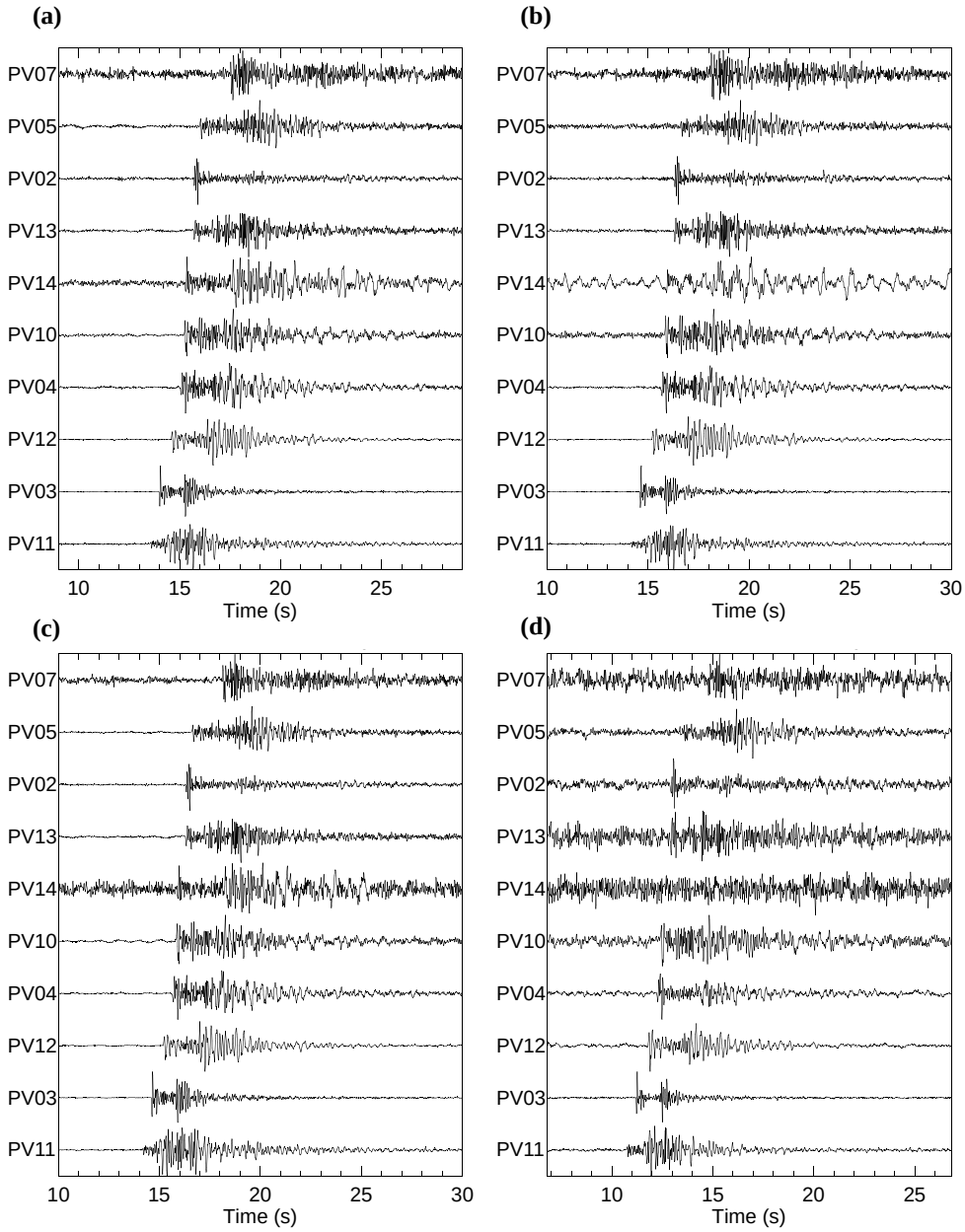

Figure 5-1 Examples of Vertical-Component Seismograms from Four Closely-Spaced Events Recorded by PVSN.

PVSN and induced by PVU injection. **Figure 5-1(a)** is an **M** 0.9 event recorded on January 29, 1994; **Figure 5-1(b)** is also an **M** 0.9 event but was located about 3 m from **(a)** and was recorded

in February 7, 1994; **Figure 5-1(c)** is also an **M** 0.9 event located 9 m from **(a)** but was recorded on February 11, 1997; and **Figure 5-1(d)** is an **M** 0.2 event located 90 m from **(a)** and recorded on October 33, 1999. Each seismogram has been 0.5-20 Hz bandpass filtered uses a 4-pole, zero-phase Bessel filter.

5.2 Local Seismic Magnitude Scale

Typically, seismologists calculate the size of an earthquake using one or more methods. In most cases, seismologists calculate magnitude for local events following a procedure calibrated for local conditions. For PVSN, we compute magnitudes from the duration of the recorded signal. This scale, called the duration or coda magnitude, is denoted **M** in this report. [For a more complete discussion of the magnitude scale for PVSN see 2000 PVSN Annual Report (Mahrer et al., 2001) and given on the accompanying CD.]

5.3 Preliminary Event Location Method

Accurately locating earthquakes requires (1) identifying arrival times of specific phases in the recorded signals, (2) appropriate array geometry, and (3) an accurate velocity model of the region through which the signals travel. As noted above, seismologists manually pick the phase arrival times for all local earthquakes recorded by PVSN. We do this to minimize uncertainty frequently found in automated (i.e., software-based) phase identification and arrival time picking. We require a minimum of four arrival times from at least three stations to locate an event. In the PVSN analysis, we pick the primary or P-wave arrival times from all stations with acceptable signal-to-noise ratios. We then pick secondary or S-wave arrival times from only the three-component stations PV11 (Davis Mesa) and PV16 (Nyswonger Mesa) and from the closest single-component station to the injection well, PV03 (Wild Steer). Although S-wave arrival times are very important to the analysis, we use only 3 stations because of the closeness of the sources to these stations. For the other stations of PVSN, the complexity in the local geology leads to mis-identifying S-phases which causes mis-locating events.

We currently determine preliminary earthquake locations using a flat, one-dimensional, layered

earth velocity model and the computer program SPONG (Malone and Weaver, 1986). [For a complete description of our Premininary Event Location Scale, see the 2003 PVSN Annual Report (Mahrer, et al, 2004) on the accompanying CD.]

5.4 Advanced Analysis: Event Re-Location

To evaluate the potential relationship of seismicity to reservoir and fluid transport characteristics, we made a significant effort to improve the accuracy of the preliminary earthquake locations (see previous section). First, we developed a three-dimensional velocity model for the Paradox Valley area using a progressive, three-dimensional velocity-hypocenter inversion (Block, 1991). In this inversion, we used a data set consisting of 682 earthquakes with **M** greater than 0.7 and good signal-to-noise ratios. Second, we performed a relative relocation of as many earthquakes as possible (i.e., clean waveforms with strong signal-to-noise ratios) using the three-dimensional velocity model developed in the first step (Waldhauser and others, 1999). Approximately 95% of the events recorded between 1991 and 2004 had sufficient signal-to-noise ratios to be included in the relative relocation. For the remaining events we used the original one-dimensional model locations. As an example of the effect on epicentral location by the relative relocation procedure, **Figure 5-2** shows the 1-D (i.e., preliminary) located and the relative relocation epicenters for 2004. Note the tighter groupings of epicenters from the relative relocation method.

The immediate goal of this modeling is reducing the arrival-time root-mean-square (rms) residuals (i.e., the difference between the observed and the model or theoretical travel times). Compared to the one-dimensional model residuals, the three-dimensional velocity model reduced the rms residuals by ~14%. The relative relocation procedure resulted in more than a 90% reduction in rms residuals relative to the three-dimensional results. The final, most-accurate earthquake epicenters for the 1991 through 2004 seismic data are shown in **Figure 5-3**, **Figure 5-4** and **Figure 5-5**. **Figure 5-4** and **Figure 5-5** show close-ups of the two regions, one region around the injection well and the second to the northwest, respectively. The linear groupings of seismic event epicenters is quite evident in these figures.

As discussed in previous annual reports (e.g., Ake et al., 2000; Mahrer et al., 2001), the loci of

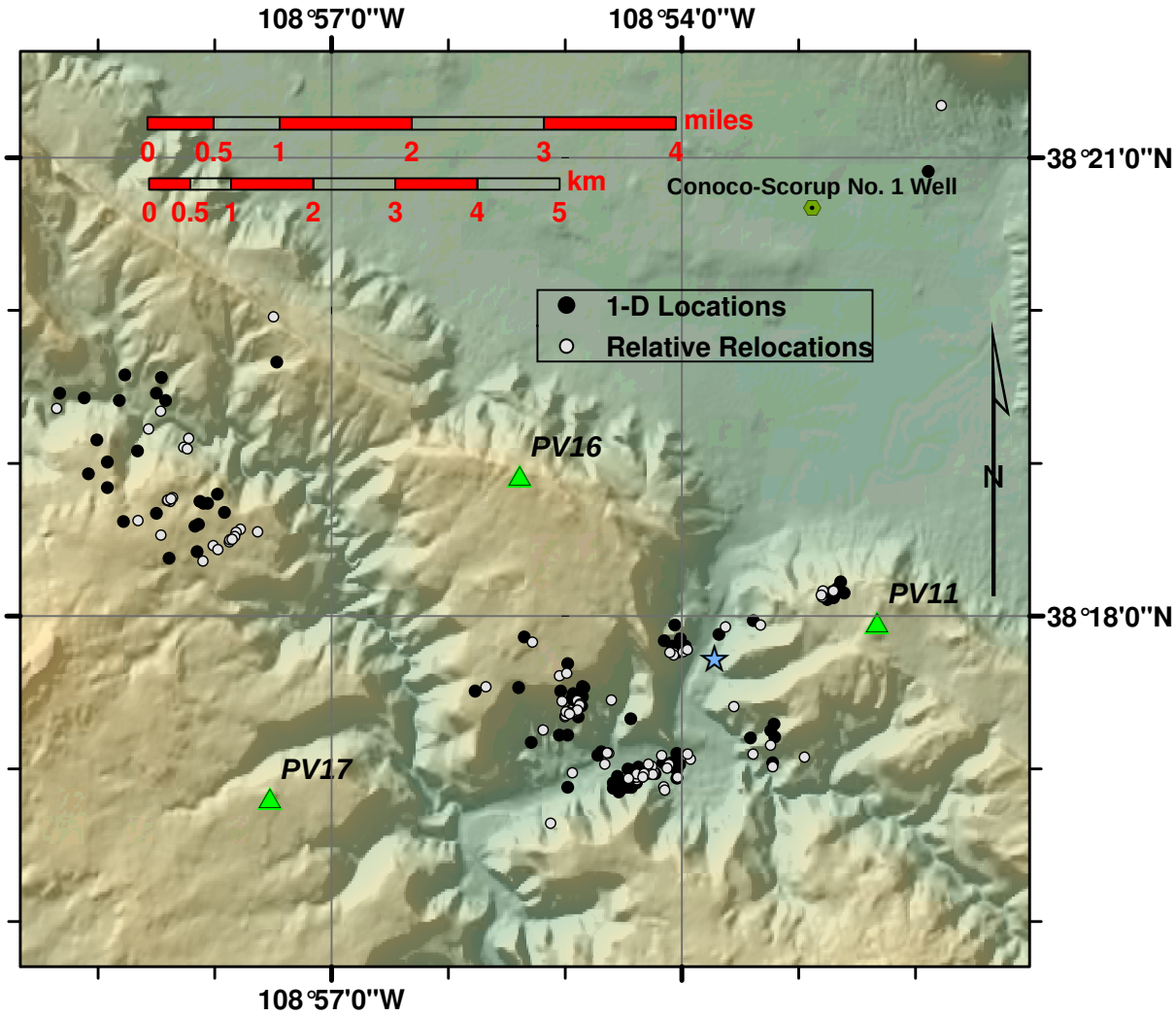

Figure 5-2 Comparison of 2004 Epicenters Determined by 1-D Model and Relative Relocation Method. Star is Injection Well; Triangles are PVSN sites.

relocated earthquakes are consistent with our interpretation that most of the tectonic stress release takes place along (existing) linear features with orientations consistent with either the two sets of focal mechanisms (set 1: N81W and N9E; set 2: N21W and N69E) or the two sets of fractures observed in the oriented core samples (primary: N69W and N74W; secondary: N38W and N42W; Ake and Mahrer, 1999). Very little seismicity appears to be occurring along planes with strike consistent with the Wray Mesa fault system, as defined by Bremkamp and Harr (1988). Bremkamp and Harr (1988) estimated the strike of the Wray Mesa fault system to be ~N55°W. It is likely that these features are the most through-going structures in the area. The locations of the linear features in **Figure 5-3**, **Figure 5-4** and **Figure 5-5** suggest communication through "con-

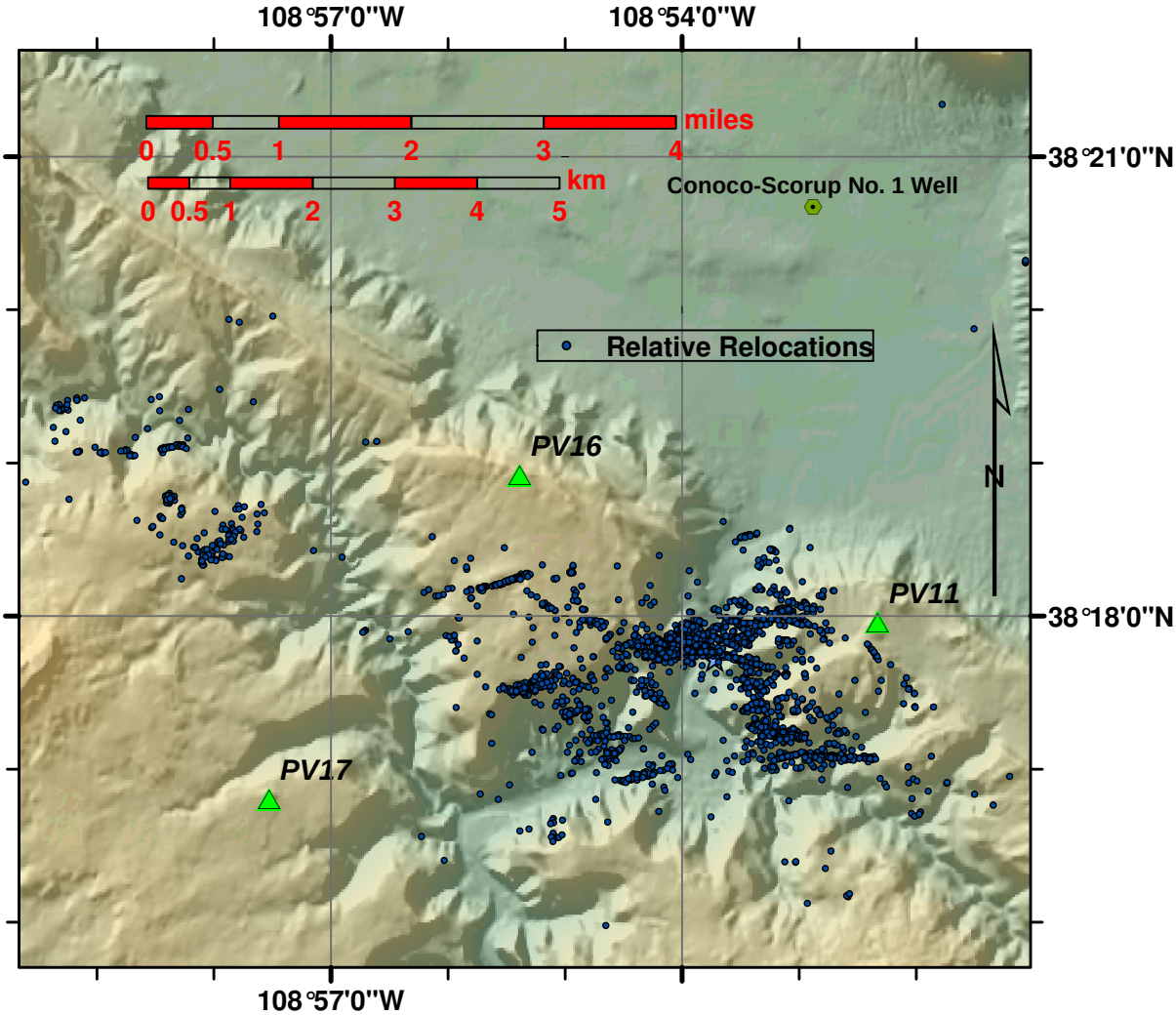

Figure 5-3 Relative-Relocated PVU Induced Seismic Epicenters from 1991 Through 2004. Star in center of main cluster is the injection well; triangles are sites of PVSN.

duits" in a ~N55°W direction. (See Microsoft Excel animation file on attached compact disk for an interpretation of conduits superimposed on the seismic linear features.) We believe this behavior suggests fluid is being preferentially carried along these steep planes with a northwest strike (i.e., the through-going elements of the Wray Mesa system). Opening of these planes will require the least energy and are less likely to induce surface-measurable events, since these planes are oriented normal to the least principal stress direction.

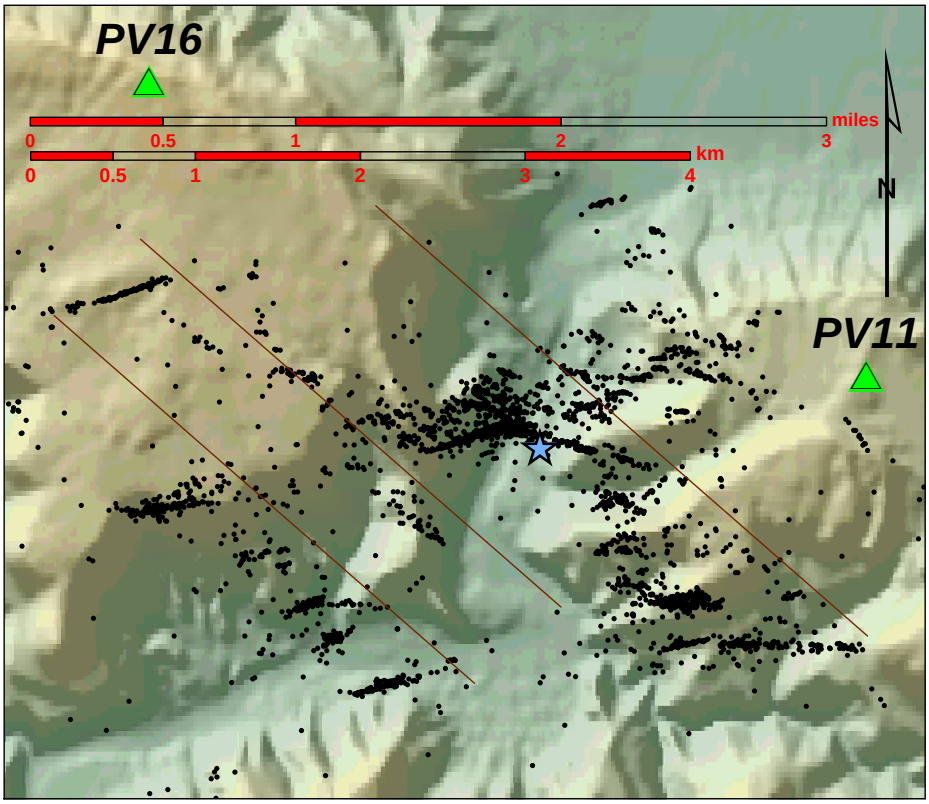

Figure 5-4 Close-up of 1991-2004 Relocated Event Epicenters in Primary Seismogenic Region Surrounding Wellbore. Star is injection well and diagonal lines are references, running N55^{o}W, paralleling the strike of the Wray Mesa Fault system.

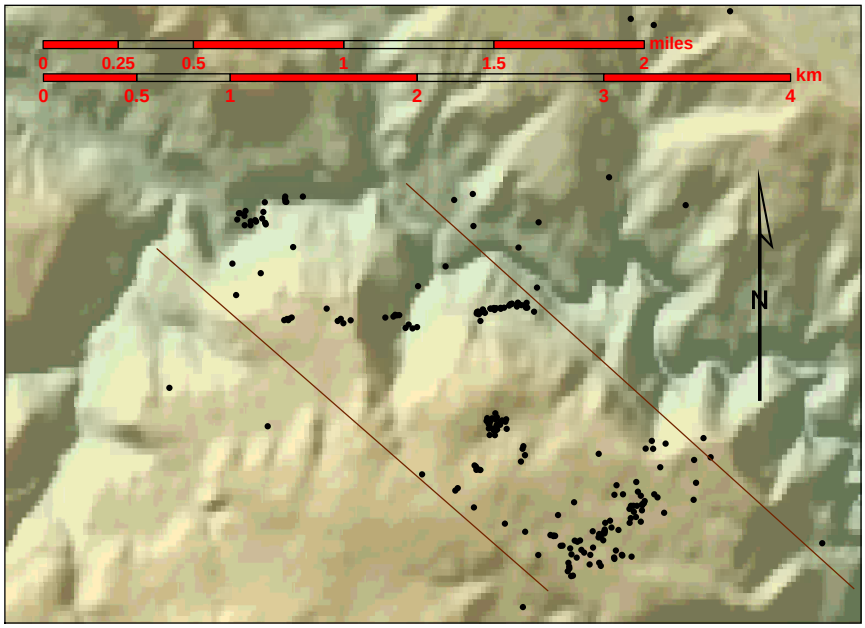

Figure 5-5 Close Up of 1991-2004 Relocated Event Epicenters in Secondary Seismogenic Region ~8.5 km Northwest of Injection well. Diagonal lines are references, running N55^{o}W, paralleling the strike of the Wray Mesa Fault system.

6.0 OBSERVATIONS

6.1 Local, Pre-Injection Seismicity

In the 1960's, the US Army high-pressure injected waste fluids ~3,000 m deep at the Denver Arsenal, north east of Denver, CO. As a result, hundreds of seismic events were induced (Healy, 1968) in a nominally aseismic region. Recognizing the implication, that the proposed injection at Paradox Valley would, most likely, induce seismicity, Reclamation prepared to record pre-injection, background seismicity in the region surrounding the proposed Paradox injection site. In 1983 the US Geological Survey began installing the first 10 stations of PVSN, PV01 through PV10 (PV06 eventually became PV15); recording seismic data began in 1986, 5 years prior to the PVU injection tests. **Figure 6-1** shows the epicenters of the pre-injection data. None of the earthquakes were within 15 km of the future injection well.

From the injection tests in 1991 through 2004, PVSN recorded and located more than 4,100 events within 10 km of the injection well. Based on the lack of pre-injection seismicity, we can safely infer that PVU injection induced these events.

6.2 Seismic Events and Well Testing (1991-1995)

As noted in **Figure 6-1**, prior to injection at PVU, the Paradox Valley region witnessed few seismic events (EnviroCorp, 1995; Ake and others, 1996) and none close to the injection well site. Between July 1991 and April 1995, PVU ran 7 injection tests. Each test consisted of a continuous pumping period followed by a wellhead shut-in to monitor downhole pressure fall off with time. The tests were implemented to qualify the well for an EPA Class V disposal well permit. (PVU Injection Well No. 1 is permitted as an EPA Class I well -- Isolate hazardous, industrial, and municipal wastes through deep injection -- run under EPA Class V guidelines -- Manage the shallow injection of all fluids to prevent contamination of drinking water resources.) **Table 6-1** summarizes the injection tests including injected volume, pumping duration, and number of local (i.e., induced) seismic events recorded. In conjunction with **Table 6-1**, **Figure 6-2** shows the injection rate and induced seismic events per day. The boxed numbers at the top of the figure identify the tests; the boxed numbers at the bottom of the figure are the number of seismic events recorded

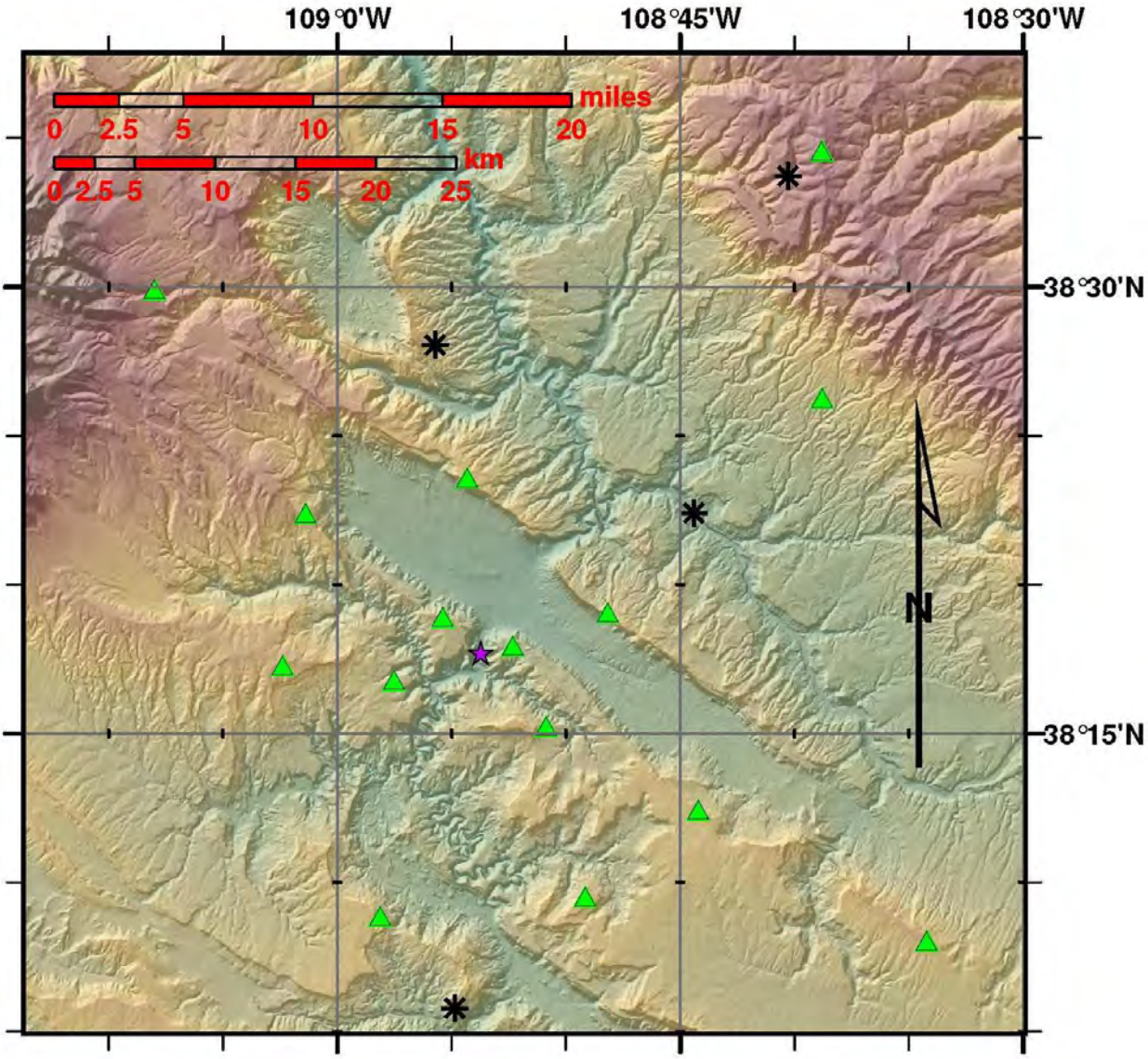

Figure 6-1 Paradox Region Natural Seismicity, 1985-1991. Asterisks are the natural seismicity, triangles show PVSN sites, and the star is the injection well.

during and immediately following the specific tests. Also noted in the figure is the 1993 acid stimulation. The stimulation was performed to increase the imbibition of the well (Envirocorp, 1995). **Figure 6-3** shows the cumulative epicenters induced by the injection tests

.

6.3 Seismic Events and Continuous Injection (1996-Present)

*{Note: We have found that the Earthworm system, discussed above, is less sensitive for detecting very small events (i.e., events < **M** 0.0) than the system it replaced. Overall these events are not*

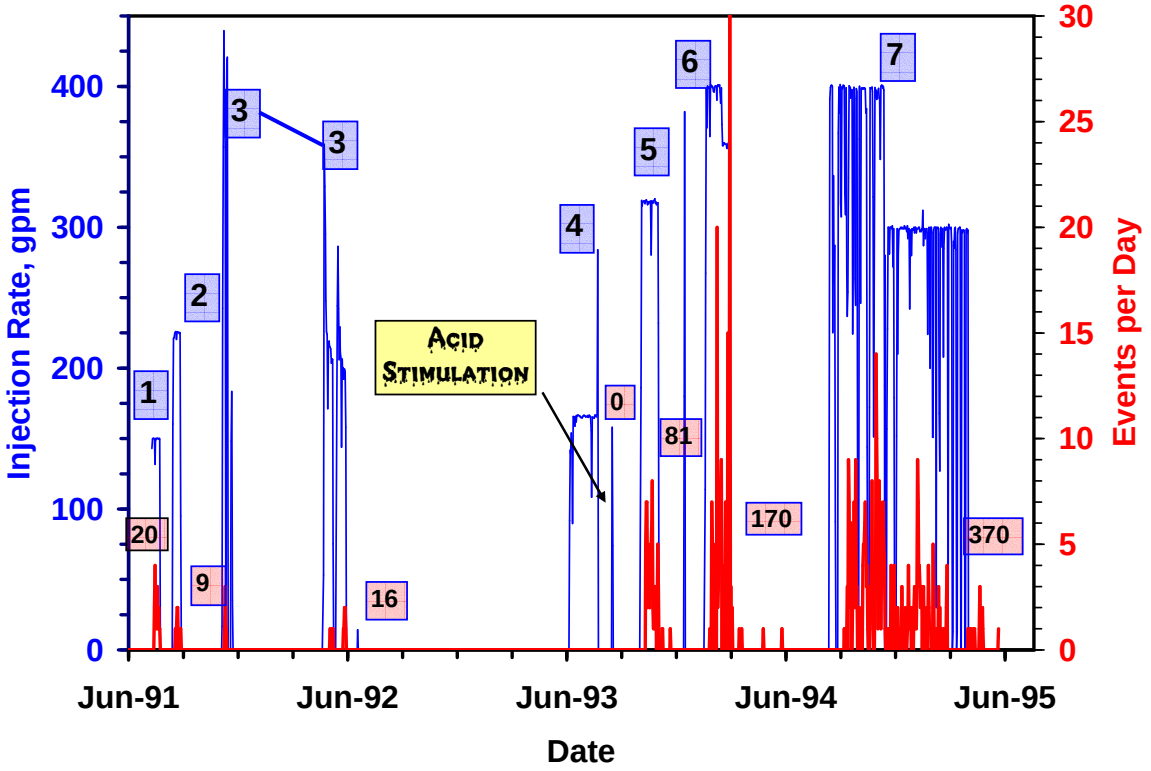

Figure 6-2 Injection Rate and Induced Events (red boxes) for Tests. Tests (blue boxes) were invoked to qualify injection well for an EPA Class V well disposal permit.

*significant, having very small signal to noise ratios (i.e., poorly constrained locations) and representing only a few percent of the old data. Therefore, for consistency with the pre-Earthworm data, all subsequent discussions and figures will only use **M** 0.0 or greater data.}*

During 2004 PVSN recorded and located 106 events with **M** 0.0 or greater. **Table 6-2** gives a year-by-year listing of event production. Note that the table does not include 1996 (it was only a partial year of pumping) and 1997 (we have some concerns about the completeness of the data set due to computer problems). We have included **Table 6-2** for comparison of 2004 data with previous years' annual activity. However, we feel that much more insight is gained when examining the Paradox seismic data by the injection phases described above. **Table 6-3** presents these data by PVU injection phase of which the 2004 data is included in *Phase IV.* Note the event count and number of days in *Phase I* in **Table 6-3** includes 1996 (111 days from pumping inception to first recorded event) and 1997 data and therefore the average events per day appear much lower than the values for 1998 and 1999. We feel that the real average events per day for *Phase I* should

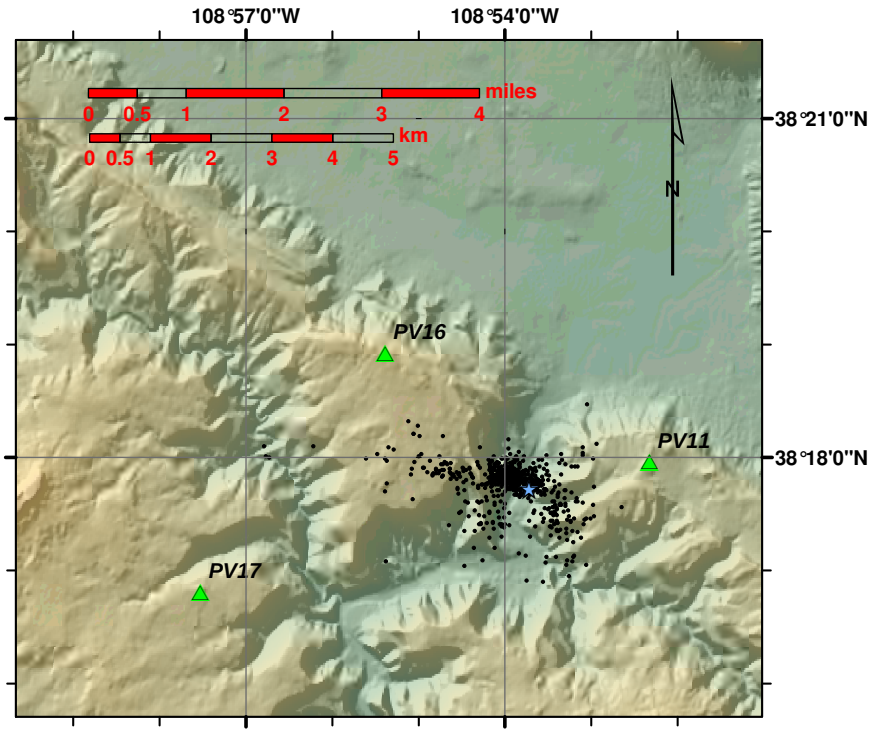

Figure 6-3 Epicenters of Seismic Events Induced By and During Injection Tests, 1991-1995. Triangles shows local stations of PVSN and star is the injection well.

match the 1998 and 1999 values at about 3.15. Therefore in **Table 6-3** we have added an * to the *Phase I* average events per day. **Table 6-3** supports our assessment that shutdowns and reduced injection rate reduce event production. In support of **Table 6-2** and **Table 6-3**, **Figure 6-4** shows histograms of monthly injection volume and monthly event production the beginning of continuous pumping in 1996 through the end of 2004. The figure shows the injection phases and emphasizes how dramatically event production has declined since mid-2000 when PVU reduced the injection rate by one third from ~345 gpm to ~230 gpm (i.e., from 3-pump injection to 2-pump injection). **Figure 6-5** and **Figure 6-6** show events per day for PVU operation since 1996 (i.e., continuous pumping) plus average daily injection rate and average daily downhole pressure, respectively.

6.4 Event Magnitudes

As shown in **Table 6-2**, in 2004, the daily seismic event rate was 0.29; this is less than 2003, but more than 2002, which are the other years of *Phase IV* injection.

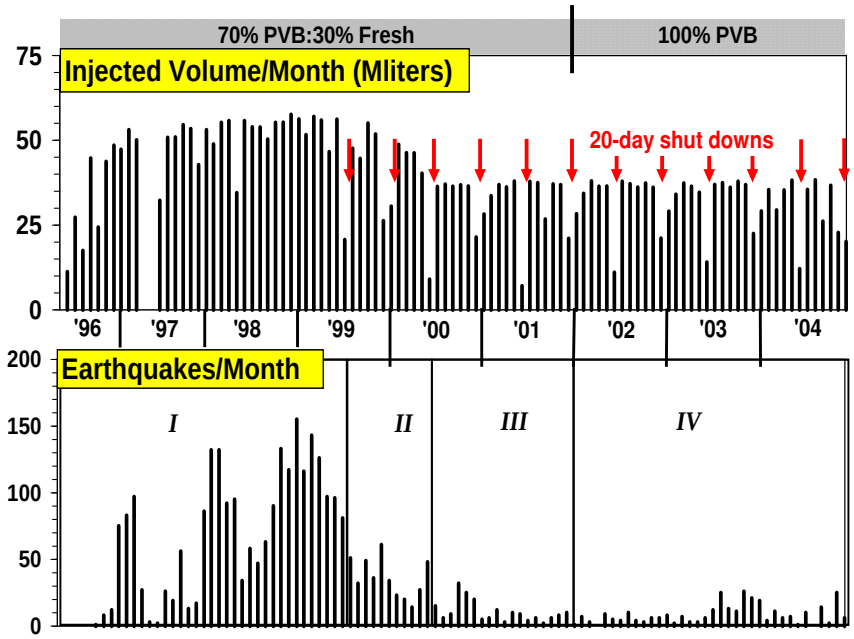

Figure 6-4 Injection Volume (top) and Earthquake Production at PVU by Month for Each Year Since Continuous Injection Began in 1996. Note the four injection phases, the bi-annual, 20-day shutdowns beginning in 1999, the reduced injection rate beginning in 2000, and the change in injectate beginning in 2002.

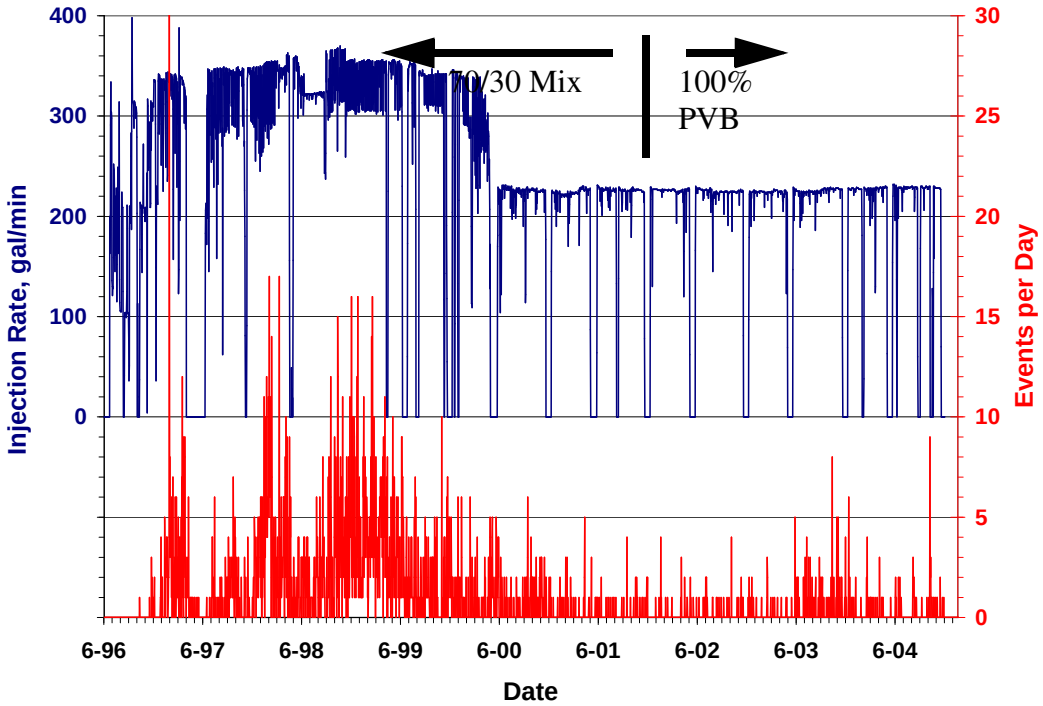

*Figure 6-5 Number of Events per Day (red) and Average Daily Injection Rate (blue) Versus Time. Event count only includes events with magnitudes **M** 0.0 and larger.*

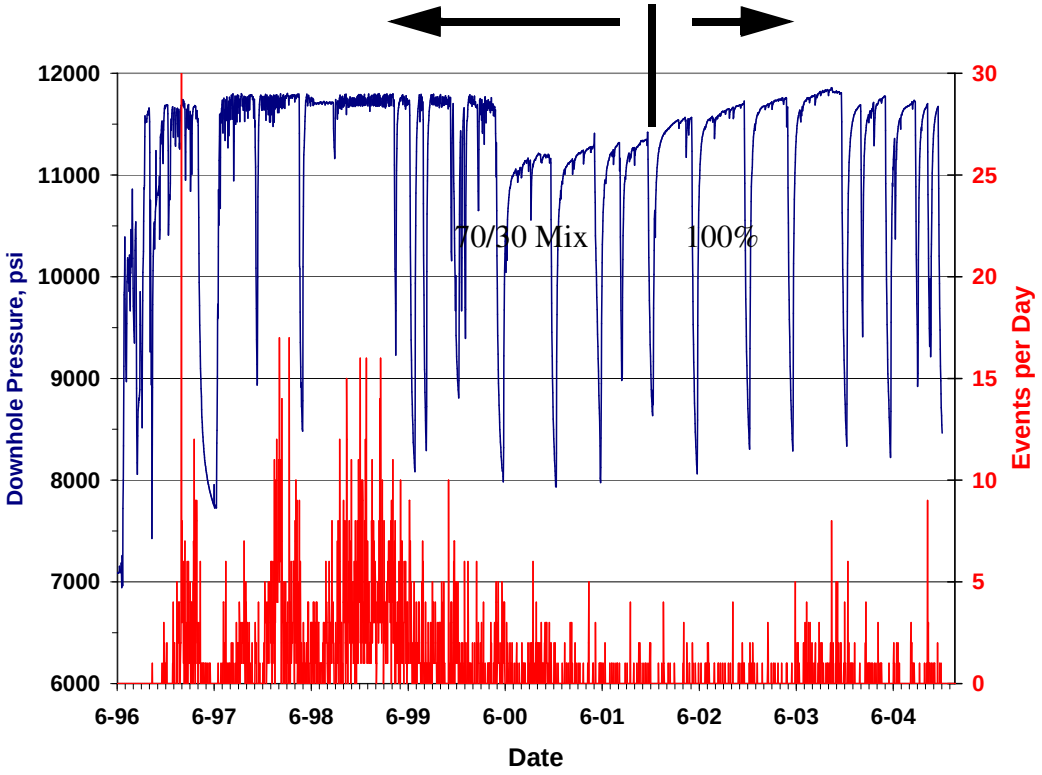

Figure 6-6 Number of Events per Day (red) and Downhole Injection Pressure (blue) Versus Time. Downhole pressure is calculated at 4.3 km (14,080 ft).

Table 6-1 Injection Tests 1991-1995

Test No.	Injected Volume	Initial Pumping Date and Duration	Injectate	Hydrostatic Pressure @ 4,300 m[a] depth	No. Induced Seismic Event
	m^3	*(date) days*	*%PVB[b]:%Fresh Water*	(MPa)	
1	11,000	(11Jul91) 14	0%:100%	42	20
2	16,000	(15Aug91) 12	33%:67%	44	9
3	54,000	(5Nov91) 54	67%:33%	47	16
4	42,000	(6Jul93) 47	0%:100%	42	0
--	38	(20Sep93) 14	28% HCl acid injection	--	--
--	34		100% fresh water flush following acid injection[c]		
5	54,000	(3Oct94) 28	70%:30%	47	81
6	89,000	(18Jan94) 41	70%:30%	47	170
7	354,000	(14Aug94) 242	70%:30%	47	370
Total	**620,000**	**438 days**	**---**	**--**	**666**

[a]Depth = Top of the casing perforation interval; i.e., the top of the injection target horizon, the Leadville Limestone

[b]PVB = Paradox Valley Brine (260,000 mg/l total dissolved solids)

[c]Injection well surface pressure became negative (i.e., below hydrostatic) following water flush of acid injection;

Table 6-2 Yearly Event Production for M>=0

Year	Induced Events	Average Events Per Day
1998	1071	2.93
1999	1051	2.88
2000	272	0.75
2001	83	0.23
2002	58	0.16
2003	137	0.37
2004	106	0.29

Table 6-3 Event Production by Injection Phase Through 2004

Phase	Induced Events	Duration	Avg. Events per Day	Injected Volume
--	--	Days	--	Ggal
I	2369	1100	2.15*	0.427
II	402	335	1.20	0.118
III	208	565	0.37	0.156
IV	301	1090	0.28	0.302
**Questionable value, see text for explanation*				

Table 6-4 shows the event magnitude distribution by year for 0.5-magnitude wide bins. **Table 6-**

Table 6-4 Distribution of Seismic Events by Year

Phase	1999		2000		2001		2002		2003		2004	
Mag. Range	**No.**	**%**	**No.**	**%**	**No.**	**%**	**No.**	**%**	**No.**	**%**	**No.**	**%**
0.0-0.4	419	39	114	40	17	21	6	10	10	7	13	12
0.5-0.9	388	36	98	35	35	42	23	40	44	32	39	37
1.0-1.4	160	15	41	15	18	22	17	29	55	40	34	32
1.5-1.9	64	6	18	6	11	13	8	14	17	12	12	11
2.0-2.4	31	2.9	7	2.5	2	2.4	3	5	11	8	5	5
2.5-2.9	5	0.5	3	1.1	0	0	1	1.7	0	0	2	2
>2.9	2	0.2	1	0.4	0	0	0	0	0	0	1	1
Total	**1070**		**282**		**83**		**58**		**137**		**106**	

4 shows that, there was about a 20% decrease in total number of events during 2004 compared to 2003. A more complete discussion of magnitudes and recurrence statistics is given below.

6.5 Events by Depth

Figure 6-7 shows the Paradox epicenters color-coded by depth in km relative to the wellhead. Note that these data show a shallowing of the event depth to the west south west, which is consistent with the description of the local geology given above. This indicates that the seismicity follows both the stratigraphic dipping and the fault-fracture structure of the Wray Mesa system.

6.6 Felt Events

By the end of 2004, PVSN recorded more than 4,100 events attributed to PVU injection. Of these, more than 99.9% were imperceptible (i.e., < **M** 2.4) to people at the surface. From 1991 to 1996 no events were felt. Between August, 1997 (i.e., the first reported felt event) and the end of 2004 about 15 events were felt. During 2004, one felt-event was reported to PVU. It was a magnitude

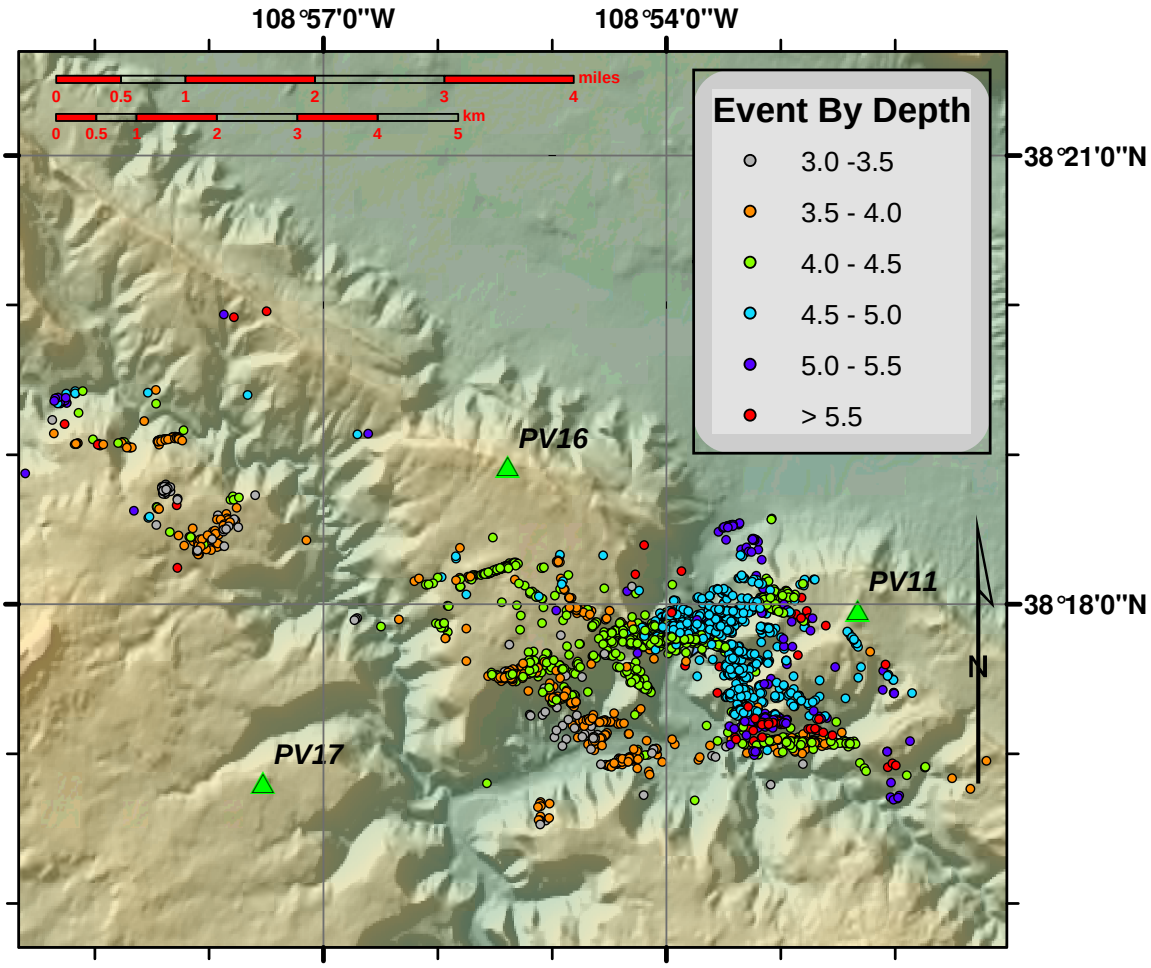

Figure 6-7 Epicenters Color-Coded by Depth, in Kilometers, Relative to Injection Wellhead.

M 3.9 occurring on November 7 and is discussed elsewhere in this report in detail.

During 1996-2004, 21 events **M** 2.5 or greater were recorded, indicating not all larger events are felt. Of the larger events, 3 occurred in 1998, 7 in 1999, and 5 in 2000. In 2000 only 1 **M** 2.5-or-greater event occurred after the reduction in injection rate following the May 27th event. In 2001 no events **M** 2.5 or greater occurred. In 2002, 1 event **M** 2.5 or greater occurred. In 2003, no events **M** 2.5 or greater occurred. In 2003, 3 events **M** 2.5 or greater occurred. In 2004, 3 events **M** 2.5 or greater occurred.

6.7 2004 Event Locations

Figure 6-8 shows a plan view (i.e., epicenters) of the 106 earthquakes induced by the PVU injection during 2004 and located using the preliminary one-dimensional model and the relative relocation method. The relocated events are plotted by the indicated magnitude bins. The magnitudes of these events range from **M** 0.0 to **M** 3.9 (see **Table 6-4**). With regard to magnitude, the error in locating events generally decreases with increasing magnitude. For smaller events, noise is proportionately larger, obscuring identification of the initial P and S-arrivals. As a result, most of our conclusions for these data are based on events with **M** > 0.6.

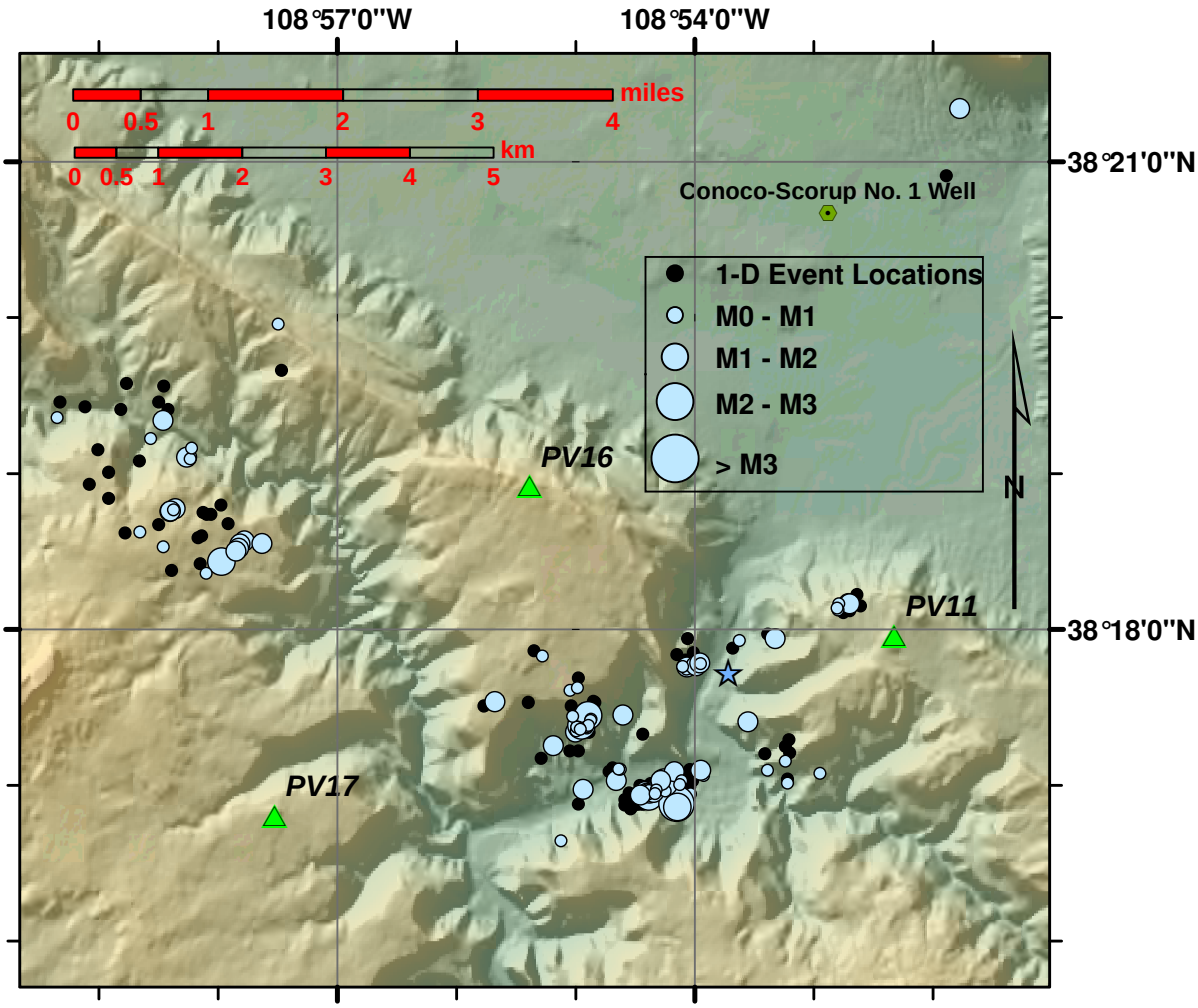

Figure 6-8 2004 Epicenters Located Using One-Dimensional Velocity Model and Relative Relocation Method. 106 events are plotted; relative relocations are plotted by magnitude. Injection wellhead is star.

Figure 6-8 shows that the epicenters recorded in 2004 are, as in previous years, contained within

two distinct regions. The first and most populated region surrounds the injection well in an elongated envelope whose long axis runs approximately NW-SE and extends to a maximum of ~4 km west of the injection well and ~2 km east of the well. The second region is centered about 8 km northwest of the injection well. The figure also shows the swarm events (discussed above) located to the north west and very near the injection well.

Figure 6-9 compares the epicenters for all events from 1991 through 2003 to the 2004 events. The figure uses only relocated data. The relocation method was discussed above and detailed in the PVSN 2000 annual report (Mahrer et al., 2001), given on the accompanying CD.

As noted earlier, **Figure 6-9** shows that the relocated 2004 events fall within the two groups defined by previous year events. As discussed in previous annual reports (e.g., Mahrer et al., 2002; Mahrer et al., 2003), the relocated epicenter and the terminations of their aligned lineations within the seismic zones suggest the strike (N55^{o}W) of the Wray Mesa fault and fracture system.

The group 8 km northwest of the well first appeared in 1997. We believe that the paucity of events between the two groups, which has been maintained for almost 8 years, indicates the zones communicate hydrologically by a conduit(s) of fluid, probably through one or more principal faults of the Wray Mesa system.

Complementing **Figure 6-8** and **Figure 6-9**, **Figure 6-10** shows a NE-SW geological cross section normal to the strike of the valley and passing through the injection well. The geology, fault structures, etc. are based on Bremkamp and Harr's (1988) original interpretation and speculation. Projected on the cross section are all events from 1991 through the end of 2002 and within 1.5 km of the viewed plane.

Figure 6-10 shows a number of features. First it shows two vertical groupings of events: one in the Precambrian near the injection well and one starting in the Leadville and rising through the salt about 1.5 km southwest of well. Most likely the second grouping is the actual location of the fault Bremkamp and Harr (1988) speculated to lie about 1.5 km west of the well. **Figure 6-10** also

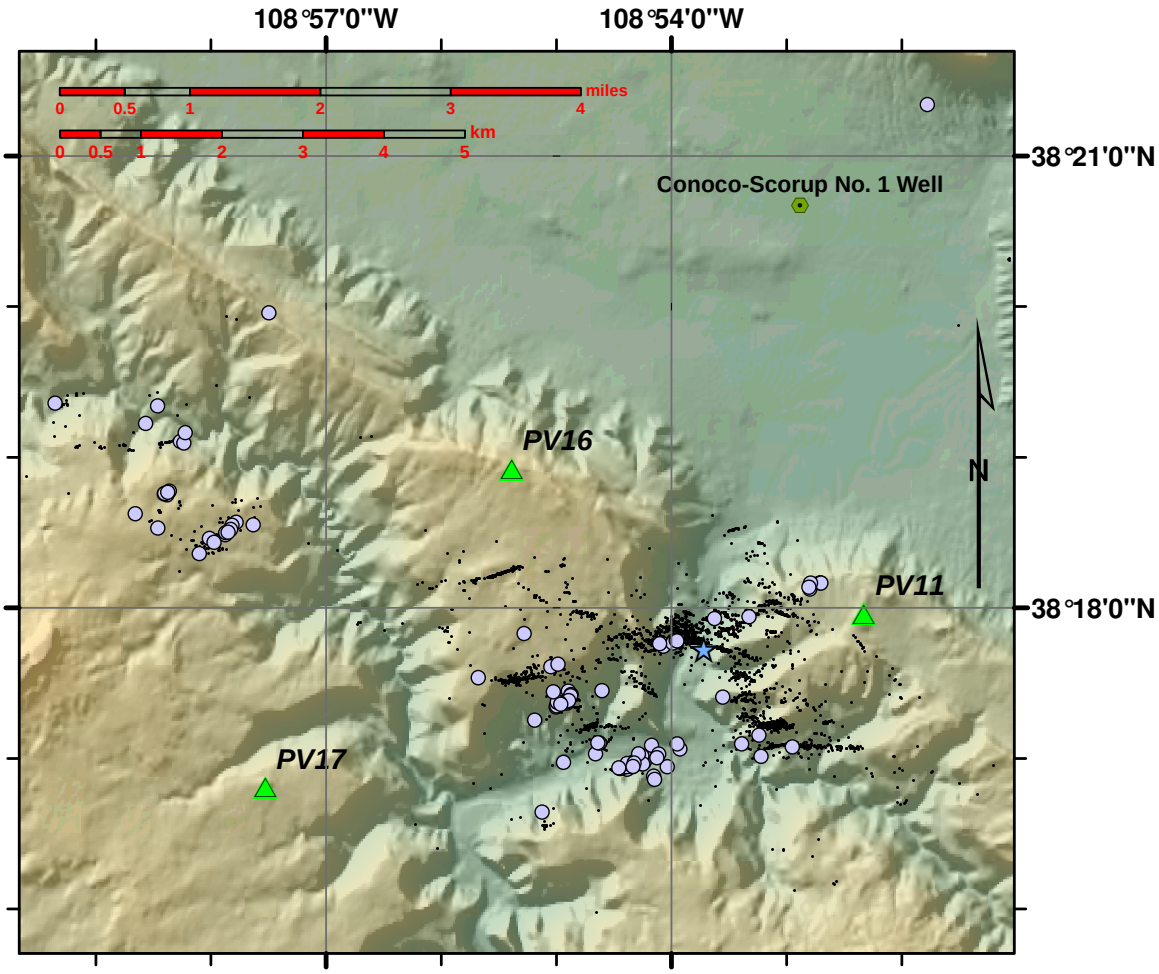

Figure 6-9 Relocated PVU-Induced Earthquake Epicenters for 2004 (circles) and years 1991-2003 (black dots). Star is PVU injection wellhead.

shows that many events near the well occur at depths between the top of the Mississippi-aged Leadville Formation, the primary injection horizon (4.3 km below surface) and the bottom of the well. This seismicity shallows to the southwest in agreement with the inferred shallowing of the Leadville Formation (Bremkamp and Harr, 1988). The figure also shows that the actual shallowing may be steeper than originally interpreted by Bremkamp and Harr.

Figure 6-10 shows a significant number of earthquakes appear below the bottom of the well in the Precambrian basement rocks. In 1998 approximately 18% of the events had depths greater than 4.8 km relative to the wellhead, the depth to the top of the Precambrian at the well. During 1999, 24% were below this depth horizon. In 2000, before the May 27th event, 30% of the events were

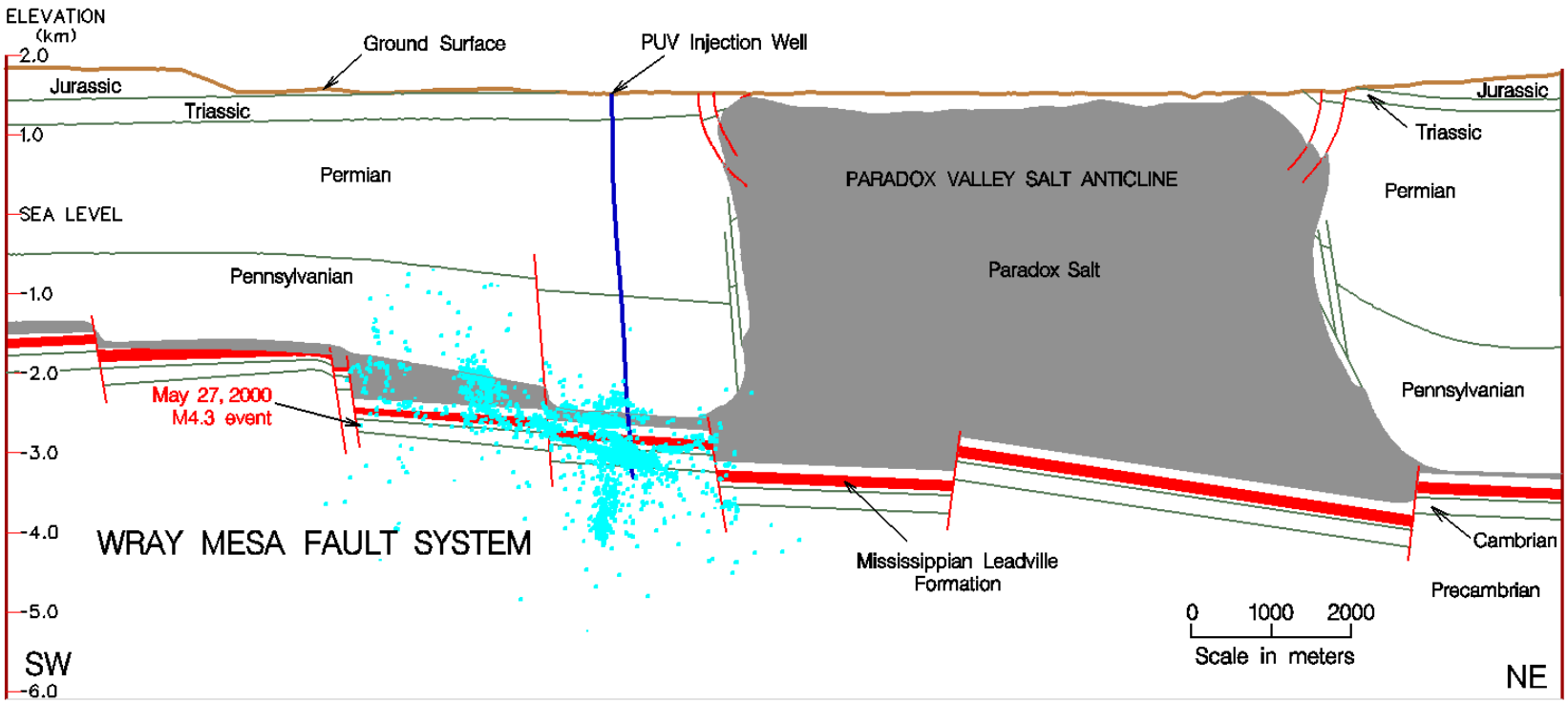

Figure 6-10 Bremkamp and Harr (1988) Cross Section Interpretation of Paradox Valley and Bordering Stratigraphy. Section passes through PVU injection well and run normal to strike of the valley. Projected on to cross section are seismic events (1991-2002) within 1.5 km of the viewed plane.

below this depth horizon. After pumping resumed in June, 16% were below this depth. In 2001, 35% were below 4.8. In 2002, about 34 of the 59 (relocated) events or 58% were 4.8 km or deeper. In 2003, 38 of the 138 (relocated) events or 28% were 4.8 km or deeper. In 2004, 11 or the 106 (relocated) event or 10% were 4.8 km or deeper. Note that since the Precambrian shallows to the west, these numbers represent a minimum number of events in the Precambrian.

6.8 1991-2003 Event Locations By Year

For comparison with the event locations in 2004 (previous section), **Figure 6-11** through **Figure 6-19** show event locations by years from initial injection testing in 1991-1995 (**Figure 6-11**) through annual figures for 1996-2003 (**Figure 6-12** - **Figure 6-19**). This time sequence shows the growth of the near-wellbore seismic zone indicating that by the end of 1998, the expansion of the seismic zone surrounding the well had reached maturity and further expansion is very slow, if at all.

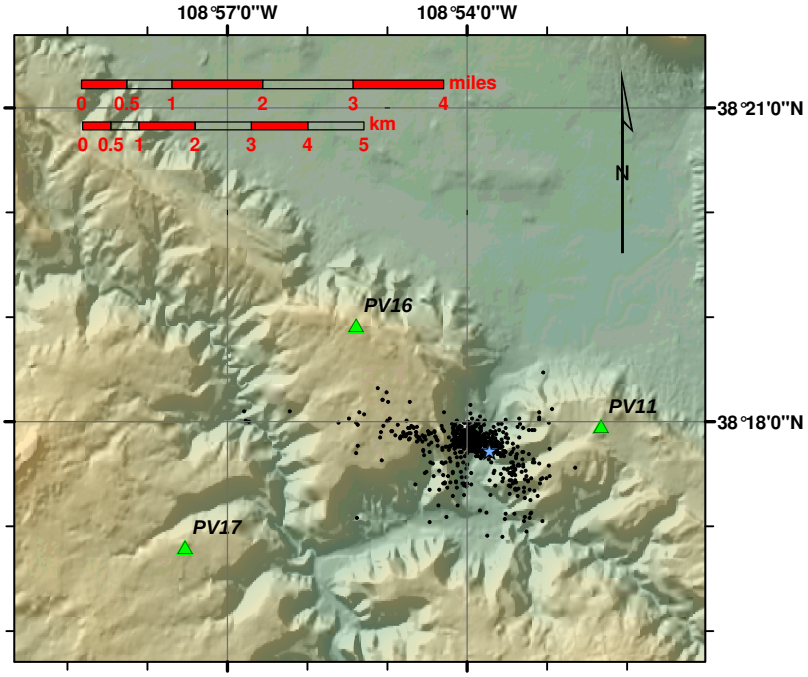

Figure 6-11 1991-1995 Epicenters. Star is injection wellhead.

6.9 Earthquake Recurrence

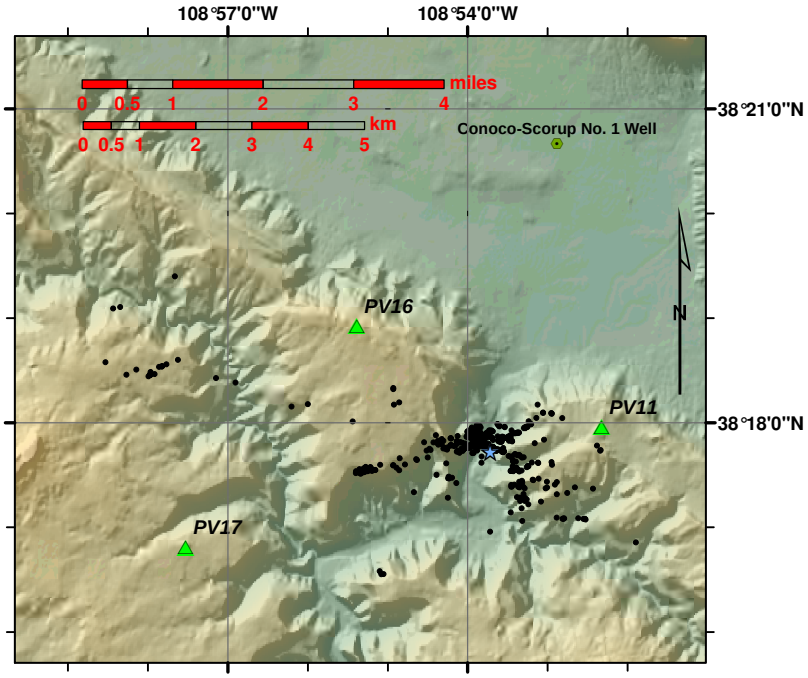

Figure 6-12 1996-1997 Epicenters. Star is injection wellhead.

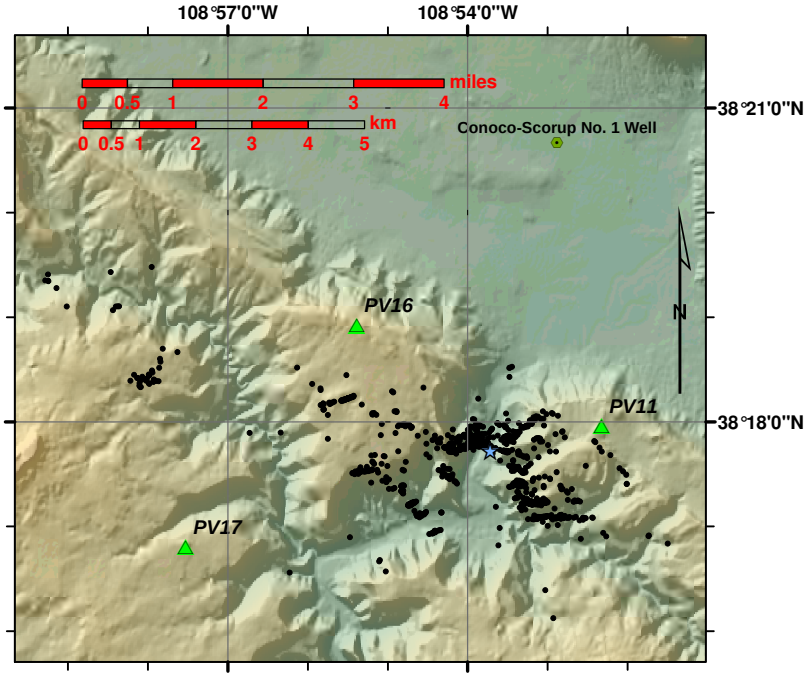

Figure 6-13 1998 Epicenters. Star is injection wellhead.

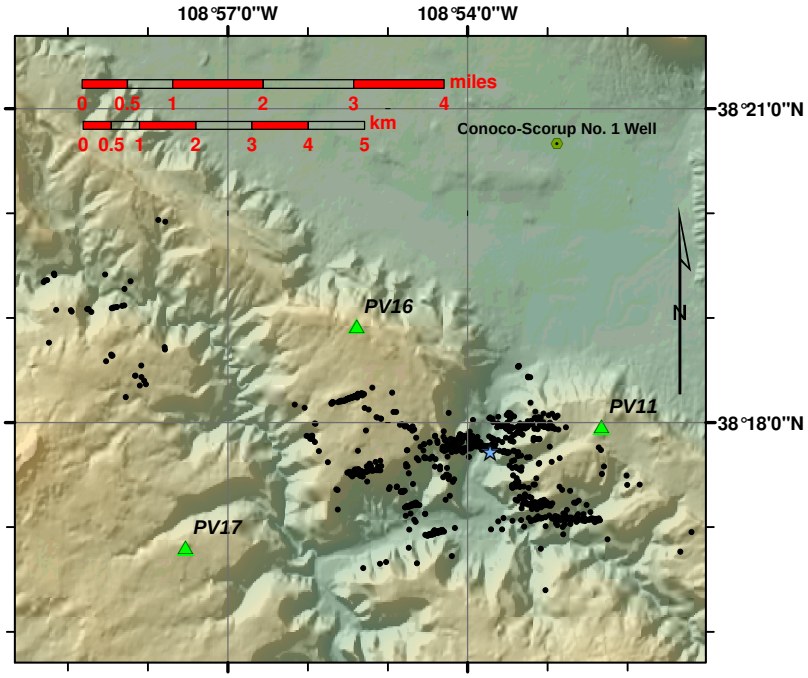

Figure 6-14 1999 Epicenters. Star is injection wellhead.

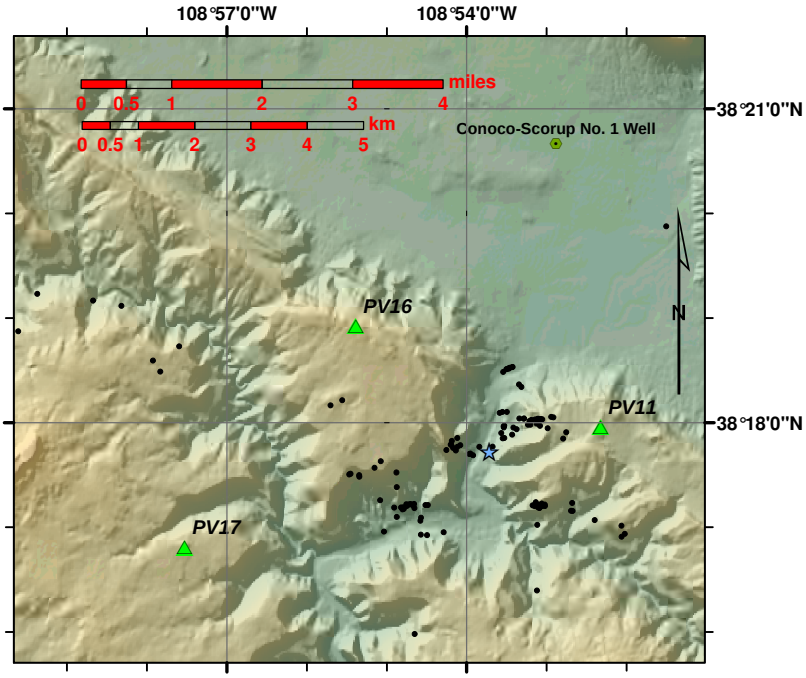

Figure 6-15 2000 January-May Epicenters. Star is injection wellhead.

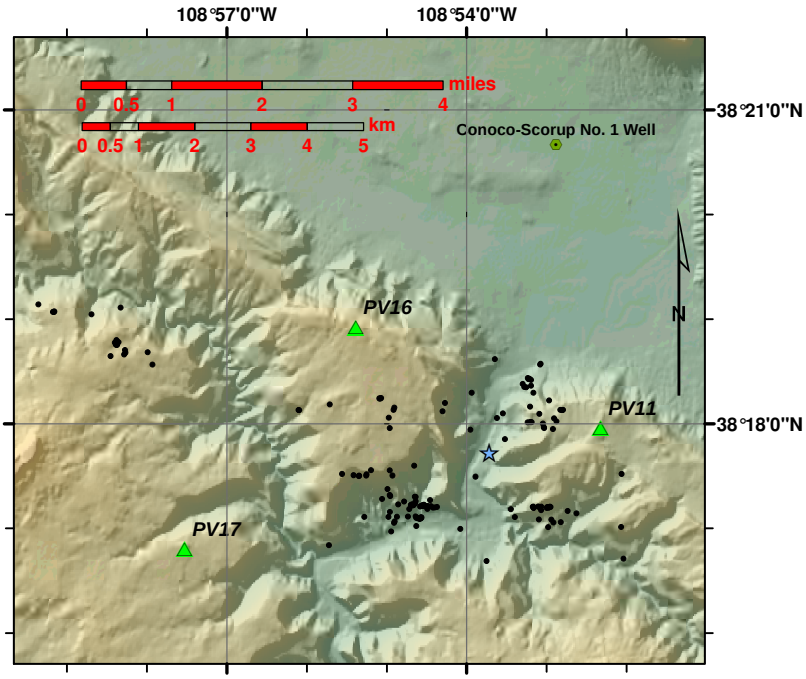

Figure 6-16 2000 June-December Epicenters. Star is injection wellhead.

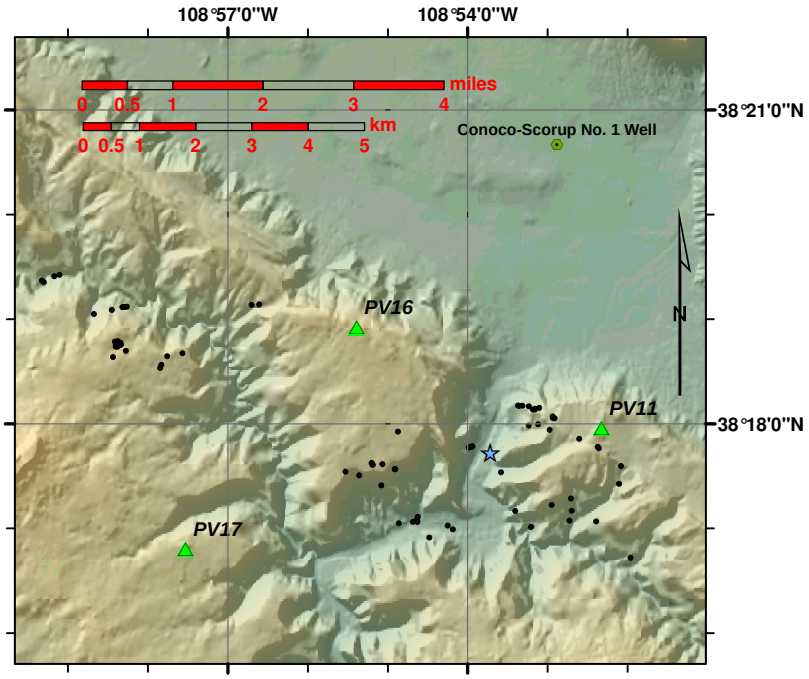

Figure 6-17 2001 Epicenters. Star is injection wellhead.

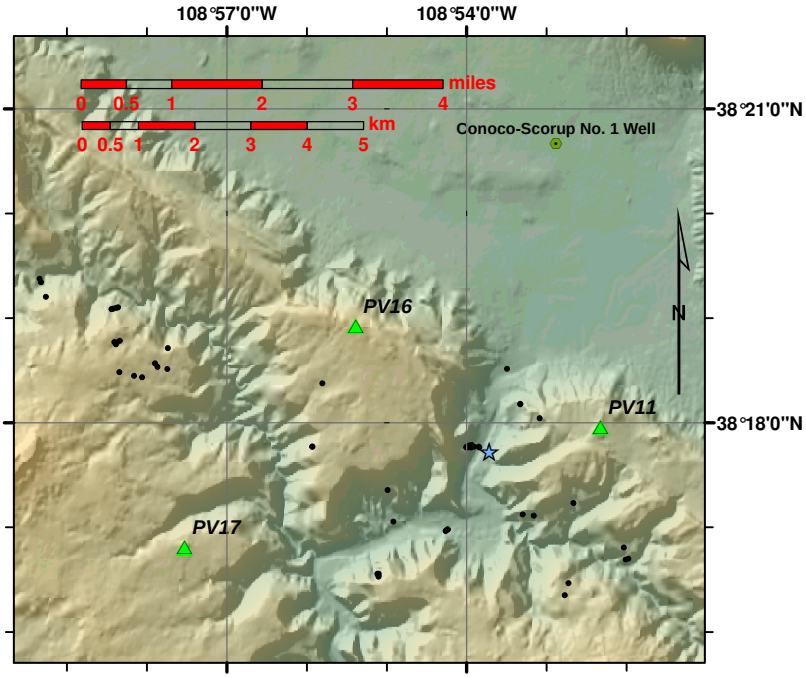

Figure 6-18 2002 Epicenters. Star is injection well head.

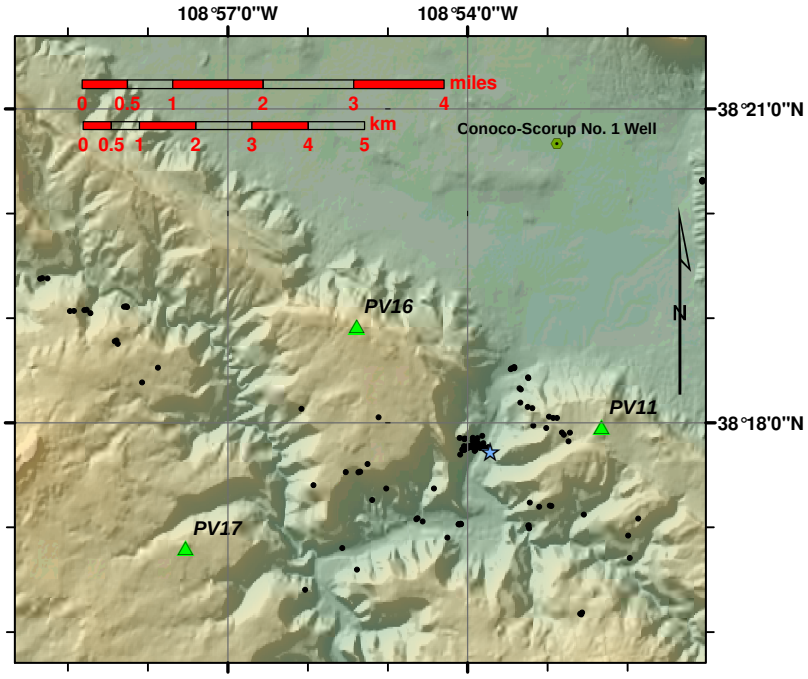

Figure 6-19 2003 Epicenters. Star is injection wellhead.

Table 6-5 shows the data and calculated *b*-values and **Figure 6-20** shows the calculated cumula-

Table 6-5 Number of Events by Magnitude Range and Pumping Phase Used in Calculating Earthquake Recurrence Curves (Figure 6-20)

Magnitude Ranges	**All** (7/96-12/04)	***Phase I*** (7/96-7/99)	***Phase II*** (7/99-7/00)	***Phase III*** (7/00-1/02)	***Phase IV*** (1/02/-12/04)
	no. events	no. events	no. events	no. events	no. events
0.5-0.9	1209	877	152	74	106
1.0-1.4	548	355	48	39	106
1.5-1.9	221	141	23	20	37
2.0-2.4	83	51	11	3	19
2.5-2.9	18	8	6	1	3
3.0-3.4	0	0	0	0	0
3.5-3.9	3	2	0	0	1
4.0-4.4	1	0	1	0	0
***b*-value**	0.892	0.963	0.901	0.858	0.651

tive recurrence data, linear fits to the data (solid lines), and back projection of the linear fits (dashed lines) for small magnitude events, respectively for the **Table 6-5** data. The *b*-value relates the change in the number of earthquakes with a unit change in magnitude. In **Figure 6-20** we plot the data such that the *b*-values are annualized (i.e., relate the change in the number of earthquakes *per year* with a unit change in magnitude). In most tectonic settings, the *b*-value is typically about 1 which means each unit change in magnitude corresponds to a factor of 10 change in number of events. For a *b*-value of 0.8, the factor changes from 10 to 10 x 0.8 or 8.

Figure 6-20 uses all the events recorded since continuous injection began through the end of 2004 and for each of the injection phases described above. These calculations assumed a maximum magnitude of 5. The flattening in the data at **M** 0.5 suggest that **M** 0.5 is the lower detection threshold of PVSN (i.e.,below ~**M** 0.5 ground motion is small and, although, some Paradox events are detected, some are not.)

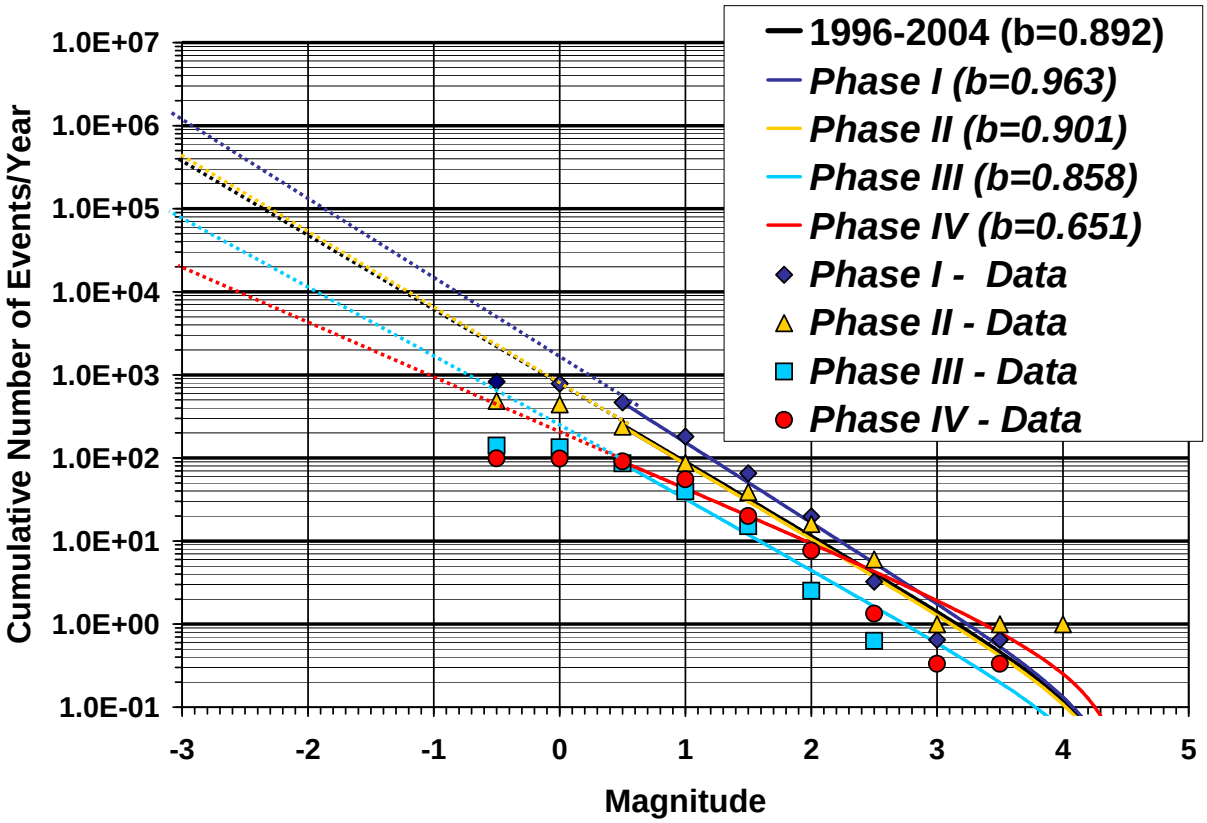

Figure 6-20 Cumulative Recurrence Curves for PVU-Induced Earthquakes, 1996 through 2004, and for Each Injection Phase. Colored symbols are data by phase; solid lines are statistical fits to the data; and dashed lines are projections of the solid lines to magnitudes below PVSN's detection threshold.

The *b*-values for *Phases I*, *II*, and possibly, *III* in **Figure 6-20** are consistent with observations of earthquake recurrence within the seismically inactive Colorado Plateau (Wong and others, 1996; LaForge, 1996). This similarity of the Paradox *b*-values to other studies in the Colorado Plateau supports the concept that during *Phase I*, *II*, and *III*, many of the induced earthquakes at the Paradox site were due primarily to the release of tectonic shear-stress. This observation agrees with our source (i.e., focal mechanism) studies of the PVSN data discussed below. However, the *b*-value for *Phase IV* is significantly lower than the earlier phases. This may mean a change in the nature of the induced seismicity. We are still investigating this possibility.

6.10 Focal Mechanisms - Preliminary Analysis

The waveforms of the 2004 data are consistent with previous years. Hence we did not feel a need

to calculate new fault plane solutions. For a complete discussion see Mahrer et al., 2004 (on attached CD).

6.11 Focal Mechanisms - Advanced

Focal mechanisms for the entire data set were calculated using *P*-wave first motion polarities and S_V/P amplitude ratios on vertical component seismograms (Kisslinger, 1980; Kisslinger and others, 1981). This has been discussed in detail in previous report (Mahrer et al., 2004: on attached CD) and is not included here.

6.12 Induced Event Slip Mode

The source mechanics of the PVU earthquakes recorded by PVSN is shear slip on existing faults and fractures. These faults are not sufficient to hold the volume of injectate emplaced at PVU. Hence, within the formations, the injection process creates additional "volume" (i.e., new fracture and pore space and open existing fractures and existing pore space) to accommodate the injectate. This means injection creates and opens tensile fractures (i.e., hydraulic fractures) into which the injectate squirts. The question then arises: Is any portion of the seismicity recorded by PVSN due to these tensile events? Based on oil and gas field hydraulic fracture studies run at pressures comparable to PVU injection pressure, the hydraulic fracture opening or aperture is on the order of a few millimeters, at most. With this size opening and subsequent fluid squirt, the (new) surface area of a fracture is on the order of 10's of square centimeters, or less. Based on calculation of seismic moment (Wells and Coppersmith,1994), **Figure 6-21** shows the slippage on surfaces this size will generate tiny events and these events will radiate minimal seismic energy. At the ground surface, this radiation is well below the detection threshold of PVSN. In addition, based on the area of the opened fracture, this radiation is in the frequency band of a few 100 hertz to a couple of kilohertz. As discussed previously, the recording systems at PVSN operate at frequencies below a few 10's of Hz and lower. Hence, based on the focal mechanics studies and the aforementioned arguments, the results of this fracture mechanics argument are consistent with the PVSN data: the ground motions recorded by PVSN are due to shear events, not tensile openings.

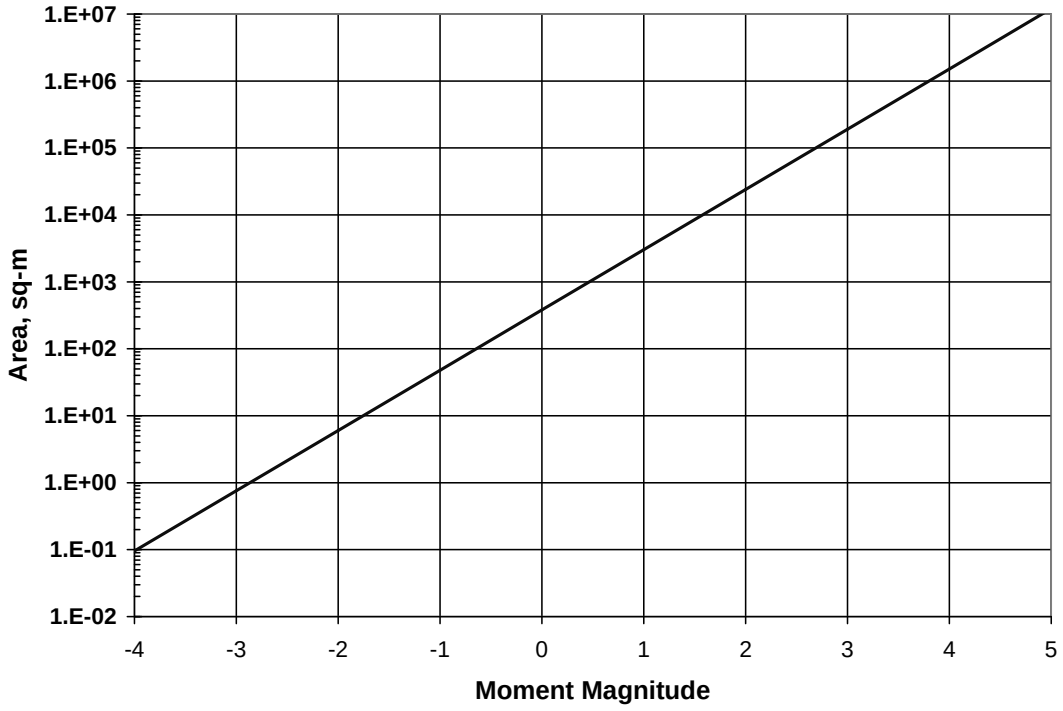

Figure 6-21 Earthquake Fault (i.e., Slip) Area Versus Earthquake Size (i.e., Moment Magnitude). The line is extrapolated from Wells and Coppersmith (1994)

6.13 Seismic Magnitude versus Location

With the highly accurate event location data, how do the locations correlate with event magnitude? **Figure 6-22** and **Figure 6-23** show all events a magnitude **M** 1.7 and greater plotted against a background of all the events. **Figure 6-22** is a plan view and **Figure 6-23** is a depth cross section looking north. Note in these figures that not all of the seismically-illuminated, linear features (i.e., the faults and fractures seismically activated by PVU injection) host larger events. Only a subclass of the fractures and faults have larger events. Also, some of the fractures and faults have many larger events and some have only one or two. Initially we expected the larger events to be more uniformly distributed. Also note that a disproportionately larger number of larger events occur in the secondary seismogenic region, ~8 km to the northwest of the injection well.

6.14 Swarm Analysis

For some years we have noted that some regions within the seismogenic zone surrounding the

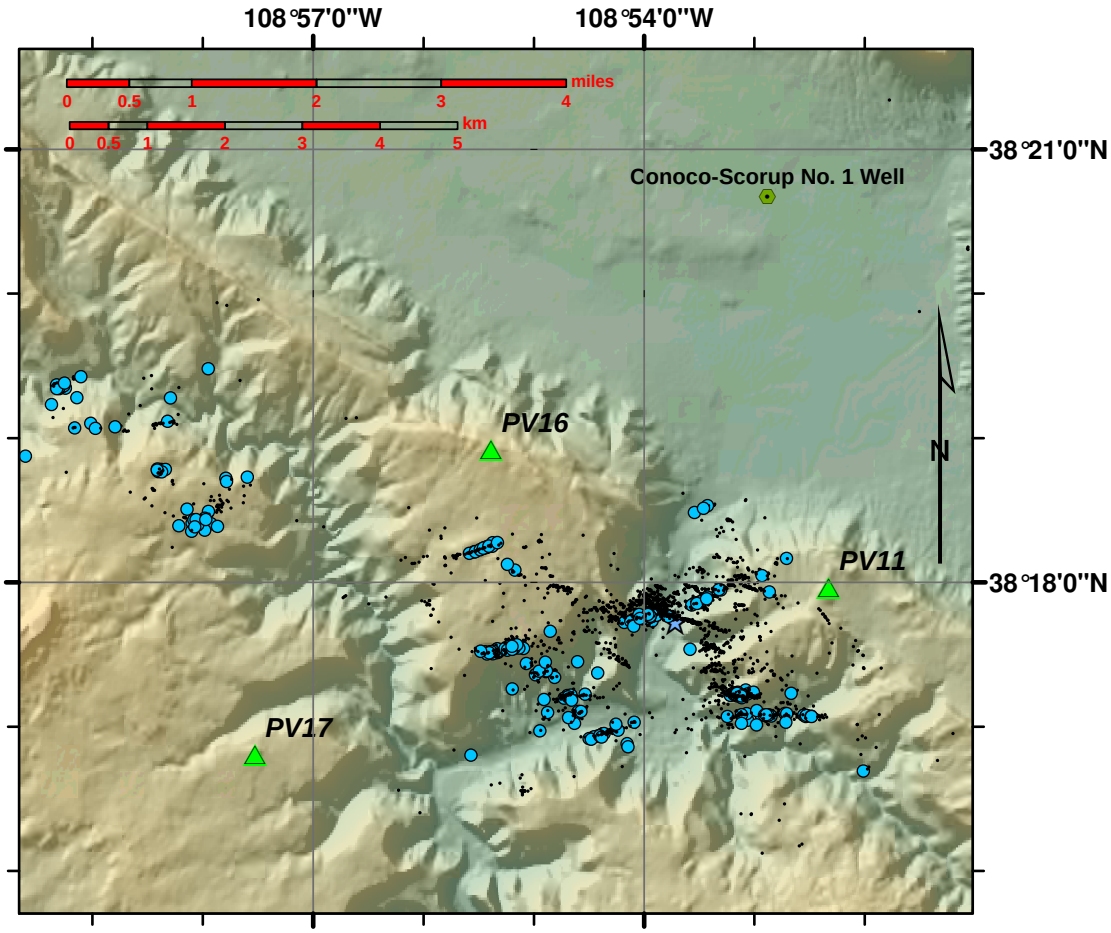

*Figure 6-22 PVU Epicenter Map of Events with Magnitude **M** 1.7 and Greater (blue circles) Superimposed on All of the Seismicity. Note that the larger events only occur along a limited subset of the faults illuminated by the induced seismicity.*

injection well seem to vacillate between active and inactive. During 2003 we isolated a region that seems to respond directly to large-scale changes in injection; during 2004 this region witnessed 7 events. We have defined the region as a square region running from -0.2 km south of the well to 0.5 km north of the well and west from the well to -0.7 km (i.e., area = ~0.5 km^2); in map view, the region is shown in **Figure 6-24**. **Figure 6-25** shows a close up of the swarm zone showing the 7 2004-events against all the events, 1991-2003. Since 1996, this region has generated ~690 or ~18% of the near-wellbore events. By comparison, it covers less than 5% of the near-well seismogenic zone.

We have found that within the region designated in **Figure 6-24** and **Figure 6-25**, the seismicity is very responsive to wellbore injection. **Figure 6-26** shows the downhole pressure (since 1996) and

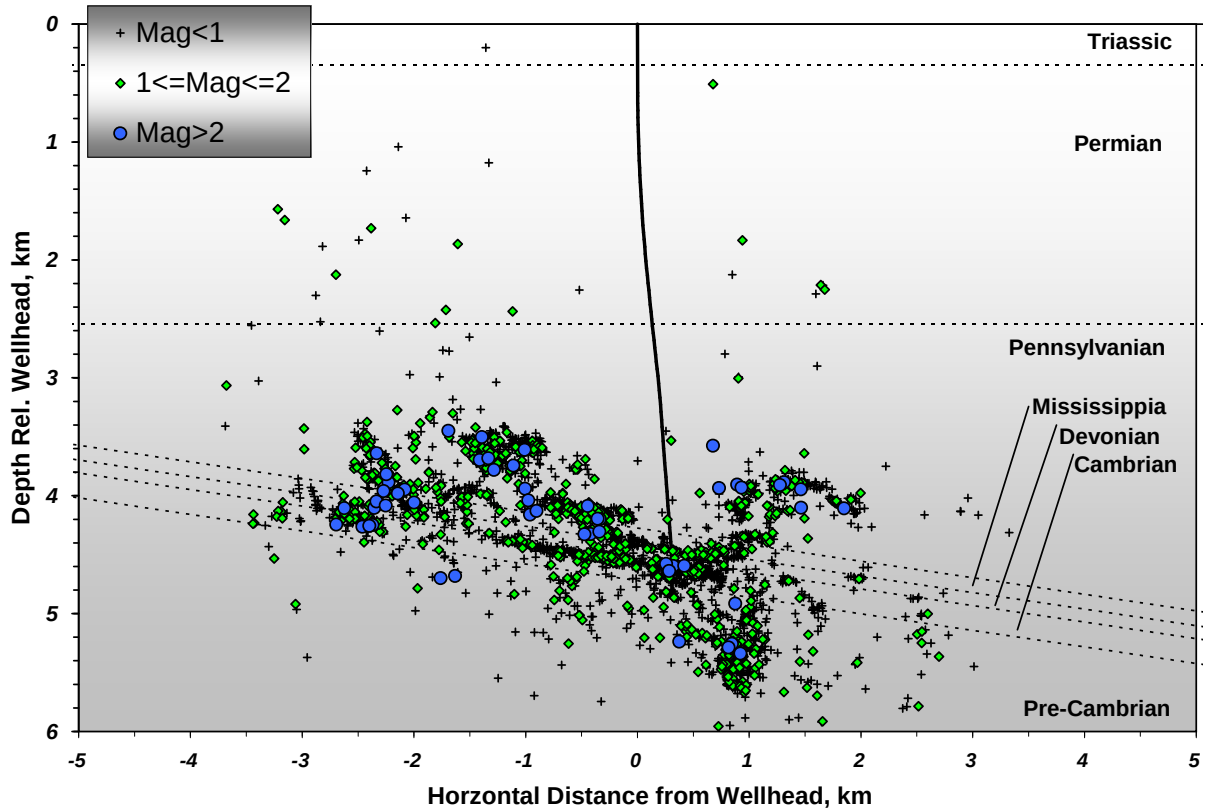

Figure 6-23 Depth Cross Section of Event Locations Looking North. Events are shown by magnitude range. Superimposed is the dipping stratigraphy (10°) based on projected data from the injection well logs and does not indicate the faulting structure. Note that the larger events only occur along a subset of the faults illuminated by the induced seismicity.

the occurrence times of events (yellow diamonds) within the swarm region (see **Figure 6-24** and **Figure 6-25**). To prevent confusion, the y-axis location of the occurrence data is arbitrary. The only important parameter of the occurrence data is time. Note how closely the gaps in the occurrence data follow the gaps (i.e., shut downs) in the pressure data. When the injection is shut down, the swarm region very quickly stops being seismically active. Normally, the delay between seismic response and injection cessation is much longer, weeks to months. In this swarm zone, this time delay is hours to a few days. Note also in **Figure 6-26**, when the downhole (injection) pressure is below a threshold of about ~80 MPa (~11,600 psi), the region becomes inactive even though PVU is still injecting.

6.15 Remote (Northern) Seismic Swarms

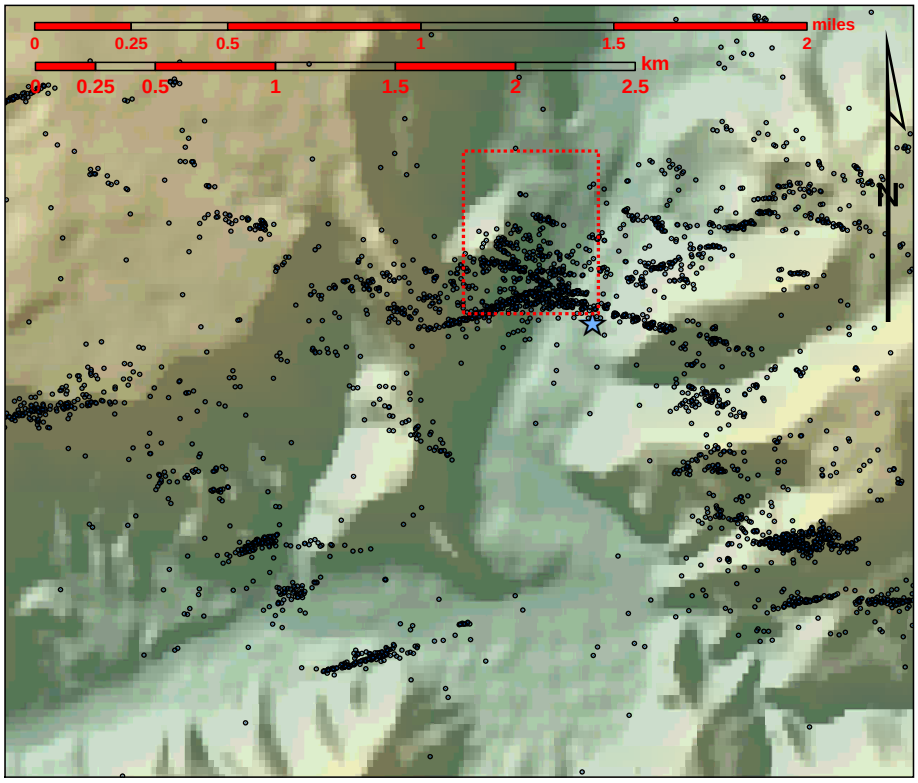

Figure 6-24 Square Region [Red with Boundaries Relative to Injection Well (star) @ North: (+0.5,-0.2) km; East (0.0,-0.7) km] Identified as an Injection-Sensitive Active Swarm Zone.

PVSN is a local seismic network, but is not limited to only events near the injection well and injection-induced events. **Figure 6-27** shows events located between 10 and 20 km north of the injection well. During 2004 this region showed no activity. However, during 2003 this region saw active swarms. One was in January and consisted of 7 events spread over about 21 days. All the events were **M**1.8 or smaller, well below human detection. This swarm is centered ~11 km north and 3 to 4 km west of the injection well. The second swarm occurred in August '03 and consisted of 16 events spanning 6 days and all of magnitude **M**1.5 or smaller. In the figure it is a very tight swarm located ~10.5 km north and ~1 km east of the injection well (northeast of PVSN station PV04). At this time, we believe these events are not induced by the PVU injection. Harr and Bremkamp (1988) and the established seismicity induced by injection do not strongly support fluid or pressure migration to the north of the well. The shape and time histories of the induced seismic regions support pressure migration to the northwest. However, we add a minor note of caution. Although they don't predict it, neither Harr and Bremkamp's model nor the present

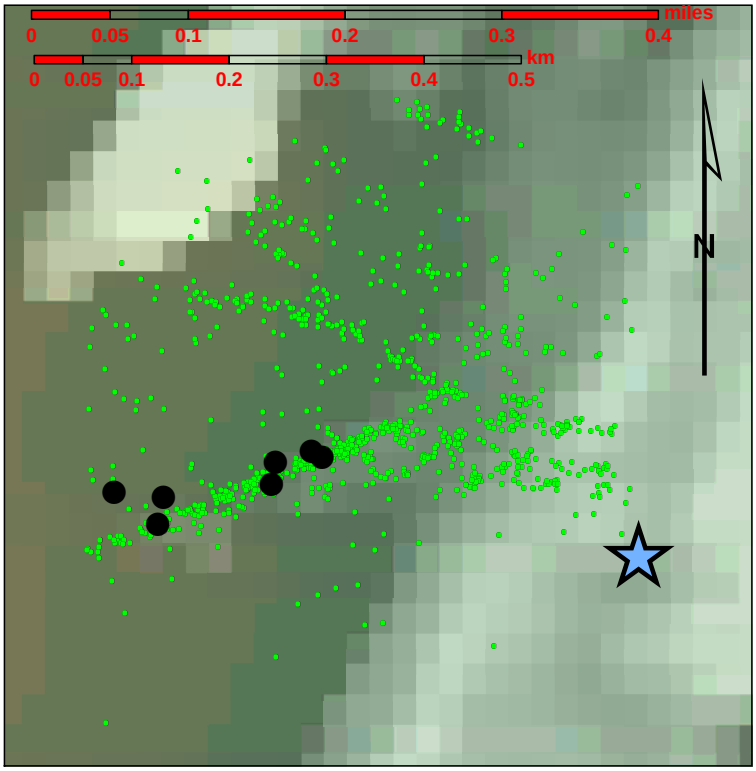

Figure 6-25 Close-Up of the 2004 Events (large circles) in Active Swarm Region Designated in Figure 6-24. Background data (small dots) are all events in region from 1991-2003. Star designates the injection wellhead.

extent of the induced seismicity preclude migration of the seismicity to the north. Also recall that in this area, PVSU recorded two events (**Figure 6-1**) between 1986 and 1991, the 5 years prior to injection.

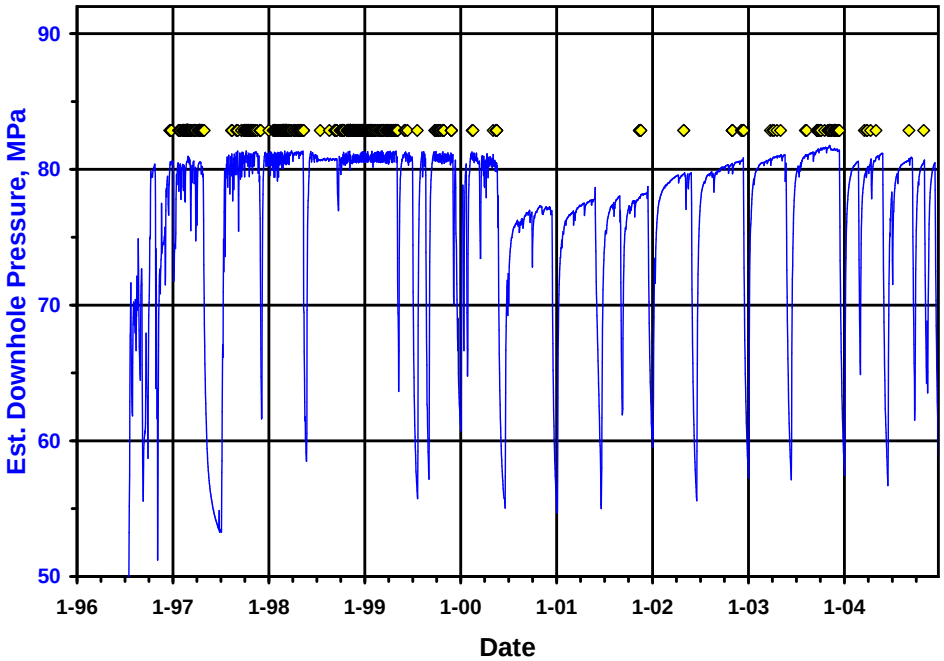

Figure 6-26 (Estimated) Downhole Pressure at 4.3 km (14,080 ft) Versus Date and Occurrence Time of Events (yellow diamonds) in the Swarm Region Shown in Figure 6-24 and Figure 6-25.

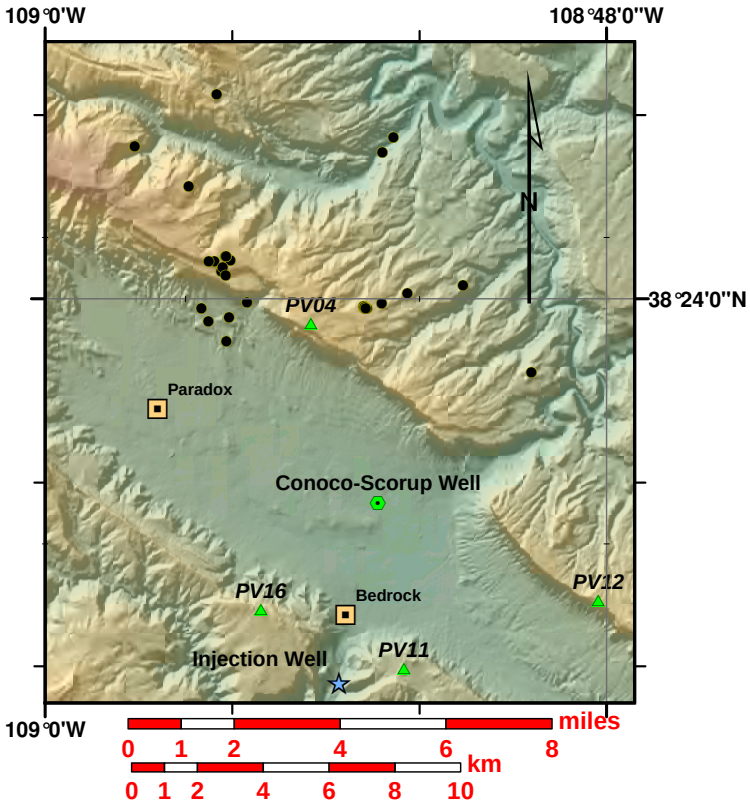

Figure 6-27 Seismically Active Swarms North of PVU Injection Well.

7.0 MODELING

7.1 Mohr Circle Analysis

7.1.1 General

[*Note*: Following is a short tutorial of the Mohr circle analysis based on Cosgrove (1995).] The Mohr circle is a graphical method for resolving the shear and normal stresses and the potential for shear and tensile failure; it is based on the maximum and minimum principal stresses of a system in compression. The equations that give shear and normal stresses from the maximum and minimum principal stresses result in a circle, the Mohr circle, when the principal (normal) stress are plotted on the x-axis and the shear stress on the y-axis of a graph (**Figure 7-1**).

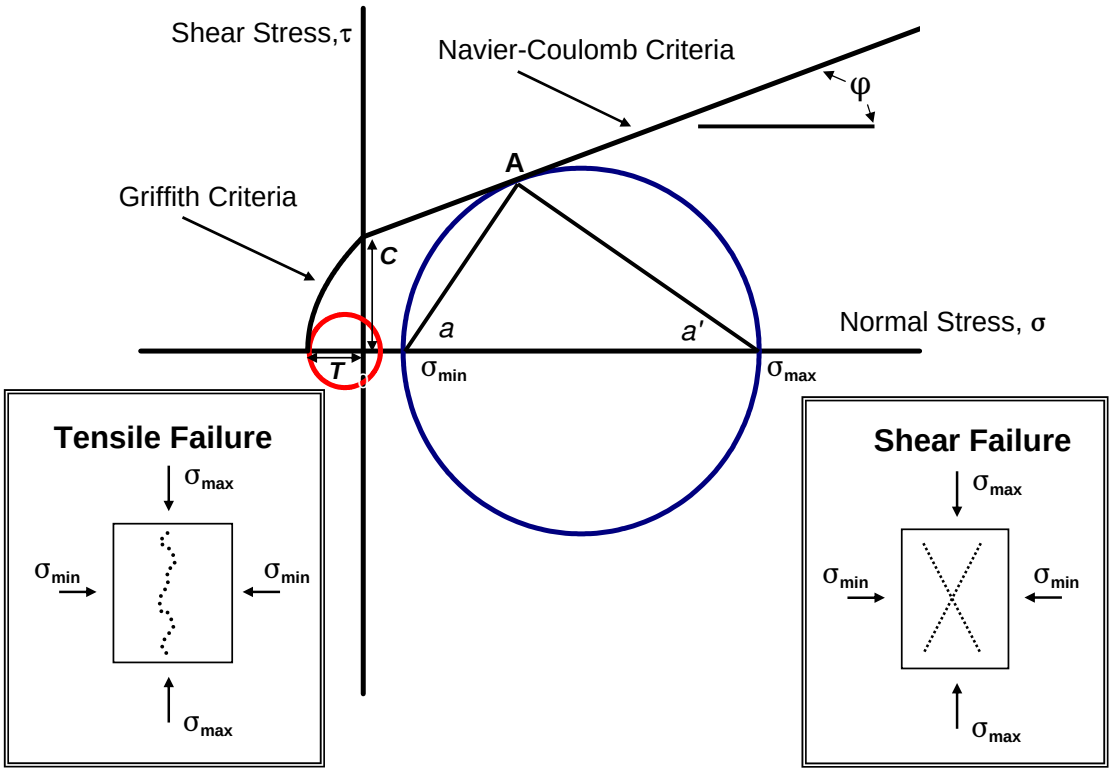

Figure 7-1 Tutorial Plot of Mohr Circles, Failure Criteria, Key Parameters.

To determine shear and tensile failure, respectively, we add the Navier-Coulomb criteria and the Griffith criteria, respectively, to the graph, as shown in **Figure 7-1**. The Navier-Coulomb criteria,

a straight line, is given by the expression

$$\tau = C + \mu \cdot \sigma_n \tag{7}$$

where τ is the peak shear stress of the eventual slip plane, C is the material cohesive strength of the rock (C=0 means no cohesive strength, a preexisting fracture), μ is the coefficient of friction of the slip plane and is frequently written as tan(ϕ) where is ϕ is called the friction angle (see **Figure 7-1**), and σ_n is the normal stress across the slip plane. The Griffith criteria, a curved surface on the left side of the graph (i.e. second quadrant) and which equals the Navier-Coulomb value at the y-axis, is given by the expression

$$\tau^2 + 4T\sigma_n - 4T^2 = 0 \tag{8}$$

where T is the tensile strength of the rock and is typically given as C=2T. As noted in **Figure 7-1**, the positive x-axis or right side of the figure corresponds to shear failure and the negative x-axis or left side corresponds to tensile failure. If the Mohr circle that describes a physical system is to the right of the Navier-Coulomb line (blue circle in **Figure 7-1**), then all fracture planes are locked by their own friction and cohesive strength. If one introduces fluid in the system through pore pressure then the Mohr circle is shifted to the left. The shift is by the amount of the pore pressure. If the shift results in the Mohr circle becoming tangent to the Navier-Coulomb line (point A in **Figure 7-1**), then a plane at a preferred angle to the maximum and minimum stress can fail (i.e., slip) in shear, as shown in **Figure 7-1** in the lower right side insert titled Shear Failure. From **Figure 7-1**, the angles **a** and **a'** give the angles of the shear failure plane with respect to the minimum and maximum principal stress, respectively: **a** = 45° - $\phi/2$ and **a'** = 45° + $\phi/2$. In order for tensile failure to occur, the Mohr circle must touch the Griffith criteria at the point $\tau = 0$, $\sigma_{min} = T$. As noted in the lower left insert in **Figure 7-1**, the failure plane will be in the direction perpendicular to the minimum principal stress. As one can see in the figure, the diameter of the Mohr circle is the maximum principal stress - minimum principal stress. For tensile failure to occur, this diameter, must be smaller than C, the cohesive (i.e., tensile) strength of the rock.

7.1.2 Paradox Injection and Mohr Circle

Figure 7-2 shows three Mohr circles for Paradox injection at 4.3 km (14,080 ft) depth. and two Navier-Coulomb failure criteria and one Griffith criteria. The solid line in the figure is the criteria for average parameters for competent (i.e., unfractured), intact limestone, as given by Hendron

(1968, p. 33) and Goodman (1980, p. 78). These are friction angle of 40° and cohesive strength of ~21 MPa. (~3050 psi). The dash failure criteria in the figure assumes the same friction angle, but with no cohesive strength.

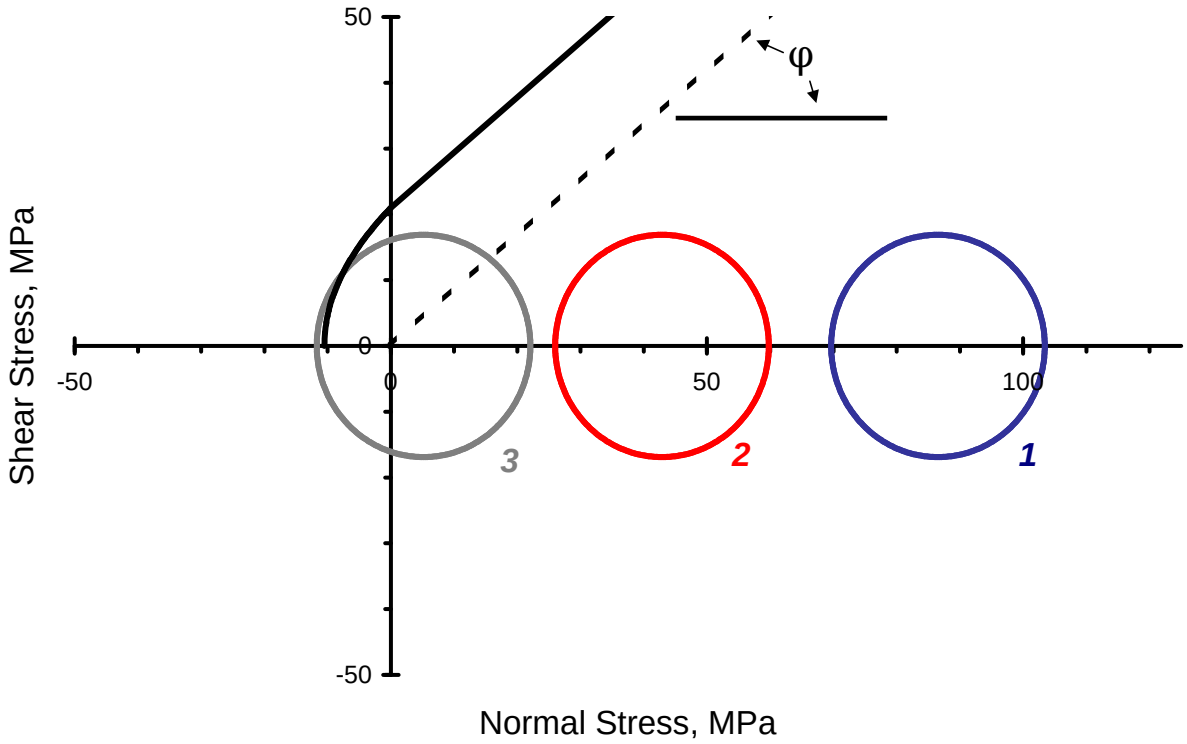

Figure 7-2 Mohr Circle Plots for Three Different States (numbered circles, see text), Navier-Coulomb (straight lines) and Griffith Failure Criteria (solid curve in second quadrant) for Average Limestone and Depth of 4.3 km Below the Surface.

Circle number 1 in **Figure 7-2** is the state of stress inferred from the well logs of mechanic properties and the inferred minimum fracture pressure (i.e., least principal stress, Envirocorp, 1995) with no fluid pressure included. Well logs estimates the assumed lithostatic or maximum principal stress as vertical and ~103 MPa (15,000 psi or 1.07 psi/ft); a hydraulic fracture test gave the least principal stress, which is horizontal, and found to be ~69.6 MPa (10,100 psi or 0.72 psi/ft). Circle 1 is totally to the right of the failure criteria and therefore, in the absence of (additional) fluid pressure, there would be no slippage across any planes. Circle 2 is the same as circle 1 but with additional fluid pressure. The pressure here is the Leadville Limestone (native) aquifer pressure at 4.3 km, ~43.6 MPa (6330 psi or 0.45 psi/ft). The addition of the native aquifer fluid pressure is not sufficient to cause failure. Circle 3 is the circle 2 with the addition of the average PVU downhole

injection (fluid) pressure (total fluid pressure = 81.4 MPa or 11,800 psi); note that portions of Circle 3 are to the left of the solid and dashed lines. Circle 3 shows that the injection pressure as PVU is sufficient to induce both shear and tensile failure.

7.2 (Projected) Total Seismic Event Production

One question that has been asked since the beginning of injection is how many microevents (i.e., events of magnitude -2.0 or -3.0 and greater) are generated by the injection. The observed PVSN data cannot answer this question, since its cutoff (i.e., smallest recorded events) ranges between **M** 0.0 and **M** -0.5, and the number of events recorded in this range is incomplete. We extrapolated the recurrence curve for the PVSN data at **M** 0.5 and greater, assuming that the Gutenberg-Richter relation (i.e., the number of events of a given magnitude are proportional to that magnitude raised to a power, the *b*-value discussed earlier) remains valid for microevents. In an earlier discussion we noted that extrapolating the 1996 and later PVSN data predicted roughly 600,000 total events of **M** -3.0 and greater for this period. However, we used a second method and we apply this method to all the PVSN data, which includes 1991-1995 data, with **M** 0.7 or greater. We used **M** 0.7 as the cutoff because we feel more confident in having a complete data set above this cutoff.

The new method is based on comparing the PVSN seismic data with seismic data from published *in situ* seismic monitorings of hydraulic fractures. Unlike the PVSN monitoring in which the seismometers are stationed at the surface, *in situ* monitoring has seismometers in wells neighboring the injection well and at or near the depth of injection. These neighboring wells can be less than 100 m from the injection well. Because of the proximity of the *in situ* seismometers to the injection, much smaller events are recorded than are recorded at the surface. Data from a series of 6 *in situ* monitoring were published by Phillips et al. (2002) and are shown in **Figure 7-3**.

Figure 7-3 shows number of seismic events produced as a function of injected volume from Phillips et al. (2002) and for Paradox. The Phillips data is divided into target zone rock type, crystalline and sedimentary, and the Paradox data is divided into the injection test data and the cumulative data, including test data plus the continuous injection data (solid red line). The dark blue dash line through the Phillips et al. data is a linear trend line. We projected a line, with the

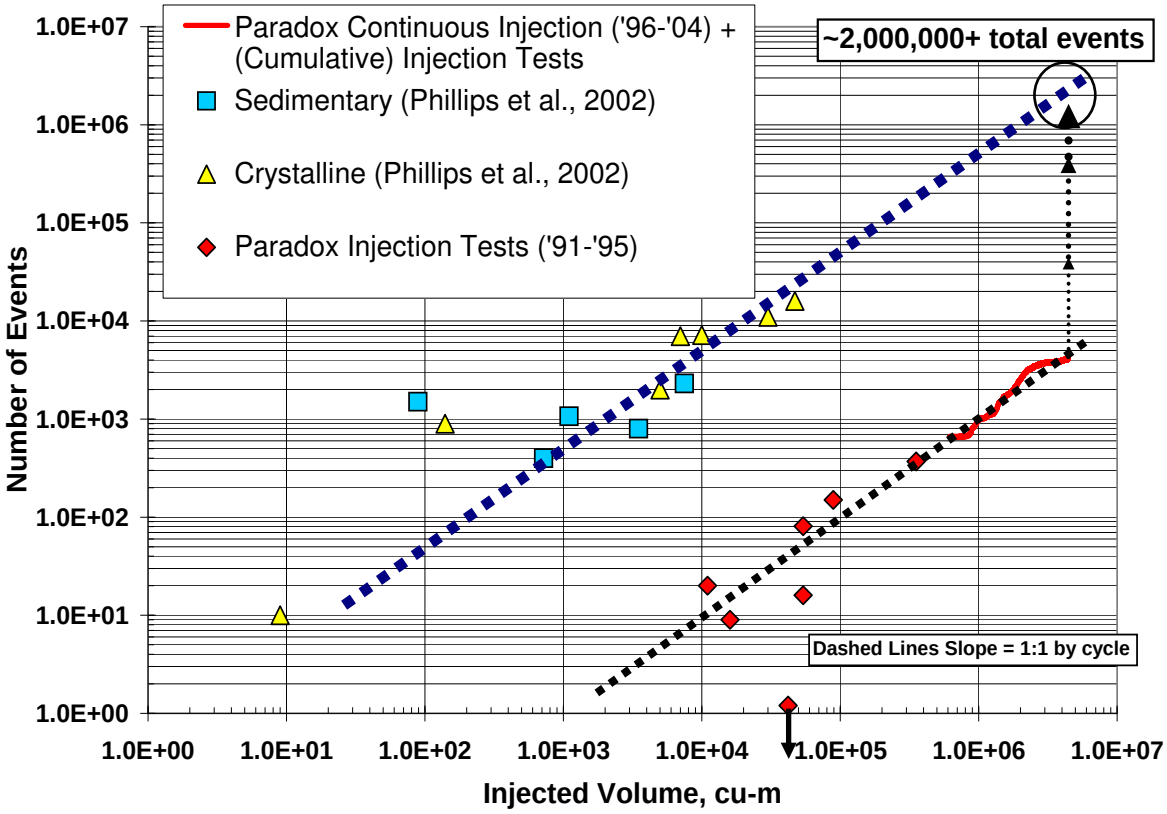

Figure 7-3 Cumulative Number of Seismic Events Produced During Deep, High Pressure Injections vs. Injected Volume. Data include in situ, at-depth and surface monitored (Paradox) injections. Lines are fitted to these data.

same slope as the Phillips et al. line, through the Paradox data. As the figure shows, it fit the Paradox data quite well. From the end of the (Paradox) red line we projected a vertical line (dashed and arrowed line in the figure) to the Phillips line. The intersection point of the Phillips et al. line and our arrowed line, indicated by the circle, is an estimate of the total number of events we would record at Paradox, if we had an *in situ* seismometry. This number is ~2,000,000 events. We then looked for the 2,000,000-events point on the back-projected recurrence curve for all the Paradox data (1991-2004), not the 1996-2004 data discussed above, and found this corresponded approximately to magnitude **M**-2.3. As a means to gage an **M**-2.3 event, we calculated an approximate area (see next section) and found its diameter (assuming a round or penny-shaped flip area) to be on the order of a few meters.

7.3 A Fractal Model to Accommodate Injectate Volume

7.3.1 Background

Since inception in 1991, PVU has injected ~4.4×10^6 m^3 of fluid. To accommodate this volume, consider a first-order approximation of a 2-km tall fracture uniformly opened 2 mm; this model requires ~1,000 km of fracture length! Looking at a map of the seismicity at Paradox, we find between 10 and 20 km of seismically-illuminated fault and fracture length and maybe 20 to 30 km of implied fault length (i.e., making robust assumptions about the main and non-seismically activated faults of the Wray Mesa system). These faults and fractures are not 2 km tall, but if we error on the side of conservatism and put an upper bound on fault height of 2 km, we find, at most, only a few percent of the total injected volume can be accommodated by the known and implied fractures, faults, joints, etc. This then begs the question of where the remaining ~95+% injectate resides. Typically injectate leaks through the walls of the main and illuminated fractures, faults, etc. into the native porosity. However, the native porosity (i.e., pre-injection small fractures and pores) for the target formations at PVU is very small. Since the injection pressure at PVU is in excess of that necessary to nucleate and grow hydraulic fractures in the target rocks, we surmise that the PVU injection is fracturing the target horizons, creating new fractures and opening preexisting but closed regions of weakness (i.e., creating new volume space to accept most of the injectate). Similar to the creation of new fracture volume at PVU, Turcotte (1997) discusses fragmentation/fracturing processes and shows that fracturing typically results a fractal distribution of fracture sizes. Following Turcotte, we developed a fractal model of fracture sizes for PVU.

7.3.2 Mathematical Foundation

The concept of fractals were first developed when it was recognized that special figures or shapes could be created whose length did not decrease under increasing magnification. Said a bit differently, under ever increasing magnification, the sides of these figures continued to show new curvature not visible under the previous magnification. If one traces (i.e. approximates) these figures with straight lines, the length of the straight lines become small, but the number of straight lines increases faster than the rate their length diminish. These figures exhibit fractal behavior. This

concept is captured in the following equation

$$N = cr^{-D} \tag{9}$$

where N is the number of entities being considered (we will consider penny-shaped fractures), c is a proportionality constant, r is a size associated with the entities (we will use r = radius of fracture wall), and D is the fractal dimension. D is an elusive parameter to define. Physically the equation describes how a distribution or group of entities fills space. For example, common geometric figures (i.e., non-fractal figures) like circles or squares have an integer fractal dimension of 2, since they are 2-dimensional bodies and fill a space as 2-dimensional bodies. Similarly, spheres or cubes have fractal dimensions of 3, since they are 3-dimensional bodies. A fractal (e.g., distribution of fractures) typically has a non-integer fractal dimension of between 2 and 3. This means if one can find a figure that emulates this distribution, the figure fills a space more completely than a 2-dimensional body and less completely then a 3-dimensional body. (A bit confusing? But that's the best the fractal gurus can offer.) Mathematically, for a fractal distribution, as developed here, D determines the increase (decrease) in number of entities in the distribution as one increments (decrements) to the next smaller size of the distribution. Note that incrementing to the next smaller size is equivalent to viewing at the next magnification step.

For the model we developed, we incremented the fracture radii in decadal increments (i.e., powers of 10). At two adjacent steps or levels in radii, r_i and r_{i+1},

$$N_{i+1}/N_i = (c(r_{i+1})^{-D})/(c(r_i)^{-D}) \tag{10}$$

which simplifies to

$$N_{i+1} = N_i \cdot (r_{i+1}/r_i)^{-D} \quad \text{since } (r_{i+1}/r_i) = 10 \tag{11}$$

To complete equation (11), we determined an initial value, N_o, for the fracture distribution. As is common for this type of modeling we will assume a thin, circular fracture or penny-shaped fracture. Based on the seismicity, we assumed an initial fracture radius of 100 m. Using an equation

from Wells and Coppersmith (1994) that relates the magnitude **M** of an earthquake and the area of slip with radius r

$$\mathbf{M} = 4.07 + 0.98 \times Log_{10}(\pi r^2) \tag{12}$$

we find that for radius of 100 m, M = ~2.6. From our seismic data we have ~20 events with M = ~2.6. Hence, we fixed N_o at 20.

7.3.3 Calculations

We begin the calculations with 20, r = 100 m penny-shaped fractures (i.e., N_o) and use equation (8) to determine N_1, the number of 10-m fractures. Then from N_1 we would calculate N_2 for 1-m fractures etc. We would calculate down to a radius of 0.01 mm. To do this calculation we need the fractal dimension D, which we have not computed, yet. To determine D, we used another fixed condition or parameter of this model, the injected volume. We solved for D by initially guessing a D and then calculating the volume of the fractures and comparing it to the injectate volume. We then adjusted D until the fracture volume approached the injectate volume as closely as possible limiting D to two decimal accuracy. To determine the volume of the fractures we assumed penny-shaped fractures with the aforementioned decadal increment in radius and fixed fracture openings. We separately calculated models with 1, 2, and 3 mm openings for all fractures with 10 mm or larger radii and assumed $0.1r$ openings for all smaller fractures. To make each model more realistic we included 3 10-km long by 1 km high (i.e., the major or through-going Wray-Mesa style faults). During the calculations, each of these faults had the same aperture as the fractally distributed faults. The results of the calculations found D equal to 2.76, 2.66, and 2.60 for apertures of 1 mm, 2 mm, and 3 mm, respectively. **Table 7-1** gives the results of the calculation noting the corresponding earthquake magnitude (Wells and Coppersmith, 1994; equation (12)) for each size fracture, if the fracture slipped; the cumulative percent volume of injectate corresponds to the total volume for each fracture size; and the number of fractures of that size, all for each of the 1-mm, 2-mm, and 3-mm models. **Figure 7-4** shows additional results of the model. In that figure, the Paradox data with magnitudes less than 0.0 are linearly projected from the data with magnitudes greater than 0.0.

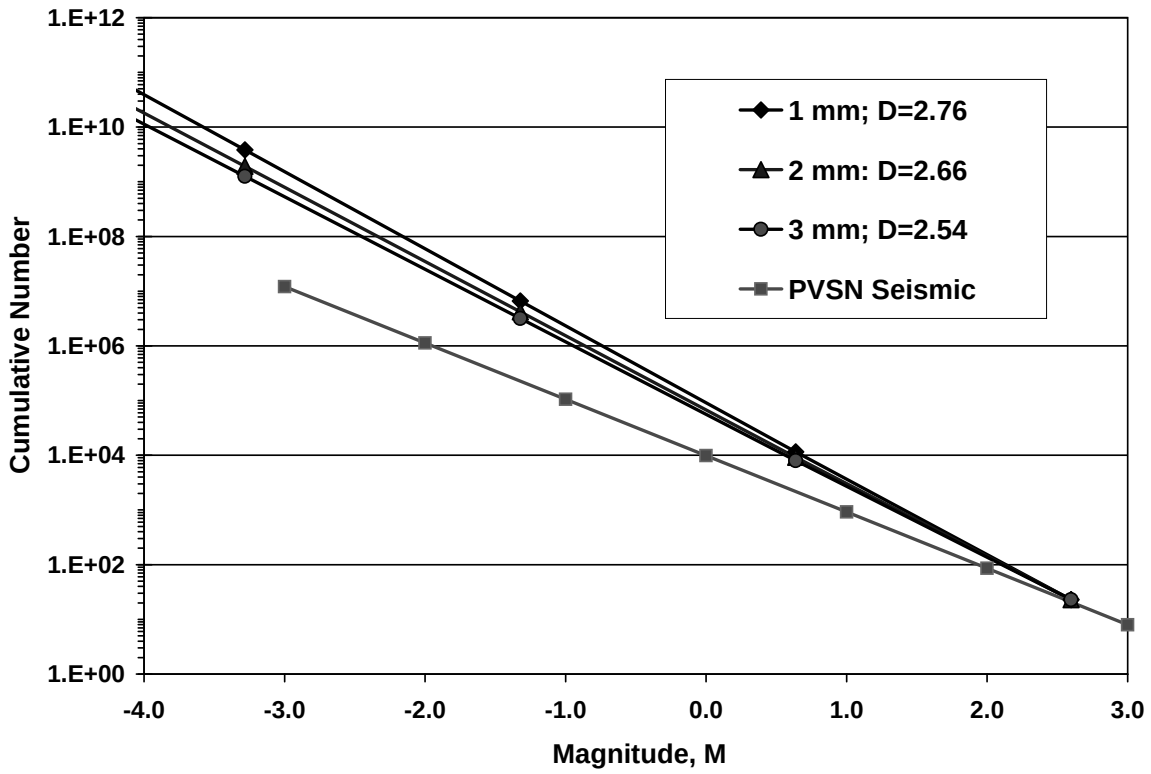

Figure 7-4 Comparison of Cumulative Number of Fractures for Various Fractal Model and PVSN Seismic Data, all versus Event Size. For the Fractal Model Magnitude is Calculated Assuming Each became Seismically Active

Table 7-1 Fractal Model Results

		Fracture Opening Models					
Radius	**W&C[a]**	**1-mm**		**2-mm**		**3-mm**	
mm	**Eq. Mag.**	**Cum.% Volume[b]**	**No. Fracs.**	**Cum.% Volume[b]**	**No. Fracs.**	**Cum.% Volume[b]**	**No. Fracs.**
1.0e+5	**M**2.6	0.02%	20	0.04%	20	0.06%	20
1.0e+4	**M**0.6	0.11%	1.1e4	0.18%	9.1e3	0.23%	8.0e3
1.0e+3	**M**-1.3	0.65%	6.6e6	0.82%	4.2e6	0.93%	3.2e6
1.0e+2	**M**-3.3	3.7%	3.8e9	3.8%	1.9e9	3.7%	1.3e9

[a]Wells and Coppersmith (1994) fault area-magnitude relation, equation (12)
[b]Percentage of injectate total volume; cumulative total given at bottom of column

Table 7-1 Fractal Model Results

		Fracture Opening Models					
Radius	**W&C[a]**	**1-mm**		**2-mm**		**3-mm**	
mm	**Eq. Mag.**	**Cum.% Volume[b]**	**No. Fracs.**	**Cum.% Volume[b]**	**No. Fracs.**	**Cum.% Volume[b]**	**No. Fracs.**
1.0e+1	**M**-5.2	21.5%	2.2e12	17.1%	8.7e11	14.8%	5.0e11
1.0	**M**-7.2	12.4%	1.3e15	15.7%	4.0e14	17.7%	2.0e14
1.0e-1	**M**-9.2	7.1%	7.3e17	7.2%	1.8e17	7.0%	8e16
1.0e-2	**M**-11.1	4.1%	4.2e20	3.3%	8.3e19	2.8%	3.2e19
		99.5%		96.1%		94.5%	

[a]Wells and Coppersmith (1994) fault area-magnitude relation, equation (12)
[b]Percentage of injectate total volume; cumulative total given at bottom of column

7.3.4 Fractal Model Implications

We recognize that the results in **Table 7-1** are based on very speculative premises, but it is very interesting to note that for all the fracture opening models, ~90% of the injectate is emplaced in fractures of 1 mm in radius or greater. If this is true, it is quite significant. It shows that at Paradox, the small to interstitial sized porosity, which is negligible, is fortunately not a factor in the operations and life of this reservoir. What is important, is maintaining the injectate pressure above the fracture pressure and creating new fracture volume in which to emplace the injectate.

Another interesting result of this model is that the fractal dimension *D* is a dynamic parameter. As more injectate invades the reservoir, *D* must increase. This assumes that the size of the reservoir is not increasing. Fortunately, the results given in **Table 7-1** are very sensitive to fractal dimension. A very small increase in D gives a substantial increase in fracture volume. Despite making this statement, further analysis is warranted. Consider the calculated number of fractures with radius 10, 1 and 0.1 mm, respectively. Roughly, each corresponds to 10^{12}, 10^{15}, and 10^{17}, respectively. In a volume of 20 km^3, this corresponds to an average fracture density of one 10-mm fracture per

$2x10^4$ cm^3, one 1-mm fracture per 20 cm^3, and five 0.1-mm fractures per cm^3, respectively. Even at 10 times the current cumulative volume (~80+ years of injecting), this model says there is still plenty of room in the reservoir to accommodate the necessary fractures (i.e., future injectate volume).

The results shown in **Figure 7-4** imply that many more fractures are created than are seismically activated. Recall that the projected number of seismic events in **Figure 7-4** is based on the number of events, specifically shear failures, that are recorded at the surface. The difference between the number of projected seismic events and the number of modeled fractures is consistent with our understanding of fracturing. Fractures most easily open against the smallest or least principal stress. The direction of fracture opening is a principal stress direction, meaning it has no shear stress across it faces and no tendency to slip dynamically, radiating seismic energy. However, once a fracture has been created, the local stress field may change with shear stress developing across the fracture face. If the shear stress becomes large enough to overcome the friction across the fracture, then the fracture can slip and radiate seismic energy. We are presently considering a model in which stress readjusts due to inflation from the injectate.

7.4 Injection Data and Fracture Modeling

As noted earlier, the 2004 seismicity generally locates within the zone defined by previous years' seismicity. From this we assume that the extent of the injectate envelope is stable or expanding very slowly, therefore much of the region occupied by the 2004 injectate lies within the envelope defined by the extent of the seismicity. That is, the new volume (i.e., rock fracturing) caused by the injectate is probably occurring within the well-centered seismogenic zone defined by the seismic envelope of previous years. The persistent spatial distribution of events suggests that the occurrence of induced earthquakes at this site (and hence fluid migration) is controlled by physical attributes, like stress, preexisting faults, planes or zones of weakness, etc., and is not a random process.

Supporting this are the results from BORFRAC, a computer code of Envirocorp (1995) that synthesized injection data based on formation parameters and fitted the synthetic data to real injec-

tion data from the 1991-1995 injection test sequence. BORFRAC synthesized the data by modeling the well and surrounding formations and their responses to high-pressure fluid invasion. In the initial BORFRAC model, Envirocorp assumed that injection created a traditional hydraulic fracture: a single vertical fracture divided into two wings, each wing extending from opposite sides of the well at the depth of the casing perforations. This model assumes that the injectate fills the fracture wings and diffuses into the formation through the native permeability of the fracture walls. This type of model predicts seismic locations confined to a very narrow elliptical envelope centered on the well and whose semi-major axial plane overlays the wings of the fracture. From the seismic data which showed a diffused network of locations, Envirocorp interpreted a network of injectate flow paths in the Leadville Formation and recognized that the traditional, double-wing model was not correct. Envirocorp upgraded the BORFRAC model from a single, double-winged fracture to a network of fractures. Using the network model, BORFRAC gave better agreement between the model data and wellbore injection data.

7.5 Seismicity, Fault Properties, and Injectate Volume

Between 1991 and the end of 2004, PVU injected ~4.4 billion liters (~1.17 billion gallons) of injectate. In response to the greater than 11,000 psi pressure, at the injection depth the injectate is compressed to ~95% of its surface volume or about 3.9 million cubic meters. As noted earlier, this volume of fluid must occupy existing space or create new space within the rock matrix. The question then is where is the injected fluid being stored, in existing space (e.g., faults, old fractures and joints, or existing pores), in new space (e.g., new fractures), or a combination of both? It is not likely that at 4.8 km (16,000 ft) depth with ~100+ MPa (~14,500+ psi) of overburden stress, there is much open space. To evaluate the existing-space hypothesis, we considered existing faults and the possibility of opening these faults.

In previous sections we showed that, in general, the injection-induced seismic events align in linear groups. We've interpreted these groups as delineating seismically-activatable faults and fractures of the Wray Mesa system. In addition, as an upper bound on available fracture and fault storage volume, we have interpreted these faults or fractures as having been reached by injectate. Noting, as discussed, the two major groupings, one surrounding the well and the other northwest

of the well, we've stated that it is likely that one or more northwestern fault(s) run(s) from the well group to the northwestern group. Based on our seismic map and the implied local faults of Bremkamp and Harr (1988), we tallied ~30 km of seismically-illuminated and implied fault length. We then assumed that the faults averaged about 0.5 km height, the height of the Leadville formation. To accommodate the full injectate volume would require opening these faults and fractures ~200 mm (~8 in). In this setting, this opening is grossly unrealistic. Based on recovered cores from hydraulic fracture experiments in the oil and gas industry (per. comm., Mike Sorrells, Teledyne Geotech), we expect the fault openings to be a maximum of a few millimeters.

If we assume that the 30 km of faults and fractures have openings between 1 and 5 millimeters, then, at any time, only a few percent of the injectate volume can be stored in these faults and fractures. This means that the injectate either has created new fractures or its has diffused into the pore spaces of the rock mass. Considering the new fracture scenario, we calculated the length of new fracture needed, assuming 0.5 km high fractures. The amount of new fracture is on the order of several thousand kilometers. This is a prohibitively large amount of fracturing. To realistically accommodate this much fracturing requires a fractal distribution for the new fractures, which we discussed earlier. A second scenario is that the fluid temporarily occupies the seismically-defined fractures and faults, and then slowly diffuses into the existing pore space of the rock. However, since we cannot quantify what percentage of fluid occupies new fractures and what percentage occupies pore space, we will assume all the injectate occupies fractures of a fractal distribution and show in the fractal model an upper bound on the amount of fracturing that is necessary to accommodate the injectate volume.

7.6 Seismicity and Effective Porosity

Our understanding is that most of the injectate eventually migrates (i.e., diffuses) from the pressure-opened fractures and faults into the rock mass (i.e., its effective porosity). To study the effective porosity we use the injection-induced seismicity.

As a first estimate for minimum necessary porosity we modeled the fluid volume as a 2-km tall vertical cylinder expanding radially by the addition of injectate. We assumed a 2-km height since

that is the vertical extent containing most of the seismicity. **Figure 7-5** shows the results, specifically the radius of the cylinder, assuming that the modeled, available porosity is being filled as the cylinder grows. To put this radius in perspective, the figure shows a number of features. First, the scatter data are the horizontal distance of the seismicity from the wellbore as a function of time. This shows the growth of the two seismic zones: the one surrounding the well and the one ~8.5 km to the northwest. For the diffusion model discussed below we only consider the zone surrounding the well. Next we've plotted the radii of five cylinders. Each cylinder corresponds to one of five porosities; in decreasing porosities these are 0.05%, 0.01%, 0.005%, 0.0025%, and 0.001%. From smallest to largest, these porosities span a factor of 50.

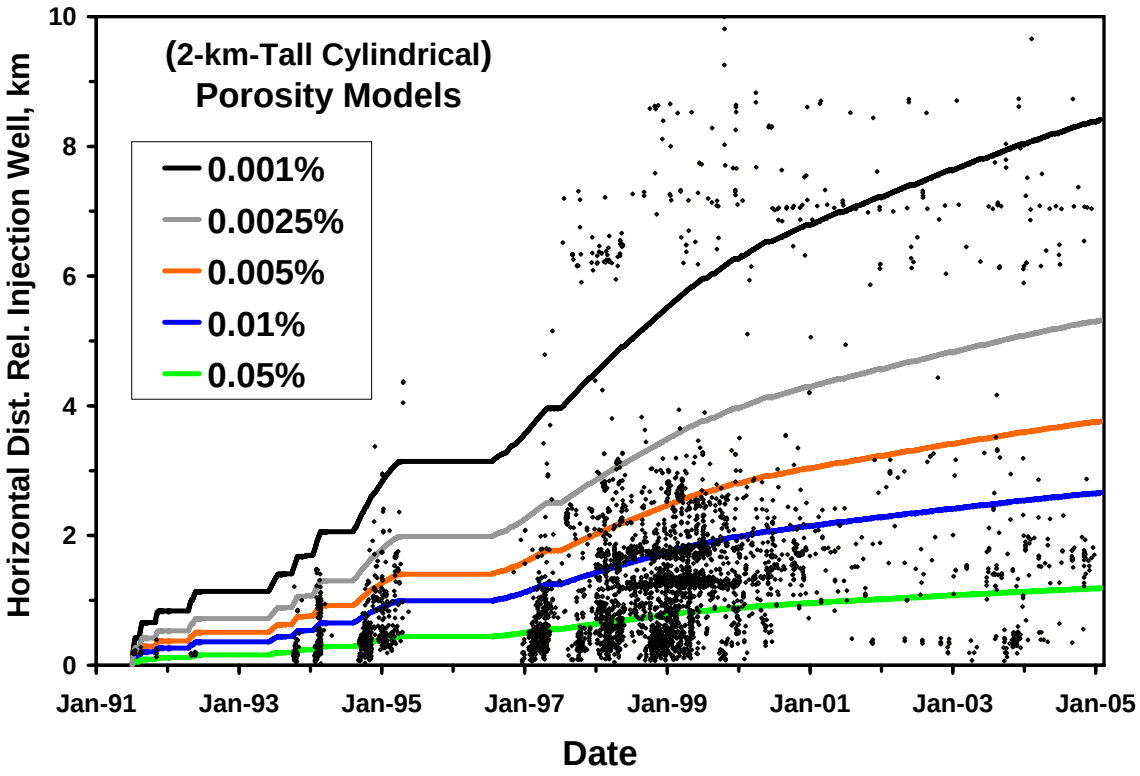

Figure 7-5 Horizontal Distance of Seismic Events from the Injection Well (black dots) and of Injectate-Porosity Model versus Time. Calculated radii of 5 models assume an expanding cylinder of injectate filling different rock porosities as a function of time for a 2-km tall cylinder of injectate.

Based in the pre-2000 seismic expansion rate in **Figure 7-5**, the models suggest a minimum necessary porosity between 0.005% and 0.0025%. In 2000 with the inception of more shut downs and

the reduced injection rate in late June, the growth of seismic zone is greatly curtailed and the model no longer fits the seismic zone expansion. This may mean that with overall reduced injection, the injectate is not being forced to move as quickly, but instead diffuses into the existing region defined by the extent of the seismicity. Using this scenario, a fixed region defined by the extent of seismicity, we assumed a seismogenic volume of about 30 cubic km. With an injected volume of about 0.004 cubic km (i.e., 4 million cubic meters), this gives a porosity of ~0.01%. This second value of porosity is not the same as our first, but, given the impreciseness of these models, they are compatible. For comparison, when Envirocorp (1995) ran its BORFRAC reservoir model to simulate the performance of the injection well and the Leadville formation, it used 0.05% porosity.

8.0 CONCLUSIONS

8.1 Specific to 2004

The general objectives of recording, analyzing, and interpreting seismicity in the Paradox Valley region were successfully carried out during 2004. The seismic data showed that the adjustment to the PVU injection schedule in 2000 continued to maintain a low level of seismicity. Relevant observations from this reporting period include:

(1) The 107 microearthquakes of 2004 locate within the two seismogenic zones defined by previous years' microearthquake locations;

(2) Induced earthquakes continued to occur ~8 km northwest of the injection well with a gap between those events and the event zone surrounding the injection well;

(3) The spatial patterns of observed seismic sources and observed seismic source mechanics seem to follow the Wray Mesa fault and fracture system and are consistent with relevant tectonic stress characteristics.

(4) A large (magnitude **M**3.9) event occurred during November 2004. The last large event (magnitude **M**4.3) occurred nearly 4 1/2 years earlier.

(5) Injection controls (i.e., reduced injection rate and biannual 20-day shut downs) were continued during 2004 and the rate of seismic event production remains very low compared to the early years of continuous pumping.

8.2 Since Inception of Continuous Pumping

Throughout the continuous pumping, beginning in 1996, the nominal injection pressure at PVU exceeds fracture pressure.

The initial induced seismicity was probably due to injectate or connate fluids reducing the friction across faults, liberating pre-existing, *in situ* tectonic stress across the faults. Later events may also include those resulting from changing the *in situ* stress due to pore and fault inflation from the injectate and displaced connate fluids.

The induced seismicity at Paradox illuminates an extensive, non-symmetric connected network of fractures, faults, joints, etc. and does not demonstrate the traditionally hydraulic fracture picture of two, vertical, symmetric fractures emanating from opposite sides of the injection well.

The surface-recorded seismic events radiate shear slippage on pre-existing faults, joints, planes of weakness, not tensile or the openings of new fractures.

Injection has induced two, distinct seismic event zones: a primary zone, asymmetrically surrounding the well to a radial distance of ~3+ km and a secondary zone, displaced ~8 km to the northwest of the injection well along the trend of the known Wray Mesa fault system. The primary zone is within a reservoir covering between 20 and 30 cubic kilometers

More than 99.9% of the over 4,000 surface-recorded events induced at the Paradox Valley injection since 1991 have magnitudes less than **M**2.0. The human detection threshold at Paradox is ~**M**2.5; There have been ~15 induced events felt at the region.

Our best estimate indicates PVU has induced ~2 million events with magnitude **M**-3.0 and greater. Being a surface array, PVSN's recording sensitivity is ~0.1% of these events which includes those events with magnitude ~0.0 and greater.

The largest seismic event, an **M**4.3 in May 2000, occurred after ~4 years of continuous injecting.

The first seismic event induced by continuous pumping occurred 111days after pumping began.

The general rate of seismicity is not uniform nor following any discernible pattern; during periods of continuous injection, there are one-day, multi-day, and multi-week quiet periods and multi-hour to multi-day active periods.

Spatially, seismic events occur as isolated events and in swarms; swarms can occur over hours to days in a single location.

The seismic swarms at Paradox are like typical earthquake swarms that culminate in one large event and some smaller foreshocks and a few smaller aftershocks or have one large event followed by 5 to 15 aftershocks.

The seismicity continuously occurs within the interior and on the border of the existing seismic zones; since mid-1999, the expansion of the zones seem negligible, if at all.

By the end of 2004, PVU injected ~0.004 cubic kilometers of injectate. Because connate fluid has been displaced and this fluid can trigger seismic events, the volumetric extent of the injectate is probably less than the volumetric extent of the seismic zone

Seismic event depths are vertically contained between ~3.5 km and ~6.0 km below the injection wellhead.

Epicenters pattern of the secondary fracture and fault network seems to align with (e.g., terminate along) the major, through-going faults of the Wray Mesa system and follows the predicted hydraulic gradient of target formation.

The major fault system aligns with the principal stress direction and acts as fluid conduits showing only minor, if any, surface-recordable seismicity.

The fault-planes defined by focal mechanism solutions (i.e., moment tensors) align with the strikes of the faults and fractures or with the predict shear planes.

Economically reasonable, 20-day shut downs has somewhat reduced the proclivity for large events by relaxing the local state of stress.

Percentage of brine (i.e.,% PVB) in injectate has not affected seismicity directly; however, it has increased the bottom-hole pressure due to the increase in specific gravity of injectate.

The storage of injectate is facilitated by the injection pressure exceeding the fracture pressure and creating new volume plus creating pathways to additional pore space; the seismically-illuminated faults and fractures can only accommodate a few percent of the injectate volume.

The *b*-value, a parameter related to the number of seismic events per size and indirectly related to repeatability of seismic events, seems to have been altered by the changes in injection phases.

9.0 MISCELLANEOUS

9.1 Supplemental Activities

Following are supplemental activities related to PVSN and the injection and seismic data:

(1) Attended Meetings (and Present Paper):

Seismological Society of America, April 2004, Palm Springs, CA

Environmental Protection Agency, Region 8 Hq, Nov 2004, Denver, CO

National Desalinization Symposium, Dec 2004, Las Vegas, NV

(2) Invited Presentations:

Kontinentales Tiefbohrprogramm der Bundesrepublik Deutschland (*German Continental Deep Drilling Program*), July 2004, Potsdam, Germany

Geophysiks Dept, Freie Universitaet, July 2004, Berlin, Germany

Heiland Lecturer, Geophysics Department, Colorado School of Mines, Sept 2004, Golden, CO.

(3) Accepted Papers for Publications:

"*Deep Injection and Closely-Monitored Seismicity at Paradox Valley, Colorado*," by J. Ake, K. Mahrer, D O'Connell, and L. Block accepted for publication in Bulletin of Seismological Society of America (April, 2005).

"*Injection Brine and Inducing Seismicity a the World's Deepest Injection Well, Paradox Valley, Southwest Colorado, USA*," by K. Mahrer, J. Bundy, J. Ake, L. Block, and D. O'Connell accepted for publications in bound proceedings of the Second International Symposium on Underground Injection Science and Technology (Berkeley, CA, Oct, 2003)

9.2 Accompanying CD File List

The accompanying CD contains 6 files:

(1) a Microsoft Excel file of the PVSN seismic data (i.e., time, date, and location of events) and contemporaneous (average) PVU injection data

(2-6) PDF files of this year's, the 2003, 2002, 2001, and 2000 PVSN annual reports

10.0 REFERENCES

Ake, J. P., D. R. H. O'Connell, L. Block, and U. Vetter, 1996. Summary report, Paradox Valley Seismic Network, Paradox Valley Project, southwestern Colorado (*draft*): Seismotectonic Report 96-9, U. S. Bureau of Reclamation, Seismotectonic and Geophysics Group, Denver, CO, 89 pp.

Ake, J., and K. Mahrer, 1999. 1998 Status report-Paradox Valley Seismic Network, Paradox Valley Project, southwestern Colorado: Technical Memorandum No. D8330-99-016, U. S. Bureau of Reclamation, Seismotectonics and Geophysics Group, Denver, CO, 18 pp.

Ake, J., K. Mahrer, and L. Block, 2000. 1999 Status report-Paradox Valley Seismic Network, Paradox Valley Project, southwestern Colorado: Technical Memorandum No. D8330-2000-012, U. S. Bureau of Reclamation, Seismotectonics and Geophysics Group, Denver, CO, 23 pp.

Anderson, J.G. and S.E. Hough, 1984. A Model for the Shape of the Fourier Amplitude Spectrum of Acceleration at High Frequencies, *Bull. Seis. Soc. Am*, v. 74, pp. 1969-1993.

Bender, B. 1983. Maximum Likelihood Estimation of *b* Values Magnitude Grouped Data, *Bull. Seis. Soc. Am*, v. 73, pp. 831-851.

Bird, P., 2002. Stress direction history of the western United States and Mexico since 85 Ma: *Tectonics*, v. 21, 10.1029/2001TC001319.

Block, L., Ake, J. and Mahrer, K, 2001, The Association between Seismicity Induced by Deep-Well Injection, Injectate Migration, and Tectonic Stresses at Paradox Valley, Colorado, *Seismological Research Letters*, v. 72, n2, p. 286. (abstract)

Block, L. V., 1991. Joint hypocenter-velocity inversion of local earthquake arrival time data in two geothermal regions: Ph. D. Dissertation, Massachusetts Institute of Technology, 448 pp.

Bremkamp, W., and C. L. Harr, 1988. Area of least resistance to fluid movement and pressure rise, Paradox Valley Unit, Salt Brine Injection Project, Bedrock, Colorado: Final unpublished report to the U.S. Bureau of Reclamation, Denver, CO., 39 pp.

Brune, J.N., 1970. Tectonic Stress and Spectra of Seismic Shear Waves from Earthquakes, *J. Geophysical Research*, v. 75, p 4997-5009.

Brune, J.N. 1971. Correction, *J. Geophysical Research*, v. 76, p 5002.

Clark, S.P. Jr. (Editor), 1966. **Handbook of Physical Constants Revised Edition, Memoir 97**, Geological Society of America, 583 pp.

Colorado Division of Minerals and Geology, 1980, Regulations of the Colorado Mined Land Reclamation Board for Coal Mining (Effective August 30, 1980), Denver Colorado.

EnviroCorp, 1995. Report of evaluation of injection testing for Paradox Valley Injection Test No. 1: EnviroCorp Project Report No. 10Y673: Final report prepared for the U.S. Bureau of Reclamation by EnviroCorp Services and Technology, Inc., Houston TX, 26 pp.

Hendron, A.J. Jr., 1968, **Mechanical Properties of Rock in Rock Mechanic in Engineering Practice**, ed by, K.G. Stagg and O. C. Zienkiewica, John Wiley & Sons, 442 pp.

Healy, J.H, W.W. Rubey, D.T. Griggs, and C.B. Raleigh, 1997. The Denver earthquakes, *Science*, v. 161, p. 1301-1310.

Kharaka, Y. K. et al., 1997, Deep well injection of brine from Paradox Valley, Colorado: Potential major precipitation problems remediated by nanofiltrations, *Water Resour. Res.*, v33(5), p. 1013-1020.

Kisslinger, C., 1980. Evaluation of S to P amplitude ratios for determining focal mechanisms from regional network observations, *Bull. Seis. Soc. Am*, v. 70, p. 999-1014.

Kisslinger, C., Bowman, J.R., and Koch, K., 1981. Procedures for computing focal mechanisms from local $(SV/P)_z$ data: *Bull. Seis. Soc. Am*, v. 71, p. 1719-1729.

LaForge, R. L., 1996. Seismic hazard assessment for Navajo Dam, Navajo Indian Irrigation Project, New Mexico: Seismotectonic Report No. 96-11, U. S. Bureau of Reclamation, Seismotectonics and Geophysics Group, Denver, CO, 34 pp.

Lee T. and T.C. Wallace, 1995. **Modern Global Seismology**, Academic Press, 521 pp.

Mahrer, K., 1999, "A Review and Perspective on Far-Field Hydraulic Fracture Geometry Studies," *J. Petroleum Science and Engineering,* 24, pp. 12-28, 1999.

Mahrer, K., L. Block, and J. Ake, 2001. 2000 Status Report-Paradox Valley Seismic Network, Paradox Valley Project, Southwestern Colorado: Technical Memorandum No. D8330-2001-007, U. S. Bureau of Reclamation, Seismotectonics and Geophysics Group, Denver, CO, 37 pp. (available on attached CD)

Mahrer, K., J. Ake, and L. Block, 2002. 2001 Status Report-Paradox Valley Seismic Network, Paradox Valley Project, Southwestern Colorado: Technical Memorandum No. D8330-2002-003, U. S. Bureau of Reclamation, Seismotectonics and Geophysics Group, Denver, CO, 35 pp.(available on attached CD)

Mahrer, K., J. Ake, D. O'Connell, and L. Block, 2004. 2003 Status Report-Paradox Valley Seismic Network, Paradox Valley Project, Southwestern Colorado: Technical Memorandum No. D8330-2004-004, U. S. Bureau of Reclamation, Seismotectonics and Geophysics Group, Denver, CO, 35 pp.(available on attached CD)

Mahrer, K., J. Ake, L. Block, and D. O'Connell, 2003. 12 Years of Injecting Brine and Inducing Seismicity near Paradox Valley, Southwest Colorado, USA, in **Soil and Rock America 2003**, 12th Panamerican Conference on Soil Mechanics and Geotechnical Engineering, 39th U.S.

Rock Mechanics Symposium, June 22-26, 2003, Proceeding Vol II, ed by P.J. Culligan, H.H. Einstein, and A.J. Whittle, Eds, pp1443-1447.

Malone, S., and C. Weaver, 1986. Informal memorandum describing earthquake location program SPONG: University of Washington Geophysics Program, Seattle, WA, 10 pp.

McGarr, A., 1976. Seismic Moments and Volume changes, *J. Geophysical Research*, v. 81, p 1487-1494.

Parker, B. H. Jr, 1992, **Gold Panning and Placering in Colorado How and Where,** Information Series 33, Colorado Geological Survey, Department of Natural Resources, Denver, CO, 83 pp.

Phillips, W.S., J.T. Rutledge, L.S. House, M.C. Fehler, 2002. Induced Microearthquake Pattern in Hydrocarbon & Geothermal Reservoirs: Six Case Studies, *Pure and Applied Geophysics*, v159, N1-3, p. 345-369/

Press, W.H., Teukolsky, S.A., Vetterling, W.T., Flannery, B.P., 1992. **Numerical recipes in FORTRAN: The art of scientific computing,** Cambridge University Press, New York, 963 p.

Turcotte, D. L., 1997. **Fractals and Chaos in Geology and Geophysics**, 2nd Edition, Cambridge University Press, 398 p.

Waldhauser, F., W. L. Ellsworth, and A. Cole, 1999. Slip-parallel seismic lineations on the northern Hayward Fault, California, *Geophysical Research Letters*, **26**, No. 23, p. 3525-3528.

Wells, D.L. and K.J. Coppersmith, 1994. New Empirical Relationships among Magnitude, Rupture Length, Rupture Area, and Surface Displacement, *Bull. Seis. Soc. Am.*, **84**, No. 4, p 974-1002.

Wong, I. G., and R. B. Simon, 1981. Low-level historical and contemporary seismicity in the Par-

adox Basin, Utah and its tectonic implications: Rocky Mountain Association of Geologists-1981 Field Conference Guidebook, p. 169-185.

Wong, I. G., S. Olig, and J. D. J. Bott, 1996. Earthquake potential and seismic hazards in the Paradox Basin, southeastern Utah: *in* Geology and Resources of the Paradox Basin, 1996 Special Symposium, A. C. Huffman, W. R. Lund, and L. H. Godwin [*eds.*], Utah Geological Association and Four Corners Geological Society Guidebook No. 25, p 251-264.